Modelling population abundance and future trajectories for Arctic marine mammals to inform Canadian sustainable fisheries management

by

Brooke Ashley Biddlecombe

A Thesis submitted to the Faculty of Graduate Studies of

The University of Manitoba

in partial fulfilment of the requirements of the degree of

DOCTOR OF PHILOSOPHY

Department of Biological Sciences

University of Manitoba

Winnipeg

Copyright © 2023 by Brooke A. Biddlecombe

Abstract

Arctic cetacean species, beluga whales (*Delphinapterus leucas*), narwhals (*Monodon monoceros)*, and bowhead whales (*Balaena mysticetus*), have a long history of subsistence harvest by northern communities, as well as various levels of exploitation from historical commercial whaling. To achieve sustainable subsistence harvest, Arctic cetacean populations must be monitored to inform management decisions. Three populations: Northern Hudson Bay (NHB) narwhal, Cumberland Sound (CS) beluga, and Eastern Canada-West Greenland (EC-WG) bowhead whales, all pose various challenges associated with building population dynamics models for management. The NHB narwhal population presents challenges surrounding inconsistent abundance estimates which limit their ability to be included into a model, this was addressed by comparing abundance estimate methodologies and calculating correction factors to adjust older estimates accordingly. The CS beluga population is endangered and is assumed to be affected by the effects of climate change, thus, the challenge of incorporating environmental variables into a population dynamics model was addressed with this population. The EC-WG bowhead whales present a challenge with achieving an abundance estimate, as their vast range makes aerial surveys, the typical method for marine mammal abundance estimation, difficult. Instead, genetic mark-recapture analyses using biopsy samples were used to estimate EC-WG bowhead whale abundance. To model population dynamics of EC-WG bowhead whales the challenge of underestimated abundance from insufficient aerial survey coverage was addressed by using telemetry data in a utilization distribution map to extrapolate abundance. Challenges associated with determining population dynamics of Arctic cetaceans can be addressed with creative problem solving, considering the types of data available and specific management goals associated with each population of focus.

Contributions of Authors

Chapter 2 and Chapter 3

Brooke Biddlecombe and Cortney Watt designed the concept, Brooke Biddlecombe led the analyses and the writing of the manuscript, and Cortney Watt provided revisions.

Chapter 4 and Chapter 5

Brooke Biddlecombe, Darren Gillis, Steven Ferguson, and Cortney Watt designed the concept, Brooke Biddlecombe led the analyses and the writing of the manuscript, and Darren Gillis, Steven Ferguson, Mads Peter Heide-Jørgensen, and Cortney Watt provided revisions. Steven Ferguson and Mads Peter Heide-Jørgensen led data collection.

Acknowledgements

I would like to thank Cortney Watt (Wheeler) for her guidance, mentorship, enthusiastic support, and the many invaluable opportunities she's provided me. I would like to thank Darren Gillis for his guidance, mentorship, and unwavering encouragement. I would also like to thank Steve Ferguson for his insight and advice, and Saman Muthukumarana for his guidance. I am also thankful to the Marine Mammal graduate student group at the Freshwater Institute for their encouragement, and Corey Smereka for being my personal morale booster. I would also like to thank Andrew Derocher for igniting my passion for Arctic research years ago.

I would like to thank my parents, Stacie and Corey Biddlecombe, for continuing to be my biggest supporters. I am also thankful for my dogs Sammie, Gus, Winnie, and Tessa, for offering endless stress relief.

For financial support I would like to thank Fisheries and Oceans Canada, the Natural Sciences and Engineering Research Council, the University of Manitoba, Nunavut Wildlife Research Trust Fund, the Nunavut Wildlife Management Board, ArcticNet Centre of Excellence, International Polar Year (Global Warming and Arctic Marine Mammals), Assiniboine Park Zoo, the Commission for Scientific Research in Greenland, the National Ocean Partnership Program, the Danish Cooperation for the Environment in the Arctic, and the Greenland Institute of Natural Resources.

Dedication

To my parents, Stacie and Corey Biddlecombe, for always encouraging my curiosity and unconditionally supporting me in all my endeavours.

Table of Contents

Abstract ii
Contributions of Authors iii
Acknowledgements iv
Dedication v
List of Tables ix
List of Figures xi

Chapter 1 1
1 Introduction 1
1.1 References 8

Chapter 2 15
2 Modelling population trajectory and probability of decline in Northern Hudson Bay narwhal 15
Abstract 16
2.1 Introduction 17
2.2 Methods 21
2.2.1 Survey abundance observations and adjustments 21
2.2.2 Model specification 22
2.2.3 Priors 25
2.2.4 Parameter Estimation and Model Diagnostics 28
2.2.5 Future Projections and Harvest Scenarios 30
2.3 Results 30
2.4 Discussion 33
2.5 References 38

Chapter 3 45
3 Incorporating environmental covariates into a Bayesian stock production model for the endangered Cumberland Sound beluga population 45
Abstract 46
3.1 Introduction 47
3.2 Material & Methods 53
3.2.1 Model Specification 53
3.2.2 Process Error Incorporating Environmental Covariates 56
3.2.3 Priors 59
3.2.4 Parameter Estimation and Model Diagnostics 62
3.2.5 Future Projections and Management Scenarios 63
3.3 Results 64
3.4 Discussion 72

3.5 References 81
Chapter 4 90
4 Estimating abundance of Eastern Canada-West Greenland bowhead whales using genetic mark-recapture analyses 90
Abstract 91
4.1 Introduction 92
4.2 Methods 95
4.2.1 Sampling 95
4.2.2 Genetic Analyses 97
4.2.3 Estimating Abundance 97
4.3 Results 101
4.4 Discussion 108
4.5 References 116
Chapter 5 123
5 Combining multiple data sources to extrapolate population estimates and model population dynamics of Eastern Canada-West Greenland bowhead whales 123
Abstract 124
5.1 Introduction 126
5.2 Methods 129
5.2.1 Location Data 129
5.2.2 Utilization distribution mapping 129
5.2.3 Extrapolation of Survey Estimates 130
5.2.4 Population model specifications 134
5.2.5 Priors 136
5.2.6 Parameter Estimation and Model Diagnostics 140
5.2.7 Future Projections and Harvest Scenarios 141
5.3 Results 143
5.4 Discussion 151
5.5 References 165
Chapter 6 175
6 Conclusion 175
6.1 References 180
Appendices 183

Appendix 1 ..... **183**
Appendix 2 ..... **187**
Appendix 3 ..... **205**
Appendix 4 ..... **210**

List of Tables

Table 2.1 Estimates of Northern Hudson Bay narwhal abundance from aerial surveys in their summering range. Total Estimates are the values calculated from the surface estimates using an availability bias adjustment factor (C_a) of 2.8, and the coefficient of variation (CV) of the total estimate. Fully Adjusted Estimates have been adjusted for both perception and availability bias. CDS = conventional distance sampling, MRDS = mark-recapture distance sampling.....**25**

Table 2.2 Prior distributions, parameters, and hyper-parameters used in the population model. "dist." denotes a hyper-parameter with its own prior distribution.....**27**

Table 3.1 Prior distributions, parameters and hyper-parameters used in the template population model (from Watt et al. 2020) and environmental covariates sea ice concentration (ICE) and sea surface temperature (SST) corresponding to process error used in the final model. "dist." denotes a hyper-parameter with its own prior distribution. Dashes indicate parameters that do not apply to the model.....**60**

Table 3.2 Model outputs for the CS beluga stock model from Watt et al. 2020 and our final model. The mean, standard deviation (SD), median (50^{th} Q), 25^{th} and 75^{th} quantiles (25^{th} Q, 75^{th} Q), 95% credibility intervals (2.5%CI, 97.5%CI) are given for the following model parameters and their priors: carrying capacity (K), process error (process), survey precision (surv), starting population (startpop), struck and loss (S&L), and population size in 2018 (N_{2018}). Coefficients for ICE (B) and SST (C) are included in the final model output. $\widehat{R}$ is the Brooks-Gelman-Rubin statistics; values < 1.05 indicate convergence of chains. N.eff is the number of effective chains after considering autocorrelation.....**65**

Table 3.3 Probability (P) that the CS beluga population, subjected to different levels of annual landed catch, will decline from the modelled 2018 population abundance estimate after 10 years of harvest. Comparing results from Watt et al. 2020 and our final model (with ICE and SST)....**71**

Table 4.1 Total number of captures from EC-WG bowhead whales in each year and each capture location, with the number of those captures that were recaptures from a previous year in parentheses.....**102**

Table 4.2 Estimated survival probability (Φ), probability of capture (*p*), super abundance estimate (*N*), and probability of individuals entering the super population (*pent*) from the top Jolly-Seber mark recapture model for EC-WG bowhead whales sampled from 2012-2021 from all sampling locations. No samples were taken in 2015.....**105**

Table 4.3 Estimated survival probability (Φ), probability of capture (*p*), super abundance estimate (*N*), and probability of individuals entering the super population (*pent*) from the top Jolly-Seber mark recapture model for EC-WG bowhead whales sampled from 2012-2021 from Pangnirtung. No samples were taken in 2015.....**107**

Table 5.1 Data used for Poisson regression analysis from EC-WG bowhead whale aerial surveys. See Figure 5.1 for strata: S1: strata 1, S2: strata 2, S3: strata 3, ES: Eclipse Sound, GB:

Gulf of Boothia, PRI: Prince Regent Inlet, AI: Admiralty Inlet, CS: Cumberland Sound, and EB: East Baffin Island. Mean BBMM refers to the standardized mean probability density of occupancy from BBMM analyses, and estimated abundance refers to reported aerial survey estimates.....**134**

Table 5.2 Prior distributions, parameters and hyper-parameters used in the population model for EC-WG bowhead whales. "dist." denotes a hyper-parameter with its own prior distribution. Dashes indicate parameters that do not apply to the model.....**140**

Table 5.3 Results of extrapolation of EC-WG bowhead whale aerial survey estimates using probability of occupancy from BBMM analyses. Unsurveyed areas were separated into high-use and low-use regions based on BBMM values, and abundance was extrapolated separately using Poisson regression results (see text for details).....**147**

Table 5.4 Model output for the EC-WG bowhead whale stock model. The mean, standard deviation (SD), median (50^{th} Q), 25^{th} and 75^{th} quantiles (25^{th} Q, 75^{th} Q), 95% credibility intervals (2.5%CI, 97.5%CI) are given for the following model parameters: carrying capacity (K), process error (process), survey precision (surv), starting population (startpop), struck and loss (S&L), and population size in 2022 (N_{2022}). $\widehat{R}$ is the Brooks-Gelman-Rubin statistics; values < 1.05 indicate convergence of chains. N.eff is the number of effective chains after considering autocorrelation.....**150**

List of Figures

Figure 1.1 Summer and winter range map for Cumberland Sound (CS) beluga, Northern Hudson Bay (NHB) narwhal, Eastern Canada-West Greenland (EC-WG) bowhead whales.....**7**

Figure 2.1 Map indicating the coverage of NHB narwhal aerial surveys included in our population model. 1982: solid; 2000: vertical; 2011: diagonal; 2018: horizontal. Inset: Map indicating the summering (solid) and wintering (hatched) ranges for the Northern Hudson Bay narwhal population with aerial survey coverage highlighted with a dashed outline.....**18**

Figure 2.2 Model estimates of NHB narwhal abundance from the model fitted to adjusted aerial abundance observations from 1982, 2000, 2011, and 2018 (black dots ± 95% log-normal CI) and harvest data from 1951-2018, and future population projections under 3 different harvest scenarios. Solid line shows the median estimates and dashed lines show the 95% credible intervals. Vertical dotted line shows separation between the modelled abundance based on aerial abundance observations and the future projections.....**31**

Figure 2.3 Probability of the NHB narwhal stock decreasing from the 2019 abundance estimate after 10 years of harvest, estimated by the model, as a function of the number of reported narwhals removed from the stock each year. Dotted lines show the corresponding probability of decline (y-axis) for various annual levels of harvest (x-axis).....**32**

Figure 3.1 Delineation of Cumberland Sound study area used to clip raster files.....**48**

Figure 3.2 Schematic of the hierarchical state space population model structure depicting linkages between state process (solid grey outline), observation process (dashed grey outline), and harvest (dotted grey outline). Grey circles indicate data, white rectangles indicate parameters to be estimated by the model, and black lines indicate dependencies between parameter and/or data. N is population size, Rmax is the maximum growth rate or rate of population increase, K is the environmental carrying capacity, εp is a stochastic term for the process error with environmental covariates, Rt are the removals for that year, calculated as reported catches, C, that are corrected for the proportion of animals that were struck and lost, $S\&L$, S is survey data, ε_{S_t} is a stochastic term for observation error, ICE is mean sea ice concentration in Cumberland sound in March, SST is mean sea surface temperature in Cumberland Sound in August, B is the coefficient being estimated by the model for ICE, C is the coefficient being estimated by the model for SST.....**55**

Figure 3.3 Mean sea ice concentration (ICE) in March and mean sea surface temperature (SST) in August as Z-score values in Cumberland Sound from 1960-2017.....**58**

Figure 3.4 Model estimates of CS beluga abundance fitted to adjusted aerial survey estimates flown in 1990, 1999, 2009, 2014 and 2017 (black dots ± 95% log-normal CI) and harvest data from 1960-2017. Process error includes the effects of sea ice concentration (ICE) and sea surface temperature (SST) in CS. Solid line shows the posterior median estimates, dashed lines show 50% credible interval, and dotted lines show 95% credible interval.....**67**

Figure 3.5 Model estimates of CS beluga abundance fitted to adjusted aerial survey estimates flown in 1990, 1999, 2009, 2014 and 2017 (black dots ± 95% log-normal CI) and harvest data from 1960-2017. A) Process error includes the effect of sea ice concentration in CS. B) Process error includes the effect of sea surface temperature in CS. Solid line shows the posterior median estimates, dashed lines show 50% credible interval, and dotted lines show 95% credible interval.....**69**

Figure 3.6 Future population projections for CS beluga under five different management scenarios based on population estimates from a stochastic stock production model including ICE and SST, fitted to adjusted aerial survey estimates flown in 1990, 1999, 2009, 2014 and 2017 (black dots ± 95% log-normal CI). Solid line shows the posterior median estimates and dashed lines show 95% credible interval.....**70**

Figure 3.7 Probability of the CS beluga stock decreasing from the 2018 abundance estimate after 10 years of harvest, as a function of the number of reported beluga removed from the stock every year. Dotted lines indicate levels of harvest (x-axis) corresponding to the probability of decline (y-axis). Red line shows probability of CS beluga stock decrease from template model (Watt et al. 2020).....**72**

Figure 4.1 Locations of EC-WG bowhead whale biopsy samples.....**96**

Figure 4.2 Annual abundance estimates for the EC-WG bowhead whale population from a Cormack-Jolly-Seber mark recapture model. Black points show annual abundance estimates, while the grey polygon indicates the confidence interval.....**104**

Figure 4.3 Comparison of abundance estimates with 95% confidence intervals from two Jolly-Seber mark recapture models for the EC-WG bowhead whale population sampled from 2012-2021. Model 1 includes samples from all locations, model 2 includes only samples collected in Pangnirtung.....**108**

Figure 5.1 Strata for EC-WG bowhead whale aerial surveys conducted in 1981 (purple; S1: strata 1, S2: strata 2, S3: strata 3), 2002 (green; GB/PRI: Gulf of Boothia/ Prince Regent Inlet, ES: Eclipse Sound), and 2013 (red; PRI: Prince Regent Inlet, GB: Gulf of Boothia, AI: Admiralty Inlet, ES: Eclipse Sound, EB: East Baffin Island, CS: Cumberland Sound).....**133**

Figure 5.2 BBMM probably of occupancy results for EC-WG bowhead whales in A) March with 1981 aerial survey coverage and B) August with 2002 and 2013 aerial survey coverage. BBMM values are relative probability density of occupancy values, and thus, have been presented as relative high and low probabilities.....**144**

Figure 5.3 Quasi-Poisson regression (blue regression line, light blue 95% confidence interval) comparing mean Brownian Bridge movement model probability density value to estimated abundance in each EC-WG bowhead whale aerial survey strata (from surveys conducted in 1981, 2002, and 2013). Linear regression shown in black, with dark grey 95% confidence interval, and polynomial regression shown in grey, with light grey 95% confidence interval. Outlier removed from regression analyses shown in red.....**146**

Figure 5.4 Future population projections for EC-WG bowhead whales under four different harvest scenarios based on population estimates from a stochastic stock production model fitted to extrapolated aerial survey estimates flown in 1981, 2002, and 2013, and genetic mark recapture estimates from 2013 and 2017 (black dots ± 95% log-normal CI). The solid line indicates the posterior median estimates and dashed lines show 95% credible intervals. A) Full model trajectory with future predictions, B) Plot enlarged to show future predictions.....**149**

Figure 5.5 Probability of EC-WG bowhead whale stock decreasing from the 2022 abundance estimate after 10 years of harvest, as a function of the number of reported bowhead whales removed from the stock every year. Dotted lines indicate levels of harvest (x-axis) corresponding to the probability of decline (y-axis). Red dotted line indicates low risk of decline.....**151**

Chapter 1

1 Introduction

Population dynamics involve changes in various aspects of a population's ecology, including size, density, and distribution, over time or space (Begon et al. 1986). The term population typically refers to a geographically or genetically isolated group of a single species, although a population's dynamics are impacted by other species that share the same ecosystem (Kareiva 1990). Population dynamics are typically dictated by certain ecological and physiological aspects of the species in question, and involve multiple population parameters, such as fecundity, mortality, immigration, emigration, and carrying capacity (Peters & Barbosa 1977, Snell 1978, McPeek & Peckarsky 1998). Dynamics are also impacted by forces exterior to the population itself, such as resource availability, predation, and competition (Begon et al. 1986, Kareiva 1990). Species can be separated into two major groups: r-selected and K-selected species (MacArthur & Wilson 1967, Pianka 1970). The "r" in r-selected refers to maximum growth rate, and thus refers to species whose combination of traits favour rapid growth, such as maximum fecundity (MacArthur & Wilson 1967, Pianka 1970). The "K" in K-selected refers to carrying capacity, referring to a species whose traits favour competitive ability, and thus population size is more likely to be regulated by restrictions in resource availability as the population approaches carrying capacity (MacArthur & Wilson 1967, Pianka 1970). K-selected species are typically long-lived, have a lower fecundity, they generally put more effort into rearing offspring, and their offspring develop more slowly (Pianka 1970, Lloyd 1987). These two species types do not exist in isolation, and often species exhibit a combination of traits that fit them on a spectrum between the two extremes (Pianka 1970).

The amplitude and temporal length of population fluctuations vary (Lande et al. 2003). There are different population growth patterns from various species and populations, but all populations exhibit some level of stochastic fluctuation. Environmental stochasticity, biotic interactions, and life history traits are a few of the many factors affecting population dynamics (Lande et al. 2003, Fitzgerald 2015). Larger more sporadic fluctuations are more typical for r-selected species because of more unstable environments, whereas K-selected species typically inhabit more stable environments, and have more stable population dynamics (Pianka 1970, Chiba 1998). Larger bodied, slow growing animals exemplify K-selected traits, as such, cetaceans are an excellent example of K-selected species (Heppell et al. 2000). Generally, populations of cetacean species are expected to have a low amount of short-term variation in abundance, with relatively stable growth. Stability of population dynamics of cetaceans (or other K-selected species) can be affected by external factors, such as a change in resource availability or increased mortality (from harvest, for example) (Kingsley et al. 2013, Wade 2018).

Arctic marine ecosystems are among many marine ecosystems that have cetacean species at the top of the food web. Arctic ecosystems are largely shaped by the presence of ice, either year-round (as with multiyear ice) or a portion of the year (as with annual ice) (Melnikov 1997). The presence of ice is linked to primary production in Arctic marine food webs, where the majority of production comes from sea ice algae and phytoplankton (Darnis et al. 2012). Moving upwards through the food web, Arctic marine ecosystems include multiple species of zooplankton, fish, and marine mammals (Darnis et al. 2012, McMeans et al. 2013). Multiple cetacean species occupy Arctic waters throughout the year, often migrating north during the summer months for feeding and mating opportunities. A subset of this group are cetaceans that remain in Arctic or sub-Arctic waters year round, and are often defined by their association with

sea ice (Kovacs et al. 2011, Laidre et al. 2015). Beluga whales (*Delphinapterus leucas*), narwhals (*Monodon monoceros)*, and bowhead whales (*Balaena mysticetus*) are the only Arctic resident cetaceans, and although they remain in the north year round, they have migrations of varying distances throughout Arctic regions, depending on the population (Richard 1991, Heide-Jørgensen et al. 2003, Richard & Stewart 2008, Richard 2010).

Narwhal, beluga, and bowhead whales, alongside multiple other Arctic species, have a long history of subsistence harvest in the north. These species have also experienced exploitation from commercial whaling throughout history (Stewart 2008, Higdon 2010, Stewart 2018). Narwhal are a common subsistence animal for communities in the Canadian Arctic (Nuttall et al. 2005, Heide-Jørgensen et al. 2013), but in the 1980's hunting quotas were put in place as a result of concerns about the ivory tusk market (Kemper 1980). Lack of data has led to uncertainty in determining true population abundance and the effectiveness of the narwhal hunting quotas that were implemented (Innes et al. 2002, Richard et al. 2010). Beluga whales have been and continue to be an important resource for Inuit populations (Tyrrell 2007), and are hunted throughout their range (Luque & Ferguson 2010). Six of the eight beluga stocks in the Canadian Arctic are listed as special concern, threatened, or endangered by the Committee on the Status of Endangered Wildlife in Canada (COSEWIC), and Cumberland Sound belugas are listed as Threatened under the Species At Risk Act since 2018. Hunting pressure is the primary cause of decline for many of these beluga stocks (Tyrrell 2007, Luque & Ferguson 2010). Bowhead whales have been subjected to both commercial and subsistence harvest as far back as ca. 1000 AD (Higdon 2010). The Eastern Canada-West Greenland bowheads were heavily harvested from 1530 – 1915, and population abundance was depleted (Higdon 2010). The population is

rebounding in more recent years (Wade et al. 2012, Rekdal et al. 2015), but past details are lacking to inform management and conservation action.

Ongoing subsistence harvest means that narwhal, beluga whales, and bowhead whales must be consistently monitored to inform management decisions, with the goal of sustainable harvest. Harvest is one of many stressors acting on Arctic cetacean populations; other anthropogenic stressors include increased shipping, increased noise pollution and oil and gas activities, as well as increased effects of climate change, namely sea ice loss (Hovelsrud et al. 2008, Huntington 2009). Impacts of climate change, including changes in sea ice extent and duration, compounded by the history of harvest in the Canadian Arctic, has affected various whale populations differently, and the direct cause of these variable responses is largely unknown due to a lack of demographic information (Wassmann et al. 2011, Laidre et al. 2015). Consistent monitoring is required to adequately assess the risk involved in management and harvest of Arctic marine mammal populations. Due to their rapidly changing ecosystems, Arctic cetaceans are impacted by a number of factors that have the potential to create discernable changes in the abundance, growth rate, and survival of a population, thus altering population dynamics (Harwood 2001, Bluhm & Gradinger 2008, Burek et al. 2008). It is difficult to make mass predictions for the effects of anthropogenic stress and environmental change on cetacean population dynamics. Between species, and even between populations of the same species, Arctic cetacean population dynamics are highly variable, and many show diverging trends (COSEWIC 2004, 2009, 2020).

Management goals for aquatic species are often determined by identifying stock status via a stock production model (Hilborn et al. 2020). Stock production models determine changes in abundance affected by harvest and can project future trajectories by analyzing demographic

information from a population (Maunder & Piner 2014). Stock production models make use of various types of biological data, such as fecundity, mortality, age structure, and growth rate, as well as fisheries data such as harvest records and harvest type (commercial or subsistence) (Pella & Tomlinson 1969, Hilborn et al. 2020). All of these aforementioned data types are not always available, particularly for aquatic populations. However, stock production models can be created using limited available data, such as catch history, for which there are often well-kept records, and existing isolated abundance estimates (Maunder & Piner 2014).

Abundance estimates are invaluable for their inclusion into modelling population dynamics. When a population has limited demographic data, often the only way stock production models are informed is through harvest history and the snapshots in time provided by abundance estimates. As such, regular, reliable abundance estimates are necessary for building stock production models that can reliably recreate population dynamics and make future predictions (Marcoux & Hammill 2016, Hammill et al. 2017, Watt et al. 2020, Ferguson et al. 2021). For Arctic cetaceans, abundance estimates are typically achieved by aerial surveys and more recently, through mark-recapture (MRC) analyses (i.e., Asselin et al. 2012, Frasier et al. 2020). Aerial surveys are typically flown via transect lines over the habitat of the animal of interest, and observations are converted to abundances estimates with subsequent distance sampling analyses (Buckland et al. 2001). While capturing cetaceans is often impractical, MRC analyses can utilize remote capture methods, such as identifying unique individuals via scars or colouration in photographs, or via genetic analyses from biopsy samples, from which abundance can be calculated (Hammond 2009). Challenges are present with abundance estimation, including logistic challenges and costs associated with working in the Arctic which can restrict factors such as aerial survey coverage, ability to collect samples, and how often surveys are completed. Other

data that may be valuable in modelling population dynamics, such as growth rate and survival, also pose collection difficulties, largely because studying Arctic cetaceans in their natural habitat for prolonged periods of time is logistically and financially challenging. Further, because interactions between demographic parameters and environmental covariates are typically indirect in cetaceans, opposed to the more direct relationships such as connections between sea ice cover and harp seal reproduction (Hammill et al. 2021). Quantifying these indirect relationships for use in models is challenging and increases model uncertainty. When considering the restrictive nature of data collection and identifying demographic relationships in Arctic cetaceans, the importance of abundance estimates for management becomes clear.

The nature of Arctic marine mammal ecology and our ability collect data presents challenges for management that require adaptive problem solving. Each population is accompanied by unique challenges, that require individual approaches to achieve valuable management perspectives. This thesis aims to address unique management goals for three Arctic cetacean populations: Northern Hudson Bay (NHB) narwhal, Cumberland Sound (CS) beluga, and Eastern Canada-West Greenland (EC-WG) bowhead whales (Figure 1.1). Chapter 2 focuses on NHB narwhal, addressing incongruencies in past aerial survey design and analyses to adjust estimates for consistency for inclusion in a population dynamics model. Chapter 3 focuses on CS beluga, with a goal of altering a population dynamics model to include the effects of environmental covariates. Harvest is one of many stressors, and inclusion of environmental variables aimed to gain information on how a changing environment contributed to population dynamics in this at-risk population. Chapter 4 focuses on EC-WG bowhead whales, specifically achieving an abundance estimate, previously identified as important for future population modelling. EC-WG bowhead whales present a challenge to estimating abundance, as their vast

range makes complete coverage via aerial survey not possible, thus a MRC analysis using genetic information from biopsy samples was used. Chapter 5 continues to focus on EC-WG bowhead whales, utilizing the abundance estimate developed from Chapter 4 alongside previous abundance estimates in a population dynamics model. The issues with aerial survey coverage that EC-WG bowhead whales present were also addressed by extrapolating abundance estimates from surveys into areas that could not be covered using available satellite telemetry data. Utilizing various types of data and addressing short comings in available data in creative ways helps move management forward and create more confidence in management decisions.

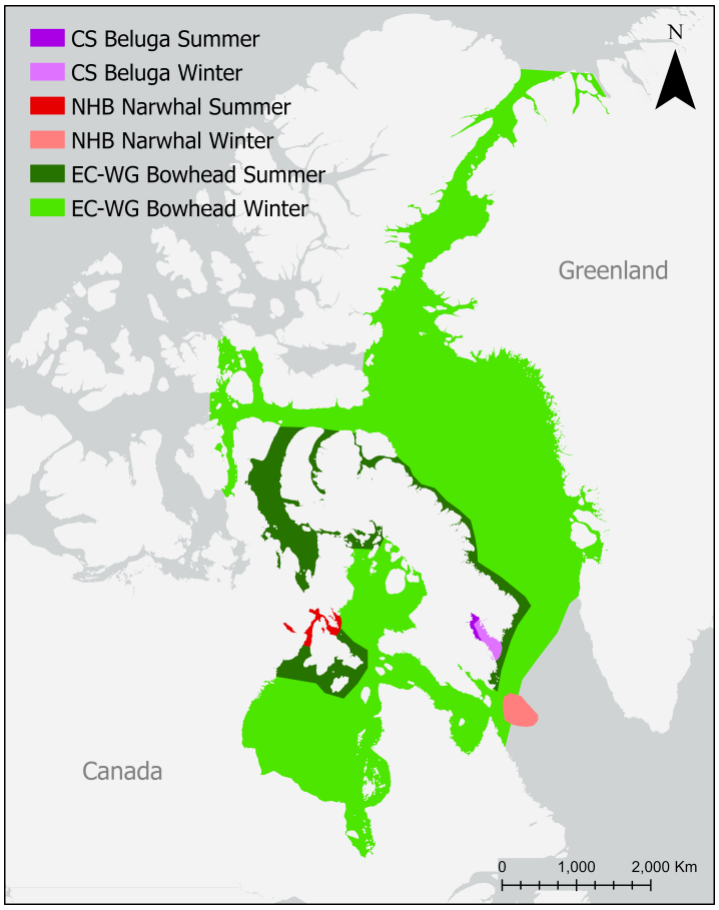

Figure 1.1 Summer and winter range map for Cumberland Sound (CS) beluga, Northern Hudson Bay (NHB) narwhal, Eastern Canada-West Greenland (EC-WG) bowhead whales.

1.1 References

Asselin NC, Ferguson SH, Richard PR, Barber DG (2012) Results of narwhal (*Monodon monoceros*) aerial surveys in northern Hudson Bay, August 2011. DFO Can Sci Advis Sec Res Doc 2012/037:iii + 23 p.

Begon M, Harper JL, Townsend CR (1986) Ecology. Individuals, populations and communities. Blackwell Science, Oxford.

Bluhm BA, Gradinger R (2008) Regional variability in food availability for arctic marine mammals. Ecol Appl 18:S77-S96.

Buckland ST, Anderson DR, Burnham KP, Laake JL, Borchers DL, Thomas L (2001) Introduction to distance sampling: estimating abundance of biological populations. Oxford University Press, Oxford.

Burek KA, Gulland FM, O'Hara TM (2008) Effects of climate change on Arctic marine mammal health. Ecol Appl 18:S126-S134.

Chiba S (1998) A mathematical model for long-term patterns of evolution: Effects of environmental stability and instability on macroevolutionary patterns and mass extinctions. Paleobiology 24:336-348.

COSEWIC (2004) COSEWIC assessment and update status report on the narwhal Monodon monoceros in Canada. Committee on the Status of Endangered Wildlife in Canada Ottawa vii + 50 pp.

COSEWIC (2009) COSEWIC assessment and update status report on the Bowhead Whale Balaena mysticetus, Bering–Chukchi–Beaufort population and Eastern Canada–West Greenland population,in Canada. Committee on the Status of Endangered Wildlife in Canada Ottawa:vii + 49 pp.

COSEWIC (2020) COSEWIC assessment and status report on the Beluga Whale Delphinapterus leucas, Eastern High Arctic - Baffin Bay population, Cumberland Sound population, Ungava Bay population, Western Hudson Bay population, Eastern Hudson Bay population and James Bay population in Canada. Committee on the Status of Endangered Wildlife in Canada Ottawa xxxv + 84 pp.

Darnis G, Robert D, Pomerleau C, Link H, Archambault P, Nelson RJ, Geoffroy M, Tremblay JE, Lovejoy C, Ferguson SH, Hunt BPV, Fortier L (2012) Current state and trends in Canadian Arctic marine ecosystems: II. Heterotrophic food web, pelagic-benthic coupling, and biodiversity. Clim Change 115:179-205.

Ferguson SH, Higdon JW, Hall PA, Hansen RG, Doniol-Valcroze T (2021) Developing a Precautionary Management Approach for the Eastern Canada-West Greenland Population of Bowhead Whales (*Balaena mysticetus*). Front Mar Sci 8:2021.

Fitzgerald LA (2015) The Interplay Between Life History and Environmental Stochasticity: Implications for the Management of Exploited Lizard Populations. Am Zool 34:371-381.

Frasier TR, Petersen SD, Postma L, Johnson L, Heide-Jørgensen MP, Ferguson SH (2020) Abundance estimation from genetic mark-recapture data when not all sites are sampled: An example with the bowhead whale. Global Ecol Conserv 22:e00903.

Hammill MO, Stenson GB, Doniol-Valcroze T (2017) A management framework for Nunavik beluga. DFO Can Sci Advis Sec Res Doc 2017/060:v + 34 p.

Hammill MO, Stenson GB, Mosnier A, Doniol-Valcroz T (2021) Trends in Abundance of Harp Seals, *Pagophilus Groenlandicus*, in the Northwest Atlantic, 1952-2019. DFO Can Sci Advis Sec Res Doc 2021/006. iv + 30 p.

Hammond PS (2009) Mark–Recapture. In: Perrin WF, Würsig B, Thewissen JGM (ed) Encyclopedia of Marine Mammals (Second Edition). Academic Press, London

Harwood J (2001) Marine mammals and their environment in the twenty-first century. J Mammology 82:630-640.

Heide-Jørgensen M, Laidre K, Wiig Ø, Jensen M, Dueck L, Maiers L, Schmidt H, Hobbs R (2003) From Greenland to Canada in ten days: Tracks of bowhead whales, *Balaena mysticetus*, across Baffin Bay. Arctic 56:21-31.

Heide-Jørgensen M, Richard P, Dietz R, Laidre K (2013) A metapopulation model for Canadian and West Greenland narwhals. Anim Conserv 16:331-343.

Heppell SS, Caswell H, Crowder LB (2000) life histories and elasticity patterns: Perturbation analysis for species with minimal demographic data. Ecology 81:654-665.

Higdon JW (2010) Commercial and subsistence harvests of bowhead whales (*Balaena mysticetus*) in eastern Canada and West Greenland. J Cetacean Res Manag 11:185-216.

Hilborn R, Amoroso RO, Anderson CM, Baum JK, Branch TA, Costello C, De Moor CL, Faraj A, Hively D, Jensen OP, Kurota H, Little LR, Mace P, McClanahan T, Melnychuk MC, Minto C, Osio GC, Parma AM, Pons M, Segurado S, Szuwalski CS, Wilson JR, Ye Y (2020) Effective fisheries management instrumental in improving fish stock status. PNAS 117:2218-2224.

Hovelsrud GK, McKenna M, Huntington HP (2008) Marine mammal harvests and other interactions with humans. Ecol Appl 18:S135-S147.

Huntington HP (2009) A preliminary assessment of threats to arctic marine mammals and their conservation in the coming decades. Mar Policy 33:77-82.

Innes S, Heide-Jørgensen M, Laake JL, Laidre KL, Cleator HJ, Richard P, Stewart RE (2002) Surveys of belugas and narwhals in the Canadian high Arctic in 1996. NAMMCO Sci Pub 4:169-190.

Kareiva P (1990) Population dynamics in spatially complex environments: theory and data. Phil Trans R Soc B 330:175-190.

Kemper JB (1980) History of use of narwhal and beluga by Inuit in the Canadian eastern Arctic including changes in hunting methods and regulations. Rep Intern Whaling Comm 30:481-490.

Kingsley MCS, Asselin NC, Ferguson SH (2013) Updated stock-dynamic model for the Northern Hudson Bay narwhal population based on 1982-2011 aerial surveys. DFO Can Sci Advis Sec Res Doc 2013/011:v + 19 p.

Kovacs KM, Lydersen C, Overland JE, Moore SE (2011) Impacts of changing sea-ice conditions on Arctic marine mammals. Mar Biodiv 41:181-194.

Laidre KL, Stern H, Kovacs KM, Lowry L, Moore SE, Regehr EV, Ferguson SH, Wiig Ø, Boveng P, Angliss RP (2015) Arctic marine mammal population status, sea ice habitat loss, and conservation recommendations for the 21st century. Conserv Biol 29:724-737.

Lande R, Engen S, Saether B-E (2003) Stochastic population dynamics in ecology and conservation. Oxford University Press, Oxford.

Lloyd DG (1987) Selection of offspring size at independence and other size-versus-number strategies. Am Nat 129:800-817.

Luque SP, Ferguson SH (2010) Age structure, growth, mortality, and density of belugas (*Delphinapterus leucas*) in the Canadian Arctic: responses to environment? Polar Biol 33:163-178.

MacArthur RH, Wilson EO (1967) The theory of island biogeography. Princeton University Press, Princeton.

Marcoux M, Hammill MO (2016) Model estimates of Cumberland Sound beluga (*Delphinapterus leucas*) population size and total allowable removals. In, DFO Can. Sci. Advis. Sec. Res. Doc. 2016/077.

Maunder MN, Piner KR (2014) Contemporary fisheries stock assessment: many issues still remain. ICES 72:7-18.

McMeans BC, Rooney N, Arts MT, Fisk AT (2013) Food web structure of a coastal Arctic marine ecosystem and implications for stability. MEPS 482:17-28.

McPeek MA, Peckarsky BL (1998) life histories and the strengths of species interactions: Combining mortality, growth, and fecundity effects. Ecology 79:867-879.

Melnikov A (1997) Arctic Sea Ice Ecosystem. CRC Press, Florida.

Nuttall M, Berkes F, Forbes B, Kofinas G, Vlassova T, Wenzel G (2005) Hunting, herding, fishing and gathering: indigenous peoples and renewable resource use in the Arctic. In Symon C, Arris L, Heal B (ed), Arctic climate impact assessment scientific report (pp. 649-690). Cambridge University Press, Cambridge.

Pella JJ, Tomlinson PK (1969) A generalized stock production model. Inter-American Tropical Tuna Commission Bulletin 13:416-497.

Peters TM, Barbosa P (1977) Influence of Population Density on Size, Fecundity, and Developmental Rate of Insects in Culture. Annu Rev Entomol 22:431-450.

Pianka ER (1970) On r- and K-Selection. Am Nat 104:592-597.

Rekdal SL, Hansen RG, Borchers D, Bachmann L, Laidre KL, Wiig Ø, Nielsen NH, Fossette S, Tervo O, Heide-Jørgensen MP (2015) Trends in bowhead whales in West Greenland: Aerial surveys vs. genetic capture-recapture analyses. Mar Mamm Sci 31:133-154.

Richard P, Laake J, Hobbs R, Heide-Jørgensen M, Asselin N, Cleator H (2010) Baffin Bay narwhal population distribution and numbers: aerial surveys in the Canadian High Arctic, 2002-04. Arctic 63:85-99.

Richard P, Stewart DB (2008) Information relevant to the identification of critical habitat for Cumberland Sound belugas (*Delphinapterus leucas*). DFO Can Sci Advis Secr Res Doc 2008/085:iv + 24 p.

Richard PR (1991) Abundance and distribution of narwhals (*Monodon monoceros*) in northern Hudson Bay. Can J Fish Aquat Sci 48:276-283.

Richard PR (2010) Stock definition of belugas and narwhals in Nunavut. DFO Can Sci Advis Sec Res Doc 2010/022:iv + 14 p.

Snell TW (1978) Fecundity, developmental time, and population growth rate. Oecologia 32:119-125.

Stewart DB (2008) Commercial and subsistence harvests of narwhals (*Monodon monoceros*) from the Canadian eastern Arctic. Arctic Biological Consultants, Winnipeg, MB for Canada Department of Fisheries and Oceans, Winnipeg, MB:ii + 97 p.

Stewart DB (2018) Commercial and subsistence catches of beluga whales (*Delphinapterus leucas*) from Cumberland Sound, Nunavut, 1840-2016. Can. Tech. Rep. Fish. Aquat. Sci. 3250: viii + 89 p.

Tyrrell M (2007) Sentient beings and wildlife resources: Inuit, beluga whales and management regimes in the Canadian Arctic. Human Ecol 35:575-586.

Wade PR (2018) Population dynamics. In: Würsig B, Thewissen JGM, Kovacs KM (ed) Encyclopedia of Marine Mammals (Third Edition). Academic Press, Cambridge.

Wade PR, Reeves RR, Mesnick SL (2012) Social and behavioural factors in cetacean responses to overexploitation: are odontocetes less “resilient” than mysticetes? J Mar Biol 2012

Wassmann P, Duarte CM, Agusti S, Sejr MK (2011) Footprints of climate change in the Arctic marine ecosystem. Glob Chang Biol 17:1235-1249.

Watt C, Marcoux M, Ferguson SH, Hammill M, Matthews C (2020) Population dynamics of the threatened Cumberland Sound beluga (*Delphinapterus leucas*) population. Arctic Sci 7 :545-566.

Chapter 2

2 Modelling population trajectory and probability of decline in Northern Hudson Bay narwhal

Brooke A. Biddlecombe[1,2] Cortney A. Watt[1,2]

[1]Freshwater Institute

Fisheries and Oceans Canada

Winnipeg, Manitoba, Canada

[2]Department of Biological Sciences

University of Manitoba

Winnipeg, Manitoba, Canada

Citation:

Biddlecombe BA, Watt CA (2022) Modeling population trajectory and probability of decline in northern Hudson Bay narwhals (*Monodon monoceros*). Marine Mammal Science 38:1357-1370

Abstract

Narwhals (*Monodon monoceros*) are an important subsistence harvest species for Inuit communities and their conservation is important for Inuit culture and ecosystem function. The Northern Hudson Bay (NHB) narwhal population, which spends summer in northern Hudson Bay, Canada, has been assessed through periodic aerial surveys from 1981-2018. To estimate the population trajectory and predict future population trends under various harvest scenarios, a Bayesian population model was fit to four aerial survey estimates and harvest data from 1951 – 2018. The model resulted in a 2019 population estimate of ~14,400 (95% CI 10,300-20,400), and an estimated starting population of 7,200 (95% CI 1,400-19,000) in 1951. The model was extended 10 years into the future under three annual harvest scenarios (current harvest: 157, low harvest: 50, and high harvest: 300) and the probability of population decline was estimated. The model predicted a 6% chance of decline with an annual harvest quota of 50 narwhal, 78% for a harvest of 157, and 95% for a harvest of 300. This updated model provides the opportunity to shape conservation efforts by estimating past population trends and how those trends, combined with management action, can affect future population dynamics.

2.1 Introduction

Many Arctic marine mammal species have a long history of subsistence harvest in northern Canada, which plays an important role in conservation and management actions (Hovelsrud et al. 2008, Wenzel 2009). Narwhal (*Monodon monoceros*) were not a common target for historical whaling (Stewart 2008), but have been and continue to be a culturally important species for Inuit communities (Heide-Jørgensen et al. 2013, Nuttall et al. 2005, Richard & Pike 1993). In the 1980's, Canada established a hunting quota of 207 narwhal in Baffin Bay and 50 in Hudson Bay as a result of concerns about the ivory tusk market (Kemper 1980). Lack of data has led to uncertainty in determining true population abundance and the effectiveness of the narwhal hunting quotas that were implemented (Innes et al. 2002, Richard et al. 2010). Alongside pressure from harvest, marine mammal populations face multiple other stressors such as habitat loss from climate change, and increased habitat disturbance as a result of oil and gas activity (Hovelsrud et al. 2008, Huntington 2009). It is important to continually monitor marine mammal populations for informed conservation action, especially as climate change continues to rapidly alter Arctic ecosystems and contribute to stressors that are projected to impact the growth and survival of these populations (Cohen et al. 2014, Wassmann et al. 2011).

Narwhals are Arctic residents, remaining in Arctic or sub-Arctic waters year-round (Kovacs et al. 2011, Laidre et al. 2015). Narwhals are predicted to be sensitive to climate change due to their direct ecological associations with sea ice (Laidre et al. 2008). There are three recognized narwhal populations, Northern Hudson Bay (NHB), Baffin Bay, and Eastern Greenland (Petersen et al. 2011). NHB narwhal summer in northern Hudson Bay and migrate through Hudson Strait to spend winters in southern Davis Strait (Richard 1991, Westdal et al.

2010) (Figure 2.1). NHB narwhal are spatially and genetically distinct from other narwhal populations in Canada and Greenland (Petersen et al. 2011).

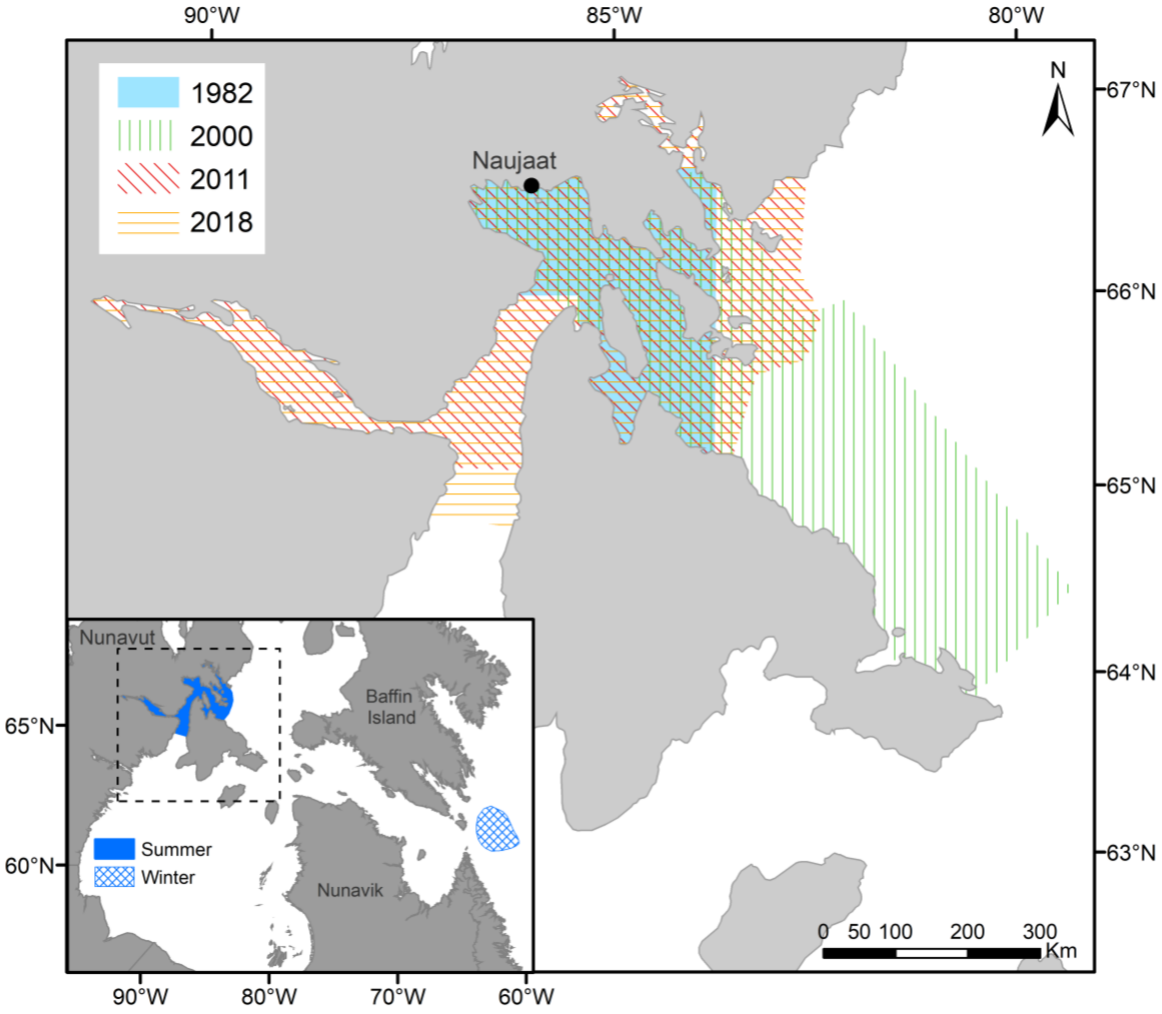

Figure 2.1 Map indicating the coverage of NHB narwhal aerial surveys included in our population model. 1982: solid; 2000: vertical; 2011: diagonal; 2018: horizontal. Inset: Map indicating the summering (solid) and wintering (hatched) ranges for the Northern Hudson Bay narwhal population with aerial survey coverage highlighted with a dashed outline.

Subsistence harvest of NHB narwhal occurs primarily near the community of Naujaat (formerly Repulse Bay), Nunavut, Canada. Non-commercial harvests of narwhal had sparse

records until the creation of a harvest quota in 1977 (Stewart 2008). NHB narwhal have a minimal commercial harvest history, as bowhead whales (*Balaena mysticetus*) were the focus of commercial whaling in this region (Stewart 2008). To promote long term conservation, surveys and resulting population estimates need to be consistently updated to aid management objectives. The NHB narwhal population is co-managed by the Canadian government and resource users, which are the Inuit communities that harvest from this population. Aerial surveys during the summer months are used to estimate narwhal abundance, as narwhal typically show long-term site fidelity to summering regions (Heide-Jørgensen et al. 2003, Richard 1991, Westdal et al. 2010). Surveys of the NHB population were flown in each year from 1981-1984, and again in 2000, 2011, and 2018 (Asselin et al. 2012, Bourassa 2003, Richard 1991, Watt et al. 2020a). To evaluate population trends, these survey estimates can be used within a modelling framework.

Aquatic populations of fish and marine mammals are often analyzed using stock production models, which estimate changes in abundance and the effect of harvest on population trajectories and are useful in monitoring (Hilborn et al. 2020, Maunder & Punt 2013). These models utilize harvest history, alongside other available demographic data which can include age structure, fecundity, mortality, and growth rate (Hilborn et al. 2020, Pella & Tomlinson 1969). It is not uncommon for commercial fisheries to have limited amounts of data and few specific population details, but stock production models are valuable because they can be created using the minimal information available (Maunder & Piner 2014). Detailed demographic data are often not available for marine mammal populations; thus, their stock production models tend to rely on population estimates from aerial surveys and harvest records (Hilborn et al. 2020, Maunder & Piner 2014). Stock production models can detect historical trends in population trajectories, and can be further applied to predict the probability of future population change under various

harvest or environmental scenarios (Duplisea et al. 2021, Watt et al. 2020b). When the probabilities of population decline under various harvest scenarios are considered in a management framework, this prediction method is referred to as a risk-based approach. The model can estimate the probability of population decline from the estimated current abundance to a defined time in the future at various harvest rates, which allows managers and resource users to select and implement harvest rates at a risk level they deem appropriate. This management approach has been used increasingly in marine mammal management in Canada in recent years for species such as beluga (*Delphinapterus leucas*) and narwhal (Kingsley et al. 2013, Marcoux & Hammill 2016, Watt et al. 2020b).

The NHB narwhal population abundance has been modelled using a stock-production model previously by Kingsley et al. (2013). However, Kingsley et al.'s (2013) model estimates had a high degree of associated uncertainty due to discrepancies in the methodologies for the surveys included in the model. The model compared survey methods, most notably the 2011 survey estimate which was analyzed using updated line-transect methods and reanalyzed as a multi-strip survey to match 1982 and 2000 survey methods. The reanalyzed estimate created a better model fit with previous estimates, but it likely underestimated true abundance, and neither analysis method could be decisively considered equivalent to the 1982 and 2000 methods. The model used a risk-based approach to predict the effect of various harvest levels on future population as described above. Due to the uncertain nature of the model estimates from these analyses the results from the risk-based analysis were not implemented for management until future surveys were performed.

The objective of this study is to use harvest data and corrected abundance observations to model the population trends of NHB narwhal and predict future trajectories under the current

harvest level of 157 narwhals per year, and high (300) and low (50) harvest scenarios. This model is important because the conservation and co-management of NHB narwhal requires an updated model to understand this population's past trends, due to the lack of certainty in previous models. Further, it is important to consistently monitor this population to actively consider how it is changing over time, what factors might be affecting populations dynamics, and for conservation of this population of narwhals.

2.2 Methods

2.2.1 Survey abundance observations and adjustments

The methodology of the 1980's surveys varied between reconnaissance, random, or systematic (i.e., stratified or targeted) in design, and using visual observers or photographic count methods. All later surveys used systematic visual observation methods. Thus, of the early surveys, only the estimate from 1982 is appropriate for use in population modeling because it was the only systematic visual survey during that time (Asselin and Ferguson 2013). Current surveys typically account for perception bias, which is the result of observers missing animals that are in the area of detection (Fuentes et al. 2015). Despite being systematic in design, the 1982 survey did not account for perception bias and was analyzed as a strip transect, which assumed that all narwhals within a 600 m strip width were observed. However, detectability declines with increasing distance from the aircraft (Buckland et al. 2001) and, therefore, this estimate is negatively biased. The survey conducted in 2000 used distance sampling analysis but did not account for perception bias, which is the result of a comparing animal detection between multiple observers, again resulting in negative bias. The 2011 survey was analyzed using mark-

recapture distance analysis, which considers the numbers of whales seen by observers in the front of the aircraft and the rear and, therefore, incorporated perception bias (Burt et al. 2014).

To make the 1982, 2000, and 2011 surveys comparable, Asselin & Ferguson (2013) re-analyzed the 2011 survey using the methods of the two older surveys. The re-analyses resulted in two new 2011 abundance estimates, one following methods used for 1982 strip transect sampling data and the other following methods used for 2000 conventional distance sampling data. In this way a ratio was calculated by which the 1982 and 2000 surveys could be adjusted to approximately equate them to the methods used in 2011. The ratio used to adjust the 1982 survey was 2.56, and the 2000 survey ratio was 2.29 (Asselin & Ferguson 2013). The standard errors (SE) for the adjusted surveys were also increased to include the uncertainty around the correction ratios. The post hoc corrections for the early NHB narwhal surveys and a new aerial survey completed in the summer of 2018 (Watt et al. 2020a) allows for the creation of an updated, potentially more accurate population model which can better support long-term conservation goals for this population.

2.2.2 Model specification

A stochastic stock production model with density dependence acting on the population growth rate was fitted with hierarchical Bayesian inference and parameter posteriors were sampled with a Markov Chain Monte Carlo (MCMC) method following Doniol-Valcroze et al. (2013) and Marcoux & Hammill (2016) with some updating (in previous formulations the process error was always additive to the abundance and therefore did not allow a negative impact of natural variation on the abundance estimation). This model utilizes aerial survey and harvest data to estimate population dynamics. To separate two stochastic processes, observation process

and state process, a hierarchical state-space model was used. Observation process describes observation error, which results from data collection. State process describes process error, which reflects natural variability in population dynamics (de Valpine & Hastings 2002).

The observation process links observed data to true population size. We determined survey error by using a multiplicative error (τ_t) term to link true population size (N_t) to aerial survey abundance observations (S_t). The observation model is log-normal, where the logarithm of the median population estimate (N_t) is applied to the Pella and Tomlinson model described below.

$$\ln(S_t) = \ln(N_t) + \tau_t$$

The state process was defined using a discrete formulation of the Pella and Tomlinson model (Innes & Stewart 2002, Pella & Tomlinson 1969), which describes the change in true population size over time. The population size at time *t* is a multiple of the previous year's population with harvest removals deducted.

$$N_t = N_{t-1} * \left(1 + (\mathrm{R}_{max}) * \left(1 - \left(\frac{N_{t-1}}{K}\right)^{\theta}\right)\right) * \varepsilon_t - R_t$$

Where: R_{max} is the maximum growth rate or rate of population increase,

K is the environmental carrying capacity,

θ defines the shape of the density-dependent function (theta) which determines how abruptly growth declines with increasing abundance,

ε_t is a stochastic term for the process error estimated annually,

R_t are the harvest removals for that year, calculated as reported catches, C_t , that are corrected for the proportion of animals that were struck and lost, $S\&L$:

$$R_t = C_t \cdot (1 + S\&L)$$

A model of this type has the potential to include age or sex structure, but our model does not, as that information is not available for this population. A male focused harvest may mitigate some of the impact of harvest (Taylor et al. 1987) on this population, but we are unable to include that dynamic at this time. We were also not able to increase the intricacy of our model by incorporating fecundity or mortality data, as there is not reliable data available for this population aside from harvest and aerial survey data.

The model was fit using harvest data from 1951 – 2018 (Appendix 1) and aerial survey data from 1982, 2000, 2011, and 2018 (Table 2.1) to estimate population dynamics for 1951 – 2018. Harvest data were available starting in 1911, but these data were too temporally sparse before 1951 to be included in the model (Stewart 2008). Surveys from 1980 and 2000 were adjusted to account for differences in survey design and analysis, and to incorporate an adjustment for perception bias, by multiplying them by 2.29 and 2.56, respectively (Asselin & Ferguson 2013) (Table 2.1). The 2011 and 2018 abundance observations had been previously adjusted for perception bias. All abundance observations were adjusted to account for animals that were diving and not visible during the survey (availability bias). Traditional knowledge was incorporated into aerial survey design by guiding the location of surveys and extent of coverage.

Table 2.1 Estimates of Northern Hudson Bay narwhal abundance from aerial surveys in their summering range. Total estimates are the values calculated from the surface estimates using an availability bias adjustment factor (C_a) of 2.8, and the coefficient of variation (CV) of the total estimate. Fully adjusted estimates have been adjusted for both perception and availability bias. CDS = conventional distance sampling, MRDS = mark-recapture distance sampling.
* denotes survey data that were used in the population dynamics model.

Survey Year	Total Estimate	CV	Observation Method	Analysis Method	Adjustment Ratio	Fully Adjusted Estimate	Citation
1981	n/a	n/a	Reconnaissance visual				Richard 1991
*1982	2,906	0.52	Systematic visual	600 m Strip	2.56	7,440	Richard 1991, Asselin and Ferguson 2013
1983	4,248	0.36	Systematic photographic				Richard 1991
1984	3,794	0.31	Systematic photographic				Richard 1991
*2000	4,978	0.40	Systematic visual	CDS	2.29	11,401	Bourassa 2003 (CV in Richard 2008), Asselin and Ferguson 2013
*2011	12,485	0.26	Systematic visual	MRDS	1.00	12,485	Asselin et al. 2012
*2018	19,232	0.28	Systematic visual	MRDS	1.00	19,232	Watt et al. 2020a

2.2.3 Priors

Prior distributions for the random variables included in the model were informed by previous cetacean population models (i.e., Marcoux & Hammill 2016, Wade 1998), and existing knowledge of narwhal/cetacean ecology. Maximum population growth rate (R_{max}) for cetaceans is often assumed to be 0.04 (Wade 1998), therefore we fixed R_{max} at 0.04 for some initial model

runs, but allowed the final model to estimate R_{max} using a uniform distribution ranging from 0.01 – 0.07 (Table 2.2). The shape parameter θ (theta) typically ranges from 1 to 7 in marine mammal populations (Taylor & Demaster 1993), which means as theta increases from 1 growth rate more abruptly declines with increasing abundance and maximum productivity occurs at a higher proportion of carrying capacity. After comparison with linear density dependence where theta =1 (details below), theta in our final model was allowed to vary between one and five (Table 2.2). Starting population size was assigned a uniform prior distribution from 1,000 to 20,000 (Table 2.2). Carrying capacity (K) was assigned a uniform distribution with a minimum of 10,000 and a maximum of 30,000 (Table 2.2).

Table 2.2 Prior distributions, parameters, and hyper-parameters used in the population model. "dist." denotes a hyper-parameter with its own prior distribution.

Parameters	Notation	Prior distribution	Hyper-parameters	Values
Survey error (t)	τ_t	*Log-normal*	μ_τ	0
			τ_τ	*dist.*
Precision (survey)	τ_τ	*		
Process error (t)	ε_t	*Log-normal*	μ_ε	0
			τ_ε	*dist.*
Precision (process)	τ_ε	*Gamma*	α_ε	1.5
			β_ε	0.00001
Density dependence	θ	*Uniform*	N_{upp}	5
shape function			N_{low}	1
Struck-and-lost	*S&L*	-	-	0.25
Initial population	N_{1951}	*Uniform*	N_{upp}	20,000
			N_{low}	1,000
Carrying capacity	*K*	*Uniform*	N_{upp}	30,000
			N_{low}	10,000
Max. growth rate	R_{max}	*Uniform*	N_{upp}	0.07
			N_{low}	0.01

** weighted by the standard error from each survey*

Harvest data underestimate the true number of narwhal removals because some animals are wounded or killed but cannot be recovered by hunters and are therefore referred to as struck and lost (S&L). Naujaat is the primary harvest community for NHB narwhal, thus, we informed S&L using the loss rate correction values for Naujaat in 1999-2005, calculated using reports from the community (Richard 2008). Mean loss rate correction in Naujaat was 0.25, and because our model does not have sufficient data to inform an updated estimate, S&L was set at 0.25.

The stochastic process error term had a log-normal distribution with a location parameter of zero. The precision parameter for process error was assigned an informative gamma(1.5, 0.00001) distribution. Gamma distributions are typical for random error precision hyperparameters, and the resulting process error term had quartiles of 0.998 and 1.002. The narrow stochastic process range reflects the assumption that because narwhals are a long-lived species, their stock dynamics have low inter-annual variability (Le Coeur et al. 2021, Morris et al. 2008). Wider process error ranges were considered but resulted in issues with model fit and lack of stochasticity in resulting process error estimates.

Uncertainty associated with aerial surveys was incorporated into model fitting by informing the prior distribution for the survey error precision parameter. The survey error term was given a lognormal distribution with a location parameter of zero. The precision parameter for survey error was specific to each survey year using a precision value calculated from each standard error (SE) independently.

2.2.4 Parameter Estimation and Model Diagnostics

A Gibbs sampler algorithm implemented in JAGS (Plummer 2003) was used to obtain posterior estimates for the parameters included in the model. Results were examined in RStudio (R Core Team, 2020; *version 1.2.5033*) using packages *R2jags* (Su & Yajima 2015; *version 0.6-1*) and *coda* (Plummer et al. 2006; *version 0.19-3*). We used a MCMC simulation method which required us to check the convergence of sample values in each parameter to a stationary distribution. Model convergence, mixing, and autocorrelation within parameters were investigated in initial and final runs of the model code.

Geweke's Diagnostic was used to test similarity between different sections of the chains and Geweke plots were visually inspected to test for mixing within each chain (Geweke 1996). Convergence between chains was validated by comparing the width of the 80% credible interval of the chains pooled with the mean widths of the 80% credible interval for each of the chains individually using the Brooks-Gelman-Rubin (BGR) diagnostic test (Brooks & Gelman 1998).

Sensitivity of model results to our updated prior for survey error precision informed by the SE from surveys was evaluated by comparing resulting trajectories from our model to an edited model which used a gamma(2.5, 0.4) prior distribution. This gamma distribution was used for survey error precision in previous population models for beluga whales (Marcoux & Hammill 2016, Watt et al. 2020b). The posterior distribution for survey error using the gamma(2.5, 0,4) prior distribution for precision included the posterior survey error estimates with precision informed by survey SEs, which confirmed that the SE informed error priors are appropriate for use in the model. We also visually inspected whether the widths of credible intervals around the median in survey years reflected the SE from each survey.

The model was run with the uniform prior described above for θ and again with $\theta = 1$, to compare the effects of linear and non-linear density dependence. Initial model runs comparing the two aforementioned priors for θ used three chains and had the number of iterations corrected to equal 10,000 after a burn in of 6,000 and thinning value of 30. We assessed outputs from initial runs by visually inspecting diagnostics for model validation, combined with consideration of biological relevance, to determine the preferred model (Table 2.2). The preferred model was run using five chains, and 100,000 iterations after a burn in of 60,000, with thinning maintained at 30.

2.2.5 Future Projections and Harvest Scenarios

To predict stock trajectory and sustainable yield of this population, the model was extended 10 years into the future under three annual harvest scenarios: 157 (the current harvest quota), 50 (a low harvest option), and 300 (a high harvest option). A relatively short period of 10 years was used due to the frequency with which harvest quotas are re-assessed for marine mammals (ideally every 5 years). The impact of each harvest level was assessed by calculating the probability of population decline over 10 years. This is the risk-based approach for assessing harvest levels and is used for populations that are considered data rich in Canada (Hammill et al. 2017).

2.3 Results

Carrying capacity (K), population size in 2019 (N_{2019}), process error, and initial population size (N_{1951}) showed rapid convergence for all chains. Autocorrelation was low in all variables, and the BGR statistics were close to 1 for all variables, indicating convergence of each chain and each model (see Appendix 1). In early model considerations, multiple runs with varied priors were performed and the model was robust to changes in priors. The preferred model is presented here.

The model shows a gradual increase in population abundance over time, which is consistent with the corrected aerial abundance observations, while also showing a general decline in population growth rate. The model posterior distributions resulted in a median maximum growth rate (R_{max}) of 0.038, the median carrying capacity (K) was estimated as 16,800, and θ was estimated as 2.94. The median starting population in 1951 was estimated as

7,200 (95% CI 1,400-19,200), and N_{2019} was estimated as 14,400 (95% CI 10,300-20,400) (Figure 2.2).

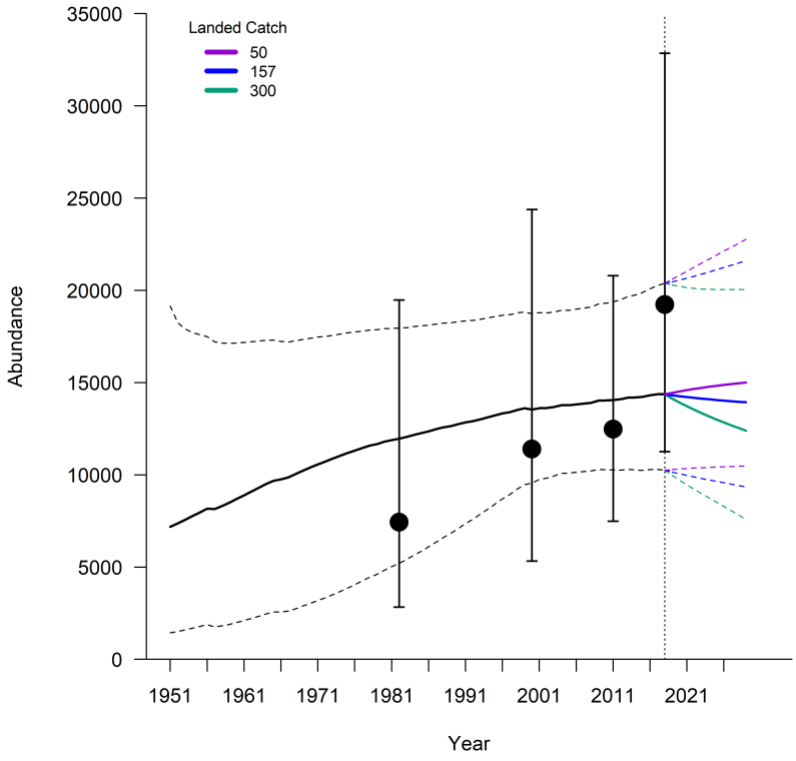

Figure 2.2 Model estimates of NHB narwhal abundance from the model fitted to adjusted aerial abundance observations from 1982, 2000, 2011, and 2018 (black dots ± 95% log-normal CI) and harvest data from 1951-2018, and future population projections under 3 different harvest scenarios. Solid line shows the median estimates and dashed lines show the 95% credible intervals. Vertical dotted line shows separation between the modelled abundance based on aerial abundance observations and the future projections.

For a risk-based approach to assessing harvest levels, the population trajectories for three harvest scenarios were plotted using the model results (Figure 2.2). These trajectories determined that after 10 years, the probability of population decline was 6% for an annual catch level of 50, 78% for a catch level of 157, and 95% for a catch level of 300 (Figure 2.3).

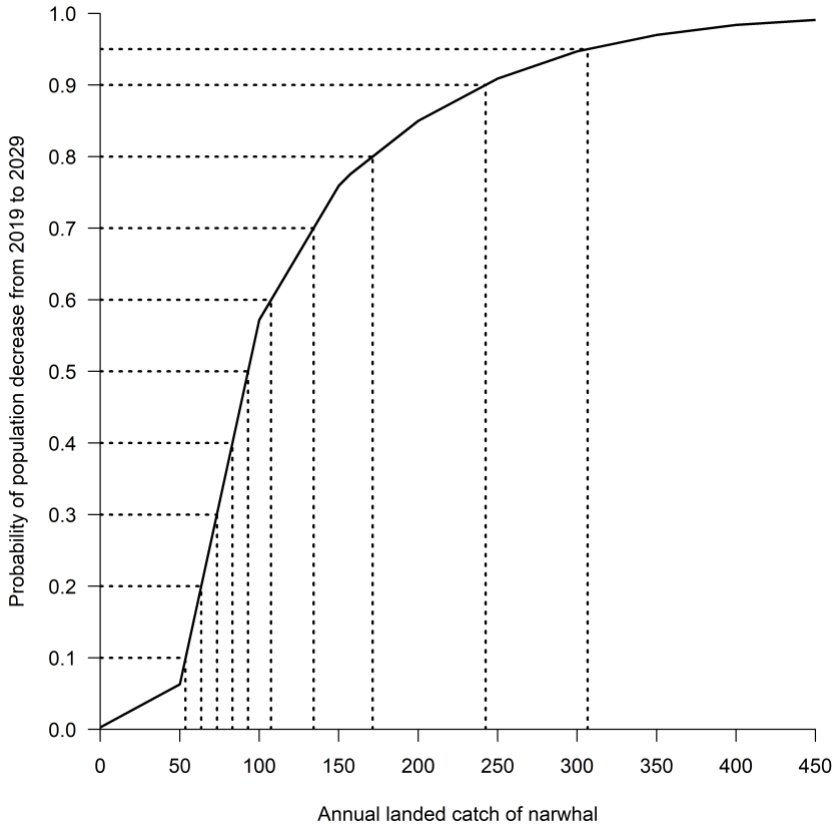

Figure 2.3 Probability of the NHB narwhal stock decreasing from the 2019 abundance estimate after 10 years of harvest, estimated by the model, as a function of the number of reported narwhals removed from the stock each year. Dotted lines show the corresponding probability of decline (y-axis) for various annual levels of harvest (x-axis).

2.4 Discussion

In this study, we used Bayesian methodology to fit a stochastic Pella-Tomlinson model (Innes & Stewart 2002, Pella & Tomlinson 1969) to narwhal aerial survey data (1982 – 2018) and a time series of catch history data (1951 – 2018). The model shows that the NHB narwhal population has increased over the entire time series from 1951-2018. There was a moderate increase in harvest levels in the early 2000's which appears to have slightly affected the population trajectory, although overall growth still occurred. The resulting model had a shaping parameter (θ) greater than one, reflecting a convex growth response (i.e., density feedback occurs at higher proportions of K), which means as the population size approaches carrying capacity the growth rate decreases closer to carrying capacity than when theta =1. Narwhal maximum population growth (R_{max}) can vary, depending on the vital rates of the population (Kingsley 1989). In our model, R_{max} was estimated as 0.038 which agrees with the commonly assumed R_{max} of 0.04 for cetaceans ($lambda_{max} = 1.04$) (Wade 1998). The aerial abundance observations fall within the 95% credible interval of the model's abundance estimates in corresponding aerial survey years. The largest discrepancy between model abundance estimate and aerial abundance observation is in 2018, this is the aerial survey with the largest SE, which translated to a larger observation error. Process error estimates showed random variation around 1, with no obvious trends over time, confirming stochasticity (see Appendix 1).

Using adjusted abundance observations allowed the model to re-create an ecologically plausible population trajectory for narwhals which shows a gradual increase over the time series. Allowing the model to estimate density dependence resulted in the population trajectory fitting the aerial abundance observations slightly better than when $\theta = 1$. Marine mammals, such as the bottlenose dolphin, an odontocete closely related to narwhal, commonly exhibit non-linear

density dependence, resulting in a θ that falls between 1 and 7 (Taylor & Demaster 1993) so the θ estimate of 2.94 is biologically plausible for narwhal as a long-lived species. The θ estimate translates to the population reaching maximum productivity at 63% of *K* with growth slowing down after that point. The 2019 population estimate of 14,400 is 86% of the estimated *K* of 16,800, which suggests that the population has reached a point of reduced growth, as is evident by the flattened curve in the latter years of the time series.

Our model assumes K is constant across the study period, although environmental changes would likely influence K over time. Narwhal are predicted to be sensitive to environmental changes caused by climate change, such as declining sea ice habitat and reduced prey availability (Laidre et al. 2008). These changes could reduce K as resources decline, which is not accounted for by our model, and thus the predicted effects of harvest may be biased. Reduced K in later years could mean that as the population increased the effects of positive density dependence may have been more influential, causing a greater reduction in growth rate. Reduced growth rate could then alter the effects of harvest, as the population may be less likely to recover from annual removals; however, management goals may also differ for a population that is close to carrying capacity and population growth may be less of a concern.

While the growth curve predicted by our model is plausible for narwhal ecology, the reason for a low initial population abundance in the 1950's, when there was little commercial whaling pressure on narwhal (Stewart 2008), is unclear. This lack of clarity is especially notable when our initial population estimate is compared to our estimated carrying capacity, which is higher by ~9,600 individuals. Narwhals have very little genetic diversity compared to other cetacean species and when considering overall population abundance estimates, narwhal have had a low female effective population size for at least 150,000 years (Louis et al. 2020). Their

genetic history could explain the constrained abundance of NHB narwhal at the start of our study period, and could continue to affect their population abundance into the future, alongside the effects of climate and anthropogenetic stressors (Hovelsrud et al. 2008, Huntington 2009). It is important to note the unexpected results at the beginning of the time series are also due, in part, to the lack of aerial surveys from the 1950s. Unfortunately, abundance observations are not available from this period to provide better model validation.

Adjustments to the aerial survey observation results from 1982 and 2000 were necessary for consistency across the time series. These surveys were adjusted post hoc, which is a potential source of error in this model. Adjustments for these earlier surveys reflect both perception bias and changes in the analytical methods used for later surveys (Asselin & Ferguson 2013). However, there is potential that the adjustments result in over- or under- estimates of the true population abundance. A further artifact of using past aerial survey abundance observations is that the latter two surveys (2011 and 2018) covered a larger area than the 1982 and 2000 surveys (Figure 2.1). The two earlier surveys may have a negative bias due to their lack of coverage in regions where narwhals were present in 2011 and 2018. We could not correct for this potential bias as the timeline for any distribution changes in NHB narwhal is unknown. The types of uncertainties described are not uncommon for models that utilize historical data.

Using the risk-based approach, the current quota of 157 reflects a 78% probability of population decline in 10 years. A 5% probability of decline is considered a low to very low risk of decline under Fisheries and Oceans Canada's Precautionary Approach (DFO 2009), and our model estimates this level of risk at a harvest level of 36. These probabilities reflect the effect of harvest with no consideration for sex; if male narwhals were targeted the effect of harvest on population dynamics would likely decrease. Compared to previous NHB narwhal population

models (Kingsley et al. 2013), there is more certainty associated with the model results from this study, indicated by reduced error around the mean, as a result of the addition of a more recent abundance observation and the incorporation of adjustments to earlier abundance observations. As a consequence of the updates applied to this model, there is more confidence in the current population estimate which can be used to assess harvest levels using population modelling with the risk-based approach.

Although our model is more well informed than the previous model, there are still shortcomings that make strict adherence to suggested harvest difficult without further data. Ultimately, the amount of reasonable risk of decline is up to managers, and decisions on harvest quotas will require consideration of surveys, model estimates, and future projections. Consistent monitoring of the NHB narwhal population will be necessary to track the effects of harvest decisions and alter quotas as managers deem necessary. Though it is important to address that due to logistic constraints surveys often do not take place as frequently as would be ideal for population modelling, so models such as ours can be useful in making use of data that is available while remaining cognizant of potential shortcomings.

Even with corrected aerial survey data and the inclusion of an updated aerial survey, our model presents some limitations and uncertainties. The posteriors for theta and R_{max} did not differ from the priors. Our prior for theta was not updated, so the resulting estimate was the median from a flat curve. We compared the model output where theta was estimated to a model with theta =1; although the two outputs did not drastically differ, we opted to allow the model to estimate theta due to the ecological relevance of positive density dependence in marine mammals (Taylor & DeMaster 1993). The posterior distribution for R_{max} was only slightly updated from the prior. The resulting estimate for R_{max} closely resembles the accepted maximum population

growth rate for cetaceans (Wade 1998) so although there was low confidence in the model estimate, it is ecologically plausible. Due to the lack of updated posteriors for these two parameters, we suggest the results not be used outside of the context of this model. Specific to our model, uncertainties surrounding posteriors can be justified, and overall our model was fit well with little cross correlation between parameters and no autocorrelation within parameters (see Appendix 1), and thus, our model still provides useful insight.

In summary, our model output estimated the past population trends of NHB narwhal and how, as this population approaches carrying capacity, the probability of decline is notable at the current harvest level; however, co-management groups should decide what level of risk is suitable. Population abundance and carrying capacity interplay to affect the predicted effects of future harvest, which supports the notion that this population should be monitored to ensure that previous management decisions are effective for conservation goals. Ideally aerial abundance observations to update models would be acquired every 5 years, but logistically that is not always possible. Due to the effect of non-linear density dependence and growth rate, response to harvest pressure will change depending on how close the population abundance is to the carrying capacity. For NHB narwhal, density dependence suggests that the growth rate will decline as the population approaches carrying capacity, as was estimated in recent years. The model in this study is a step towards the long-term monitoring required for conservation of NHB narwhal. NHB narwhal are identified as special concern, and as a species endemic to the Arctic and sensitive to habitat loss, their future as climate change progresses is uncertain. Population dynamics models can be used to inform conservation action and promote monitoring of all subsistence harvested marine mammal populations.

2.5 References

Asselin NC, Ferguson SH (2013) A re-analysis of northern Hudson Bay narwhal surveys conducted in 1982, 2000, and 2011. DFO Can. Sci. Advis. Sec. Res. Doc. 2013/019, iv + 9 p.

Asselin NC, Ferguson SH, Richard PR, Barber DG (2012) Results of narwhal (*Monodon monoceros*) aerial surveys in northern Hudson Bay, August 2011. DFO Can. Sci. Advis. Sec. Res. Doc. 2012/037, iii + 23 p.

Bourassa MN (2003) Inventaires de la population de narvals (*Monodon monoceros*) du nord de la baie d'Hudson et analyse des changements démographiques depuis 1983. M.Sc. thesis, Université du Québec à Rimouski, xii + 69 p.

Breed GA, Matthews CJ, Marcoux M, Higdon JW, LeBlanc B, Petersen SD, Orr J, Reinhart NR, Ferguson SH (2017) Sustained disruption of narwhal habitat use and behavior in the presence of Arctic killer whales. PNAS 114:2628-2633.

Brooks SP, Gelman A (1998) General methods for monitoring convergence of iterative simulations. J Computat Graphical Stat 7:434-455.

Burt ML, Borchers DL, Jenkins KJ, Marques TA (2014) Using mark–recapture distance sampling methods on line transect surveys. Methods Ecol Evol 5:1180-1191.

Cohen J, Screen JA, Furtado JC, Barlow M, Whittleston D, Coumou D, Francis J, Dethloff K, Entekhabi D, Overland J, Jones J (2014) Recent Arctic amplification and extreme mid-latitude weather. Nat Geosci 7:627-637.

de Valpine P, Hastings A (2002) Fitting population models incorporating process noise and observation error. Ecol Monogr 72:57-76.

DFO (2009) A fishery decision-making framework incorporating the precautionary approach. Government of Canada. https://www.dfo-mpo.gc.ca/reports-rapports/regs/sff-cpd/precaution-eng.htm.

Doniol-Valcroze T, Gosselin J-F, Hammill MO (2013) Population modeling and harvest advice under the precautionary approach for eastern Hudson Bay beluga (*Delphinapterus leucas*). DFO Can. Sci. Advis. Sec. Res. Doc. 2012/168, iii + 31 p.

Duplisea DE, Roux M-J, Hunter KL, Rice J (2021) Fish harvesting advice under climate change: A risk-equivalent empirical approach. PLOS ONE 16:e0239503.

Fuentes MMPB, Bell I, Hagihara R, Hamann M, Hazel J, Huth A, Seminoff JA, Sobtzick S, Marsh H (2015) Improving in-water estimates of marine turtle abundance by adjusting aerial survey counts for perception and availability biases. J Experim Mar Biol Ecol 471:77-83.

Geweke J (1996) Evaluating the accuracy of sampling-based approaches to the calculation of posterior moments. In: M Bernardo, JM Berger, AP Dawid, AFM Smith (Eds.), Bayesian Statistics 4 (pp. 169-193). Oxford University Press.

Hammill M, Stenson GB, Doniol-Valcroze T (2017) A management framework for Nunavik beluga. DFO Can. Sci. Advis. Sec. Res. Doc. 2017/060. v + 34p.

Heide-Jørgensen MP (2018) Narwhal: *Monodon monoceros*. Encyclopedia of Marine Mammals (pp. 627-631). Elsevier.

Heide-Jørgensen MP, Burt LM, Hansen RG, Nielsen NH, Rasmussen M, Fossette S, Stern H (2013) The significance of the North Water Polynya to Arctic top predators. Ambio 42:596-610.

Heide-Jørgensen MP, Dietz R, Laidre KL, Richard P, Orr J, Schmidt HC (2003) The migratory behaviour of narwhals (*Monodon monoceros*). Can J Zool 81:1298-1305.

Heide-Jørgensen MP, Richard P, Dietz R, Laidre K (2013) A metapopulation model for Canadian and West Greenland narwhals. An Conserv 16:331-343.

Hilborn R, Amoroso RO, Anderson CM, Baum JK, Branch TA, Costello C, De Moor CL, Faraj A, Hively D, Jensen OP, Kurota H, Little LR, Mace P, McClanahan T, Melnychuk MC, Minto C, Osio GC, Parma AM, Pons M, Segurado S, Szuwalski CS, Wilson JR, Ye Y (2020) Effective fisheries management instrumental in improving fish stock status. PNAS 117:2218-2224.

Hovelsrud GK, McKenna M, Huntington HP (2008) Marine mammal harvests and other interactions with humans. Ecol Appl 18:S135-S147.

Huntington HP (2009) A preliminary assessment of threats to Arctic marine mammals and their conservation in the coming decades. Mar Policy 33:77-82.

Innes S, Heide-Jørgensen M, Laake JL, Laidre KL, Cleator HJ, Richard P, Stewart RE (2002) Surveys of belugas and narwhals in the Canadian high Arctic in 1996. NAMMCO Sci Pub 4:169-190.

Innes S, Stewart RE (2002) Population size and yield of Baffin Bay beluga (*Delphinapterus leucas*) stocks. NAMMCO Sci Pub 4:225-238.

Kemper JB (1980) History of use of narwhal and beluga by Inuit in the Canadian eastern Arctic including changes in hunting methods and regulations. Rep Intern Whaling Comm 30:481-49.

Kingsley M (1989) Population dynamics of the narwhal *Monodon monoceros:* an initial assessement (Odontoceti: Monodontidae). J Zool 219:201-208.

Kingsley MCS, Asselin NC, Ferguson SH (2013) Updated stock-dynamic model for the Northern Hudson Bay narwhal population based on 1982-2011 aerial surveys. DFO Can. Sci. Advis. Sec. Res. Doc. 2013/011, v + 19 p.

Kovacs KM, Lydersen C, Overland JE, Moore SE (2011) Impacts of changing sea-ice conditions on Arctic marine mammals. Mar Biodiv 41:181-194.

Laidre KL, Stern H, Kovacs KM, Lowry L, Moore SE, Regehr EV, Ferguson SH, Wiig Ø, Boveng P, Angliss RP (2015) Arctic marine mammal population status, sea ice habitat loss, and conservation recommendations for the 21st century. Conserv Biol 29:724-737.

Laidre KL, Stirling I, Lowry LF, Wiig O, Heide-Jorgensen MP, Ferguson SH (2008) Quantifying the sensitivity of Arctic marine mammals to climate-induced habitat change. Ecol Appl 18:S97-S125.

Le Coeur C, Storkey J, Ramula S (2021) Population responses to observed climate variability across multiple organismal groups. Oikos 130:476-487.

Lefort KJ, Garroway CJ, Ferguson SH (2020) Killer whale abundance and predicted narwhal consumption in the Canadian Arctic. Glob Chang Biol 26:4276-4283.

Louis M, Skovrind M, Samaniego Castruita JA, Garilao C, Kaschner K, Gopalakrishnan S, Haile JS, Lydersen C, Kovacs KM, Garde E, Heide-Jørgensen MP, Postma L, Ferguson SH, Willerslev E, Lorenzen ED (2020) Influence of past climate change on phylogeography and demographic history of narwhals, *Monodon monoceros*. Proceed Royal Soc B 287:20192964.

Mansfield AW, Smith TG, Beck B (1975) The Narwhal, *Monodon monoceros*, in Eastern Canadian Waters. J Fish Res Board Can 32:1041-1046.

Marcoux M, Hammill MO (2016) Model estimates of Cumberland Sound beluga (*Delphinapterus leucas*) population size and total allowable removals. DFO Can. Sci. Advis. Sec. Res. Doc. 2016/077. pp. iv + 35 p.

Maunder MN, Piner KR (2014) Contemporary fisheries stock assessment: many issues still remain. ICES 72:7-18.

Maunder MN, Punt AE (2013) A review of integrated analysis in fisheries stock assessment. Fish Res 142:61-74.

Morris WF, Pfister CA, Tuljapurkar S, Haridas CV, Boggs CL, Boyce MS, Bruna EM, Church DR, Coulson T, Doak DF, Forsyth S, Gaillard J-M, Horvitz CC, Kalisz S, Kendall BE, Knight TM, Lee CT, Menges ES (2008) Longevity can buffer plant and animal populations against changing climatic variability. Ecology 89:19-25.

Nuttall M, Berkes F, Forbes B, Kofinas G, Vlassova T, Wenzel G (2005) Hunting, herding, fishing and gathering: Indigenous peoples and renewable resource use in the Arctic. In Symon C, Arris L, Heal B (Eds.), Arctic climate impact assessment scientific report (pp. 649-690). Cambridge University Press.

Pella JJ, Tomlinson PK (1969) A generalized stock production model. Inter-American Tropical Tuna Commission Bulletin 13:416-497.

Petersen SD, Tenkula D, Ferguson SH (2011) Population genetic structure of narwhal (*Monodon monoceros*). DFO Can. Sci. Advis. Sec. Res. Doc. 2011/021, vi + 20 p.

Plummer M (2003) JAGS: A program for analysis of Bayesian graphical models using Gibbs sampling. In: Proceedings of the 3rd International Workshop on Distributed Statistical Computing. Vienna, Austria.

Plummer M, Best N, Cowles K, Vines K (2006) CODA: Convergence diagnosis and output analysis for MCMC. R News 6:7-11.

R Core Team (2020) R: A language and environment for statistical computing. In R Foundation for Statistical Computing, Vienna, Austria.

Richard PR (1991) Abundance and distribution of narwhals (*Monodon monoceros*) in northern Hudson Bay. Can J Fish Aquat Sci 48:276-283.

Richard PR (2008) On determining the Total Allowable Catch for Nunavut odontocete stocks. DFO Can. Sci. Advis. Sec. Res. Doc. 2008/022, iv + 12 p.

Richard P, Laake J, Hobbs R, Heide-Jørgensen M, Asselin N, Cleator H (2010) Baffin Bay narwhal population distribution and numbers: aerial surveys in the Canadian High Arctic, 2002-04. Arctic 63:85-99.

Richard PR, Pike DG (1993) Small whale co-management in the Eastern Canadian Arctic: a case history and analysis. Arctic 46:138-143.

Stewart DB (2008) Commercial and subsistence harvests of narwhals (*Monodon monoceros*) from the Canadian eastern Arctic. Arctic Biological Consultants, Winnipeg, MB for Canada Department of Fisheries and Oceans, Winnipeg, MB, ii + 97 p.

Strong JT (1989) Reported harvests of narwhal, beluga and walrus in the Northwest Territories, 1948-1987. Canadian Data Report of Fisheries and Aquatic Sciences 734, iv + 14 p.

Su Y-S, Yajima M (2015) R2jags: Using R to Run 'JAGS'. R package version 0.5-7. Available: https://cran.r-project.org/web/packages/R2jags/.

Taylor BL, Demaster DP (1993) Implications of non-linear density dependence. Mar Mamm Sci 9:360-371.

Taylor MK, DeMaster DP, Bunnell FL, Schweinsburg RE (1987) Modeling the sustainable harvest of female polar bears. J Wildl Manage 51:811-820.

Wade PR (1998) Calculating limits to the allowable human-caused mortality of cetaceans and pinnipeds. Mar Mamm Sci 14:1-37.

Wassmann P, Duarte CM, Agusti S, Sejr MK (2011) Footprints of climate change in the Arctic marine ecosystem. Glob Chang Biol 17:1235-1249.

Watt CA, Hornby C, Hudson J (2020a) Narwhal (*Monodon monoceros*) abundance from the 2018 aerial survey of the Northern Hudson Bay population. DFO Can. Sci. Advis. Sec. Res. Doc. 2020/nnn., iv + p.

Watt CA, Ferguson SH (2015) Fatty acids and stable isotopes (δ13C and δ15N) reveal temporal changes in narwhal (*Monodon monoceros*) diet linked to migration patterns. Mar Mamm Sci 31:21-44.

Watt CA, Marcoux M, Ferguson SH, Hammill M, Matthews C (2020b) Population dynamics of the threatened Cumberland Sound beluga (*Delphinapterus leucas*) population. Arctic Sci 7:545-566.

Wenzel GW (2009) Canadian Inuit subsistence and ecological instability—if the climate changes, must the Inuit? Polar Res 28:89-99.

Westdal K, Richard P, Orr J (2010) Migration route and seasonal home range of the northern Hudson Bay narwhal (*Monodon monocero*s). In: Ferguson SH, Loseto LL, Mallory ML (Eds.), A little less arctic: top predators in the world's 71 largest northern inland sea, Hudson Bay (pp.71-92). Springer.

Chapter 3

3 Incorporating environmental covariates into a Bayesian stock production model for the endangered Cumberland Sound beluga population

Brooke A. Biddlecombe[1,2] and Cortney A. Watt[1,2]

[1]Freshwater Institute

Fisheries and Oceans Canada

501 University Crescent

Winnipeg, Manitoba, R3T 2N6

[2]Department of Biological Sciences

University of Manitoba

Winnipeg, Manitoba, R3T 2N2

Citation:

Biddlecombe BA, Watt CA (2022) Incorporating environmental covariates into a Bayesian stock production model for the endangered Cumberland Sound beluga population. Endangered Species Research 48:51-65

Abstract

The Cumberland Sound (CS) beluga (*Delphinapterus leucas*) population inhabits Cumberland Sound on eastern Baffin Island, Nunavut, Canada and is listed as Threatened under the Species at Risk Act. Population dynamics of CS beluga whales have been modelled in the past, but the effect of environmental covariates on these models has not previously been considered. An existing Bayesian population model fitted to CS beluga whale aerial survey data from 1990 – 2017 and harvest data from 1960 – 2017 was modified to include sea ice concentration (ICE) and sea surface temperature (SST). ICE and SST were extracted for all years from the Cumberland Sound study area in March and August, respectively, and incorporated into the state process component of the state space model. The model resulted in a 2018 population estimate of 1,245 (95% CI 564 – 2,715) whales, and an initial population (N_{1960}) estimate of 5,147 (95% CI 1,667 – 8,779). Determining sustainable harvest by calculating the probability of population decline estimated 30% probability of decline after 10 years with a harvest of ~15 whales annually. Compared to the previous model without environmental covariates, which followed a relatively linear trajectory, our model had more noticeable peaks and troughs in the population trend and wider credible intervals. The model suggested harvest levels be reduced by ~7 individuals for low risk of decline management goals. The novelty of this approach for beluga whales provides an opportunity for further model development via the addition of various other abiotic and biotic variables related to beluga whale ecology.

3.1 Introduction

Beluga whales (*Delphinapterus leucas*) are toothed whales with an extensive history of subsistence use by Inuit in the Arctic which continues today (Richard & Pike 1993, Wenzel 2009). Cumberland Sound (CS) beluga whales are a separate beluga stock that spend summers in northern CS, commonly aggregating in Clearwater Fiord, and the rest of the year in the main waters of CS (de March et al. 2002, de March et al. 2004, Richard & Stewart 2008, Turgeon et al. 2012) (Figure 3.1). The CS beluga population was significantly reduced by commercial whaling between 1868 and 1939 (Mitchell & Reeves 1981). CS beluga are the only beluga population listed as Threatened under the Species At Risk Act (SARA 2017), and are considered endangered by the Committee on the Status of Endangered Wildlife in Canada (COSEWIC 2004). This listing makes this a population of interest as harvest levels can have potentially severe impacts on the population trajectory due to the small current population size, estimated at ~1,400 individuals from an aerial survey in 2017 (Watt et al. 2020).

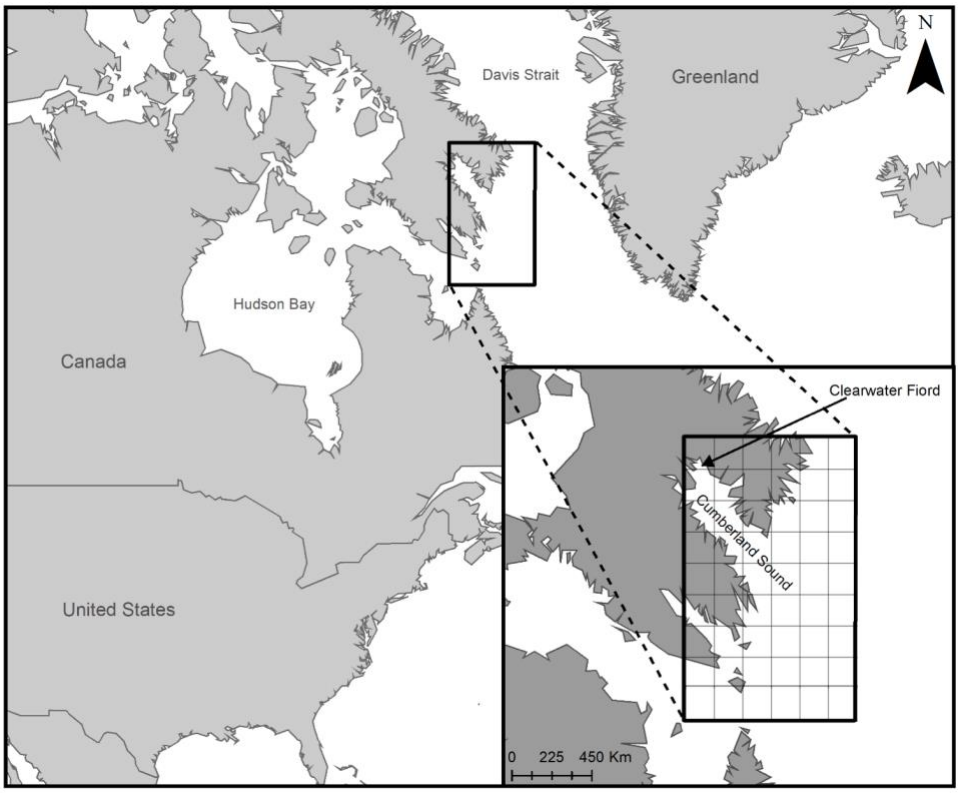

Figure 3.1 Delineation of Cumberland Sound study area used to clip raster files. Grid lines represent the size of pixels in environmental raster files.

Population assessments are an important aspect of species population management because they allow population changes to be monitored over time, providing the opportunity to mitigate those changes if necessary. Stock production models are a common way of assessing fisheries abundance (Pella & Tomlinson 1969, Horbowy 1996, Marcoux & Hammill 2016, Hilborn et al. 2020). A stock production model analyzes various types of demographic information from a population to determine changes in abundance from harvest and project future abundance (Maunder & Punt 2013). Stock assessment models are used for monitoring aquatic populations because even if data is lacking, models can still be created using available

information such as catch history, which often has well-kept records (Maunder & Piner 2014, Best & Punt 2020).

Marine mammal population assessments began utilizing techniques from fisheries stock production models in the 1960's, because previous management methods were resulting in rapid declines of many cetacean populations (Wade 2018). Although the structure is similar, the terminology and output goals for fisheries versus marine mammal stock production models differ to reflect their different goals. In fisheries, stock production models function primarily to provide biological reference points to inform quotas and identify overfishing in stocks (Hilborn & Walters 2013, Wade 2018). For marine mammal applications, stock production models are altered to calculate parameters such as removal level, pre-exploitation population size, or maximum net productivity level (MNPL), and have become an effective way to utilize commonly available data to address cetacean population dynamics (Baker & Clapham 2004, Wade 2018). Stock assessment models for both fisheries and marine mammals can be altered to include more detail, such as sex and age data (Hilborn & Walters 2013, Mosnier et al. 2014), but for many marine mammal populations this type of data is lacking. While a large amount of information about a population's past, present, and future can be gained from stock production models they often do not incorporate other biotic and abiotic aspects of the ecosystem that are potentially important determinants of population dynamics. Typically, these variables are ignored for many species because of a lack of data on the relationship between environmental change and population dynamics (Maunder & Piner 2014).

The CS beluga population has been modeled previously using a Bayesian state-space model, informed by historical harvest data and aerial survey data (Watt et al. 2020). The impact of various harvest levels was assessed by calculating the probability of population decline in 10

years. Within a management framework, predicting the effect of various harvest scenarios on the probability of population decline is considered a risk-based approach and is appropriate for evaluating populations that are considered 'data-rich'. Data-rich in this context is defined as having three or more abundance estimates within a 15-year period (Stenson & Hammill 2008). This approach allows those involved in population management to make decisions based on the risk of decline they deem appropriate. Potential Biological Removal (PBR) is another method for addressing management objectives, focused on quantifying the number of animals that can be removed from a stock while allowing a stock to reach or stay at its MNPL after 100 years (Wade 1998). Using the risk-based approach Watt et al. (2020) suggested that a harvest quota of 20 individuals would correspond to a 50% probability of population decline. The priors for this model were determined using traditional knowledge, previous cetacean models, and knowledge of cetacean ecology (i.e., Wade 1998, Marcoux & Hammill 2016). As with many other cetacean population models (Wade 1998, Thomsen et al. 2011, Jacobson et al. 2020), the existing CS beluga model lacks detail due to many unknowns in beluga demography and did not consider how environmental change may be impacting the population. There are still many unknowns surrounding environmental effects on beluga whale survival and fecundity (Laidre et al. 2015). Previous cetacean knowledge can provide a basis of knowledge for population models, but the lack of reliable data impedes the inclusion of details, such as direct effects of an environmental variable on any population parameter, into current models. Although direct environmental effects are unclear, there is evidence suggesting that changing sea ice dynamics, and subsequent changes in food availability, will affect beluga whale body condition, and thus population size through negative effects on survival (Laidre et al. 2008, Choy et al. 2020). Predicted effects are indirect,

but there is value in including environmental effects into population models to garner a better understanding of population wide effects.

Arctic marine ecosystems have undergone rapid change over the past four decades (Comiso 2012, Singh et al. 2013, Parkinson 2014). Climate change has contributed to a 4.7% decline in sea ice extent per decade and a decrease of five days/decade on average in the length of the sea ice season across the Arctic (Comiso 2012, Parkinson 2014, Yadav et al. 2020). Accompanying loss of sea ice, there has been a general increase in sea surface temperature in all regions north of 60˚N (Singh et al. 2013). These environmental changes are predicted to affect Arctic marine mammals, although the ability to predict the specific effects that environmental change will have on populations is limited (Burek et al. 2008, Laidre et al. 2008, Kovacs et al. 2011). Beluga are expected to be sensitive to climate change, influenced by stressors such as ice entrapment – triggered by rapid changes in weather, reduced availability of ice-associated prey, and increased predation pressure from killer whales expanding north (Laidre et al. 2008, Kovacs et al. 2011, Laidre et al. 2012). Most of these predicted effects are indirect, and thus, difficult to quantify and relate to specific aspects of beluga population dynamics. The direct effects of sea ice data have been included in a population model for harp seals (Hammill et al. 2021), but compared to cetaceans, seals have more available data and thus more explicitly identified relationships between variables and population parameters.

Several environmental variables that have been predicted to affect beluga populations, among those, sea ice extent is a recurring concern due to the close association beluga whales have with sea ice (Laidre et al. 2008). Alongside accessing prey that inhabit under-ice areas, sea ice cover acts as refuge from killer whale predation (Shelden et al. 2003, Bluhm & Gradinger 2008). Due to these associations with ice, variations in sea ice cover affect beluga behaviour and

have been predicted to affect survival (Kovacs et al. 2011). Sea ice in CS melts in the summer (Maslanik et al. 2011, Yadav et al. 2020) so to understand the relationship between sea ice and beluga whales, sea ice concentration (ICE) values in winter are more ecologically relevant. In contrast, summer months do not accurately reflect the condition of the ice in a given year. Though studied less than ICE, sea surface temperature (SST) is another important environmental variable in beluga ecology (Blix & Steen 1979, Aubin et al. 1990). SST impacts beluga whales because warmer waters promote molting and the proliferation of new skins cells, and are important for calf thermoregulation (Sergeant 1973, Blix & Steen 1979, Aubin et al. 1990). Calves are born with a thin blubber layer and thus, benefit from a warmer habitat initially until they amass thicker, more insulating blubber. Colder than usual water in estuaries has been linked to decreased survival of beluga calves (Blix & Steen 1979), though this relationship remains understudied. Conversely, increased SST caused by climate change has been predicted to depress calf survival rates, especially alongside other stressors such as reduced prey biomass and increased environmental contaminants (Williams et al. 2021). Both molting and calving occur in the summer months, so fluctuations in summer SST are likely to have an impact on beluga whales. ICE and SST can have short- and long-term impacts on beluga populations (O'Corry-Crowe 2009, Kovacs et al. 2011). Due to sea ice's connections to refuge from predation, declining sea ice is predicted to have short-term effects on mortality; long-term effects are more likely to relate to prey availability (such as cumulative effects of limited prey consumption) and be difficult to predict (Laidre et al. 2008). Recent research suggests that changing sea ice dynamics are already affecting beluga through reduced body condition connected to reduced prey availability (Choy et al. 2020). The short-term effects of SST are likely related to calf thermoregulation, as a year with unusually low or high summer temperatures could affect calf

survival, and thus, have immediate effects on population dynamics (Blix & Steen 1979, O'Corry-Crowe 2009). SST also affects beluga molting (Aubin et al. 1990); low temperatures may inhibit molting and cell proliferation potentially affecting abundance through reduced body condition, but unsuitable conditions may need to be prolonged for notable population-wide effects.

The objective of this study is to incorporate environmental covariates, specifically ICE and SST, into a stock production model to include the effects of environmental variation on estimates of CS beluga population trends. Further, we aim to compare models with and without covariates to determine how the inclusion of environmental variables might alter predicted future trajectories, and thus, population management plans.

3.2 Material & Methods

3.2.1 Model Specification

The CS beluga stochastic stock production model from Watt et al. (2020) was used as a template to incorporate the effect of environmental covariates on population dynamics (Figure 3.2). The model was structured with density dependence acting on population growth rate fit to aerial survey data from 1990-2017 and harvest history from 1960-2017 using Bayesian Markov Chain Monte Carlo (MCMC) methods to estimate population dynamics from 1960-2017. In this hierarchical state-space model data are considered to be the outcome of two distinct stochastic processes: a state process and an observation process (de Valpine & Hastings 2002). The state process arises from underlying population dynamics and evaluation of stock size over time and is a discrete formulation of the Schaefer model (Schaefer 1954), which allows both positive and negative effects on growth rate. The state process uses population parameters and error

(quantifying random variation in population dynamics) to estimate true population size annually. Population size, N_t, is a function of the previous year's population:

$$N_t = N_{t-1} * \left(1 + (R_{max}) * \left(1 - \frac{N_{t-1}}{K}\right)\right) * \left(\varepsilon_p\right)_t - R_t \quad (1)$$

Where: R_{max} is the maximum growth rate or rate of population increase,

K is the environmental carrying capacity,

$(\varepsilon_p)_t$ is a stochastic term for the process error with environmental covariates,

R_t are the removals for that year, calculated as reported catches, C_t , that are corrected for the proportion of animals that were struck and lost, $S\&L$:

$$R_t = C_t \cdot (1 + S\&L) \quad (2)$$

S&L is also a way to account for potential under-reporting in catch history. S&L data themselves can be under-reported, but because we have no available S&L data for CS beluga, we must rely on the prior being informed by data from eastern Hudson Bay beluga (see Watt et al. 2020).

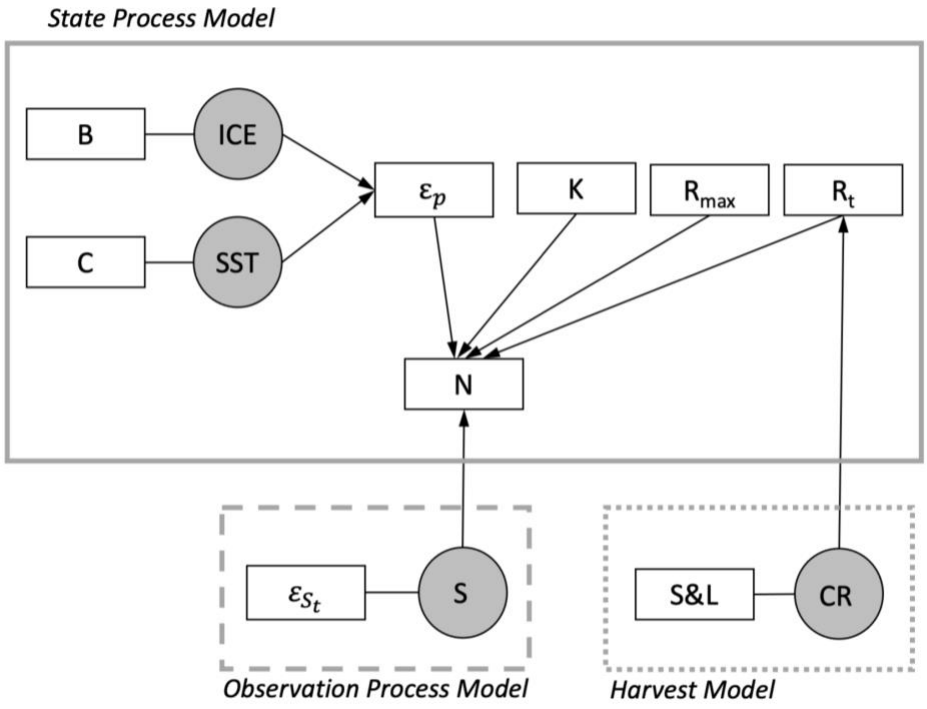

Figure 3.2 Schematic of the hierarchical state space population model structure depicting linkages between state process (solid grey outline), observation process (dashed grey outline), and harvest (dotted grey outline). Grey circles indicate data, white rectangles indicate parameters to be estimated by the model, and black lines indicate dependencies between parameter and/or data. *N* is population size, R_{max} is the maximum growth rate or rate of population increase, *K* is the environmental carrying capacity, ε_p is a stochastic term for the process error with environmental covariates, R_t are the removals for that year, calculated as reported catches, CR, that are corrected for the proportion of animals that were struck and lost, $S\&L$, S is survey data, ε_{S_t} is a stochastic term for observation error, *ICE* is mean sea ice concentration in Cumberland sound in March, *SST* is mean sea surface temperature in Cumberland Sound in August, *B* is the coefficient being estimated by the model for *ICE*, *C* is the coefficient being estimated by the model for *SST*.

The observation process is the relationship between true population size (N_t) and observed data (S_t), associated with random uncertainties, or observation error (ε_{S_t}), in data collection and abundance estimation. The logarithm of the median population estimate (N_t) from this log-normal model is applied to the state process model described above.

$$\ln(S_t) = \ln(N_t) + \varepsilon_{S_t} \quad (3)$$

A model of this type would benefit from the inclusion of age or sex structure, especially considering one of our chosen covariates, SST, potentially has a differing effect based on age. Unfortunately, our model does not contain information on age or sex for this population, as there are no reliable data available at this time.

Included surveys occurred in 1990, 1999, 2014, and 2017; all surveys were systematic visual in design. All surveys were adjusted to account for availability bias, and the 2017 survey was adjusted for perception bias (as per Watt et al. 2020).

3.2.2 Process Error Incorporating Environmental Covariates

To capture more of the natural variation within the population, process error was modified from the previous template model to include the effects of environmental variation. ICE and SST were incorporated into the process error term (see Appendix 2 for details). Both ICE and SST are spatially gridded data with a 1 x 1 degree resolution consisting of monthly averages and were obtained from the HadISST data set (Rayner et al. 2003).

The model requires the process error to have annual values for each covariate, so to avoid the loss of nuance in interannual variation, we chose to use a single month based on ecological

significance to beluga, instead of an annual average. We used ICE data from March of each year from 1960-2018 as, on average, March is the month of highest sea ice extent across the Arctic (Maslanik et al. 2011, Stroeve et al. 2012). For SST, we used August data, as August, on average, is the month with highest sea surface temperatures (Shea et al. 1992, Chambault et al. 2018). We chose ICE and SST maximum months *a priori* based on ecological relevance, but we also considered minimum months for either variable, and intra-annual patterns in ICE and SST. Months with minimum ICE and SST values, August and March respectively, were explored, as well as the same month for both ICE and SST. ICE values in August largely reflected a lack of ice cover, which was not valuable for representing environmental variation. SST values in March were not ecologically applicable to beluga whales, compared to summer months, as variability in SST was predicted to have the most impact on beluga whale summer ecology. We decided not to explore the use of minimum months further as minimum ICE in August represents a time when sea ice cover has less ecological importance to beluga, as well minimum SST in March was too highly correlated with ICE in March (Pearson correlation coefficient of -0.97) to be considered independent of ICE. Similarly, when the same months were tested for ICE and SST across the year, correlation remained high. Finally, annual averages were also tested, but using all the values within a year dampened the extremes in ecologically relevant months for which we were aiming to investigate the effects.

We used a 6 x 9 pixel polygon to extract data from the environmental raster files specific to CS (Figure 3.1). The mean of all pixels in the resulting clipped raster files from each year were calculated and the mean values were translated into a Z-score for ICE and SST separately. Z-scores were used in the process error so the environmental variables in the model reflected the variation of each value from the mean for all years during the study period of 1960-2018 (Figure

3.3). We used a Pearson correlation test to determine if there was collinearity between ICE and SST and if they could be incorporated into the same model. The resulting correlation coefficient was -0.12, which is low enough to allow for the incorporation of both environmental covariates into the model (Vatcheva & Lee 2016). We also tested the square of SST in initial model runs to determine if there was a non-linear relationship, where extreme high and lows had a negative impact on population size. The inclusion of SST^2 decreased model fit and thus was not explored further.

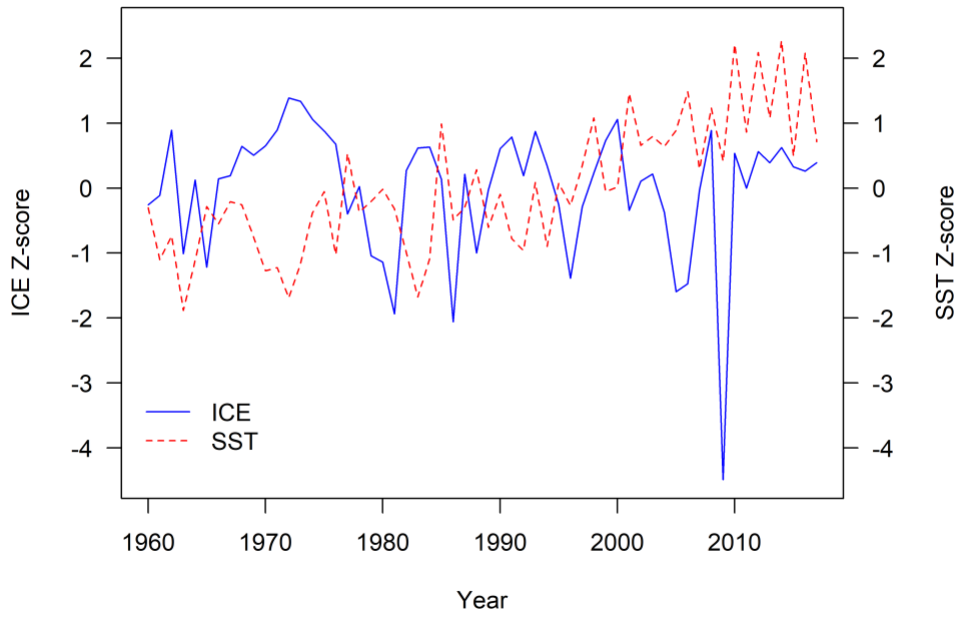

Figure 3.3 Mean sea ice concentration (ICE) in March and mean sea surface temperature (SST) in August as Z-score values in Cumberland Sound from 1960-2017.

3.2.3 Priors

The majority of priors remained the same as those in the template model (Table 3.1) from Watt et al. (2020). The stochastic process error term ε_p was altered to include the additive effects of ICE and SST. The equation below was used for the location parameter of process error, with the precision hyperparameter (ε_{pr}) free to vary to account for error not explained by the covariates (see Appendix 2 for details).

$$(\varepsilon_p)_t = (B*ICE_{t-1} + C*SST_{t-1}) + \varepsilon_{pr} \quad (4)$$

Where:

ICE is mean sea ice concentration in Cumberland sound in March,

SST is mean sea surface temperature in Cumberland Sound in August,

B is the coefficient being estimated by the model for ICE,

C is the coefficient being estimated by the model for SST,

t is annual time,

ε_{pr} is the random error in the process precision parameter

Table 3.1 Prior distributions, parameters and hyper-parameters used in the template population model (from Watt et al. 2020) and environmental covariates sea ice concentration (ICE) and sea surface temperature (SST) corresponding to process error used in the final model. "dist." Denotes a hyper-parameter with its own prior distribution. Dashes indicate parameters that do not apply to the model. * denotes variables that differ or are new from the template model.

Parameters	**Notation**	**Prior distribution**	**Hyper-parameters**	**Values from Watt et al. (2020)**	**Values for model with ICE and SST**
Survey error (t)	ε_{st}	Log-normal	μ_s	0	0
			τ_s	*dist.*	*Dist.*
Precision (survey)	τ_s	*Gamma*	α_s	*2.5*	*2.5*
			β_s	*0.4*	*0.4*
*Process error (t)	ε_{pt}	Log-normal	μ_p	0	*B*ICE + C*SST*
			τ_p	*dist.*	*Dist.*
*Precision (process)	τ_p	Gamma	α_p	1.5	1.5
			β_p	0.00005	0.001
*ICE coefficient	B	Normal	μ_B	-	0
			τ_B	-	5
*SST coefficient	C	Normal	μ_C	-	0
			τ_C	-	5
Struck-and-lost	*S&L*	Beta	α_{sl}	3	3
			β_{sl}	4	4
*Initial population	N_{1960}	Uniform	N_{upp}	4,000	9,000
			N_{low}	1,000	1,000
Carrying capacity	*K*	Uniform	K_{upp}	15,000	15,000
			K_{low}	2,000	2,000
*Lambda	λ	Uniform		0.01-0.05	0.01-0.07

Both ICE and SST were multiplied by independent coefficients and were autoregressive to an order of one to allow the model to determine the effect each environmental covariate had

on process error, and thus, population dynamics in the following year. We focused on one year autoregressive effects, although it is ecologically plausible that these covariates may have effects over a greater time span, and this would be valuable to test in future models. Prior distributions for coefficients were informed by the necessity for coefficients to fall between -1 and 1. Initial exploratory runs were performed with each covariate alone in the model, and both covariates together. The best fit model included both covariates, both with coefficients assigned normal(0, 5) distributions. The model was also re-run with each covariate individually to explore the effect of each covariate alone.

The stochastic process error term ε_p included in the state process equation (Eqn. 1) was assigned a lognormal distribution with a location parameter set by the process error equation (Eqn. 4) described above. The precision parameter for the process error term was assigned a moderately informative gamma(1.5, 0.001) distribution. The precision term within the precision parameter was reduced as compared to the precision parameter in Watt et al. (2020) to allow the opportunity for process error to increase and have more of an effect on interannual variation in the population trajectory. Precision for process error was high in the Watt et al. (2020) model because, as a long-lived species, beluga whales were not expected to exhibit a high amount of annual stock variation. We decreased precision to allow the model to explore more variation, to accommodate uncertainty surrounding the covariates. Initial runs of the model showed that the prior distributions for starting population and R_{max} in the template model appeared to constrain the posterior distributions. Both parameters had uniform distributions in the template model, so the starting population distribution was widened to a uniform(1,000 – 9,000) distribution and R_{max} was widened to a uniform(0.01 – 0.07) distribution (Table 3.1). The updated starting population distribution allows space for the model to estimate a slightly higher population in

1960 if necessary. R_{max} in the template model was informed by known rates of population increase in odontocetes, which can range from 0.02 – 0.06 (Wade & Angliss 1997, Wade 1998, Lowry et al. 2008), which also informed our prior.

3.2.4 Parameter Estimation and Model Diagnostics

Posterior estimates for all parameters included in the model were obtained using a Gibbs sampler algorithm implemented in JAGS (Plummer 2003). Rstudio (R Core Team 2020; *version 1.2.5033*, R *version 4.0.2*) packages *R2jags* (Su & Yajima 2015; *version 0.6-1*) and *coda* (Plummer et al. 2006; *version 0.19-3*) were used to examine the results. We used an MCMC chain simulation method and visually inspected trace plots to check the convergence of parameters. Initial runs of the code investigated model convergence, mixing, and autocorrelation within parameters. Model fit was determined using the diagnostics described below and Deviance Information Criterion (DIC), although DIC did not have a difference >2 between any of the models (Burnham & Anderson 2002), so other diagnostics assessing convergence were used preferentially.

We visually inspected Geweke plots to test for mixing within each chain and used the Geweke Diagnostic test of similarity between different sections of the chains (Geweke 1996). The Brooks-Gelman-Rubin (BGR) diagnostic test was used to validate convergence between chains by comparing the width of the 80% credible interval (CI) of the chains pooled with the mean widths of the 80% CI for each of the chains individually (Brooks & Gelman 1998). Probability of direction was computed to determine if the posterior distributions for ICE and SST coefficients significantly differed from zero. Probability of direction (pd) refers to the probability

that a parameter is strictly positive or negative and is often used as a Bayesian proxy for the frequentist p-value, whereby pd = 95% equates to p = 0.1, and pd = 97.5% equates to p = 0.05.

In initial model runs, we used three chains which had the number of iterations corrected to equal 10,000 after a burn in of 6,000 and thinning value of 30. Once a top model was determined, that model was run using five chains, and 100,000 iterations after a burn-in of 60,000, with thinning maintained at 30.

3.2.5 Future Projections and Management Scenarios

In order to predict stock trajectory and sustainable yield, the model was extended 10 years into the future under five different management scenarios reflecting annual harvests of 5, 10, 20, 30, and 41individuals. Although a 10-year trajectory is relatively short, it was chosen because ideally harvest quotas for marine mammals are re-assessed every five years. The current harvest quota is 41 individuals, and because CS beluga are endangered and not predicted to recover at the current quota (Watt et al. 2020), only harvests below the current quota were considered for projections. We explored how adding environmental covariates changed the probability of decline from the template model.

To continue the comparison of our model to the template model from Watt et al. (2020), we estimated PBR using a recovery factor (F_R) of 0.1 for a threatened declining stock (Hammill et al. 2017).

The equation for PBR threshold is:

$$PBR = N_{min} \cdot 0.5 \cdot R_{max} \cdot F_R \quad (5)$$

Where: R_{max} is the maximum rate of population increase. The default value for cetaceans is 0.04; however, in our calculation we used the R_{max} estimated by the model.

F_R is a recovery factor (between 0.1 and 1), and

N_{min} is the estimated population size using the 20-percentile of the posterior distribution resulting from the model or the 20-percentile of the log-normal distribution (Wade 1998) of the aerial survey estimate.

Animals that are harvested, as well as those that are struck and lost (S&L), not reported, and those with other sources of human caused mortality are all included in PBR estimates, thus, we need to estimate total allowable landed catch (TALC) which is calculated as:

$$TALC = PBR - S\&L \quad (6)$$

where S&L is estimated in the model.

3.3 Results

The final CS beluga model, adapted from Watt et al. (2020) (Table 3.2), included ICE for the month of March and SST for the month of August in CS from 1960-2017. Differences between results for the three models tested (ICE alone, SST alone, and ICE and SST together) were minimal. DIC and BGR values were not distinguishable between the three models, and convergence of all parameters was similar. DIC from all covariate models were >2 larger than the DIC of the base model without environmental covariates (see Table 3.2). Due to the similarities, model selection for covariate inclusive models was led by Geweke Diagnostic test results, where the z-scores for multiple parameters in the ICE and SST model were lower than

those in models with the covariates alone. The focal update of our final model was the addition of environmental covariates which resulted in updated variable estimates (Table 3.2). There was rapid convergence of all chains for carrying capacity (K), population size in 2018 (N_{2018}), process error, initial population size (N_{1960}), and $S\&L$. Convergence of each chain was indicated by low autocorrelation in all variables (Figure S1), and a BGR statistic < 1.05 for all variables (Table 3.2).

Table 3.2 Model outputs for the CS beluga stock model from Watt et al. 2020 and our final model. The mean, standard deviation (SD), median (50^{th} Q), 25^{th} and 75^{th} quantiles (25^{th} Q, 75^{th} Q), 95% credibility intervals (2.5%CI, 97.5%CI) are given for the following model parameters and their priors: carrying capacity (K), process error (process), survey precision (surv), starting population (startpop), struck and loss (S&L), and population size in 2018 (N_{2018}). Coefficients for ICE (B) and SST (C) are included in the final model output. $\widehat{R}$ is the Brooks-Gelman-Rubin statistics; values < 1.05 indicate convergence of chains. N.eff is the number of effective chains after considering autocorrelation.

Model	Parameter	Mean	SD	2.5%CI	25th Q	50th Q	75th Q	97.5%CI	$\widehat{R}$	n.eff
Watt et	K	8,233	3,567	2,907	5,067	7,875	11,258	14,607	1.001	$5.00x10^5$
al. (2020)	K.prior	8,489	3,752	2,321	5,238	8,486	11,730	14,678	1.001	470,000
DIC=77.86	$lambda_{Max}$	1.03	1.01	1.01	1.02	1.03	1.04	1.05	1.001	130,000
	$lambda_{Max}$.prior	0.03	0.01	0.01	0.02	0.03	0.04	0.05	1.001	$5.00x10^5$
	error.process	1.00	0.01	0.98	1.00	1.00	1.00	1.02	1.001	413,103
	prec.process	30,092	24,521	2,213	12,231	23,736	41,112	93,588	1.001	97,000
	prec.process.prior	29,982	24,439	2,189	12,115	23,673	41,061	93,179	1.001	$5.00x10^5$
	prec.surv	6.97	3.30	2.09	4.56	6.45	8.82	14.79	1.001	$5.00x10^5$
	prec.surv.prior	6.25	3.95	1.04	3.34	5.44	8.28	16.06	1.001	370,000
	startpop	3,077	537	2,042	2,667	3,100	3,519	3,946	1.001	160,000
	startpop.prior	2,499	867	1,075	1,747	2,496	3,252	3,926	1.001	$5.00x10^5$
	S&L	0.38	0.16	0.10	0.25	0.36	0.49	0.72	1.001	$3.00x10^5$
	S&L.prior	0.43	0.18	0.12	0.30	0.42	0.55	0.78	1.001	$5.00x10^5$
	N_{2018}	1,127	320	617	915	1,090	1,293	1,864	1.001	450,000
Model	B	0.069	0.175	-0.274	-0.049	0.07	0.189	0.409	1.002	2300
with ICE										
and SST	B.prior	0	0.447	-0.876	-0.301	0.001	0.302	0.876	1.001	$5.00x10^5$
	C	0.022	0.041	-0.063	-0.005	0.023	0.05	0.1	1.001	6300
DIC=81.66	C.prior	-0.001	0.448	-0.879	-0.303	-0.001	0.301	0.874	1.001	$5.00x10^5$
	K	6,730	3,674	2,283	3,557	5,666	9,504	14,394	1.001	290000
	K.prior	8,496	3,751	2,325	5,251	8,494	11,739	14,679	1.001	$5.00x10^5$
	deviance	77.94	2.66	74.06	76.069	77.494	79.349	84.336	1.001	32000
	$Lambda_{max}$	0.038	0.017	0.012	0.024	0.038	0.053	0.068	1.001	260000
	$Lambda_{max}$.prior	0.04	0.017	0.011	0.025	0.04	0.055	0.068	1.001	$5.00x10^5$
	prec.process	1,523	1,226	125	628	1,205	2,080	4,700	1.001	160000
	prec.process.prior	1,502	1,226	108	608	1,184	2,058	4,679	1.001	410000
	prec.surv	5.89	3.051	1.551	3.661	5.364	7.544	13.245	1.001	94000
	prec.surv.prior	6.244	3.948	1.038	3.341	5.434	8.28	16.042	1.001	$5.00x10^5$
	startpop	5,211	2,075	1,667	3,496	5,147	6,940	8,779	1.001	120000
	startpop.prior	5,000	2,308	1,200	3,002	5,001	6,995	8,800	1.001	420000
	struck.and.lost	0.407	0.17	0.111	0.279	0.397	0.526	0.755	1.001	$1.00x10^5$
	struck.and.lost.prior	0.428	0.175	0.118	0.297	0.422	0.553	0.777	1.001	220000
	N_{2018}	1,344	569	564	974	1,245	1,591	2,715	1.001	27000

The estimated maximum growth rate (R_{max}) was 1.038 (CI: 1.012- 1.068), S&L was estimated as 1.40 (CI: 1.11-1.78), and carrying capacity (K) was estimated at 5,666 (CI: 2,283-14,394). In 1960, the starting population was estimated at 5,147 (95% CI 1,667 – 8,779), and the estimated value for N_{2018} was 1,245 (95% CI 564 – 2,715) (Figure 3.4).

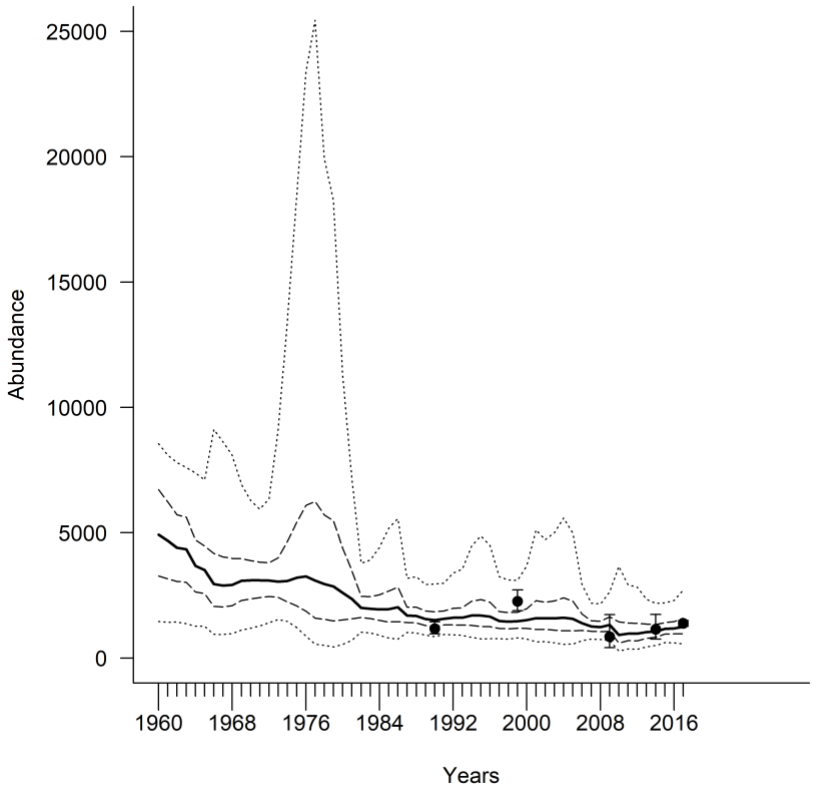

Figure 3.4. Model estimates of CS beluga abundance fitted to adjusted aerial survey estimates flown in 1990, 1999, 2009, 2014 and 2017 (black dots ± 95% log-normal CI) and harvest data from 1960-2017. Process error includes the effects of sea ice concentration (ICE) and sea surface temperature (SST) in CS. Solid line shows the posterior median estimates, dashed lines show 50% credible interval, and dotted lines show 95% credible interval.

The coefficient for ICE (B) was estimated as 0.070 (-0.27 – 0.41), and the coefficient for SST (C) was estimated as 0.023 (-0.06 – 0.10). These coefficients control the extent to which ICE and SST affect fluctuations in population trajectory. ICE and SST were translated into Z-scores so negative values reflect years below the mean, and positive values reflect years above the mean for the study period. The positive values of both B and C mean that ICE and SST values directly affect the direction of population fluctuations. The probability of direction was 65.44% for B, and 70.98% for C, suggesting both covariate coefficients overlap zero, this supports the increased DIC for the covariate inclusive model. We also ran the model with ICE and SST separately (see Appendix 2 for model outputs). In both cases the coefficients for ICE and SST remained positive, 0.002 and 0.013 respectively, but were lower than when both were included in the same model. Separate covariate models also resulted in less variation in the population trajectory over the study period compared to the final model (Figure 3.5).

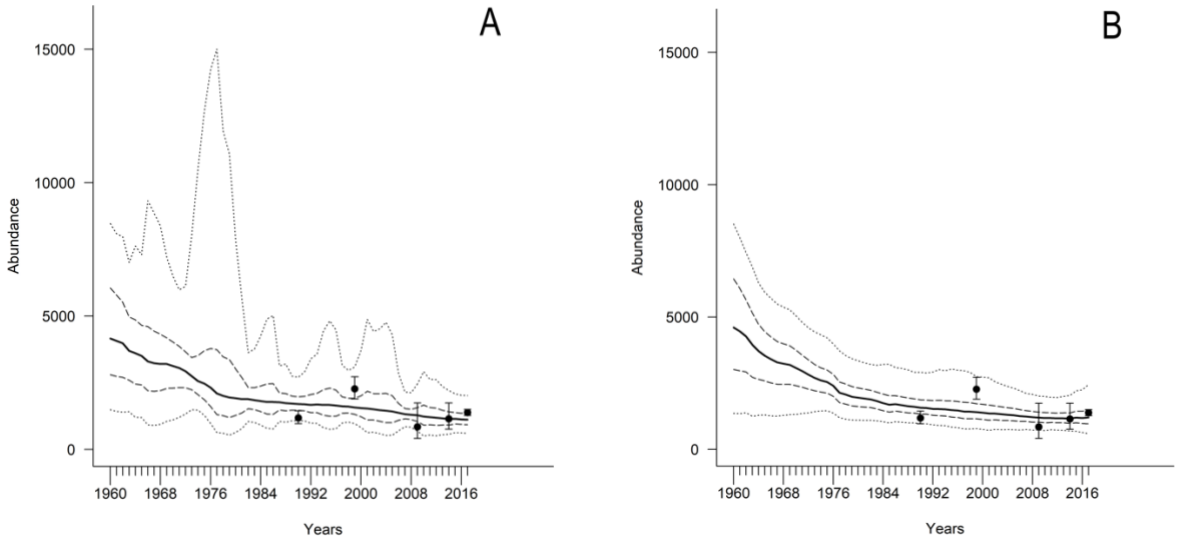

Figure 3.5 Model estimates of CS beluga abundance fitted to adjusted aerial survey estimates flown in 1990, 1999, 2009, 2014 and 2017 (black dots ± 95% log-normal CI) and harvest data from 1960-2017. A) Process error includes the effect of sea ice concentration in CS. B) Process error includes the effect of sea surface temperature in CS. Solid line shows the posterior median estimates, dashed lines show 50% credible interval, and dotted lines show 95% credible interval.

To assess the impacts of different management strategies on the population, the model was used to plot the trajectories of five harvest scenarios (Figure 3.6). The probability of population decline after 10 years was 83% for a harvest of 41, 66% for a harvest of 30, 42% for a harvest of 20, 18% for a harvest of 10, and 9% for a harvest of 5 (Table 3.3, Figure 3.7). Using the N_{2018} estimate from the model, the PBR was estimated at 2, and TALC was estimated at 1 individual.

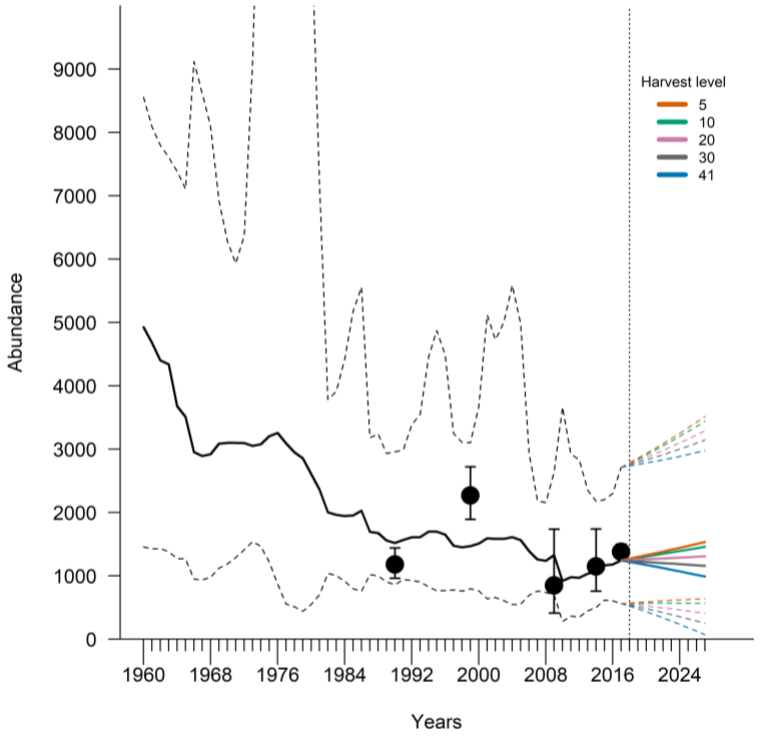

Figure 3.6 Future population projections for CS beluga under five different management scenarios based on population estimates from a stochastic stock production model including ICE and SST, fitted to adjusted aerial survey estimates flown in 1990, 1999, 2009, 2014 and 2017 (black dots ± 95% log-normal CI). Solid line shows the posterior median estimates and dashed lines show 95% credible interval.

Table 3.3 Probability (P) that the CS beluga population, subjected to different levels of annual landed catch, will decline from the modelled 2018 population abundance estimate after 10 years of harvest. Comparing results from Watt et al. 2020 and our final model (with ICE and SST).

Landed Catch	P(%) Watt et al. 2020	P (%) with ICE and SST
5	1	9
10	11	18
20	50	42
30	83	66
41	96	83

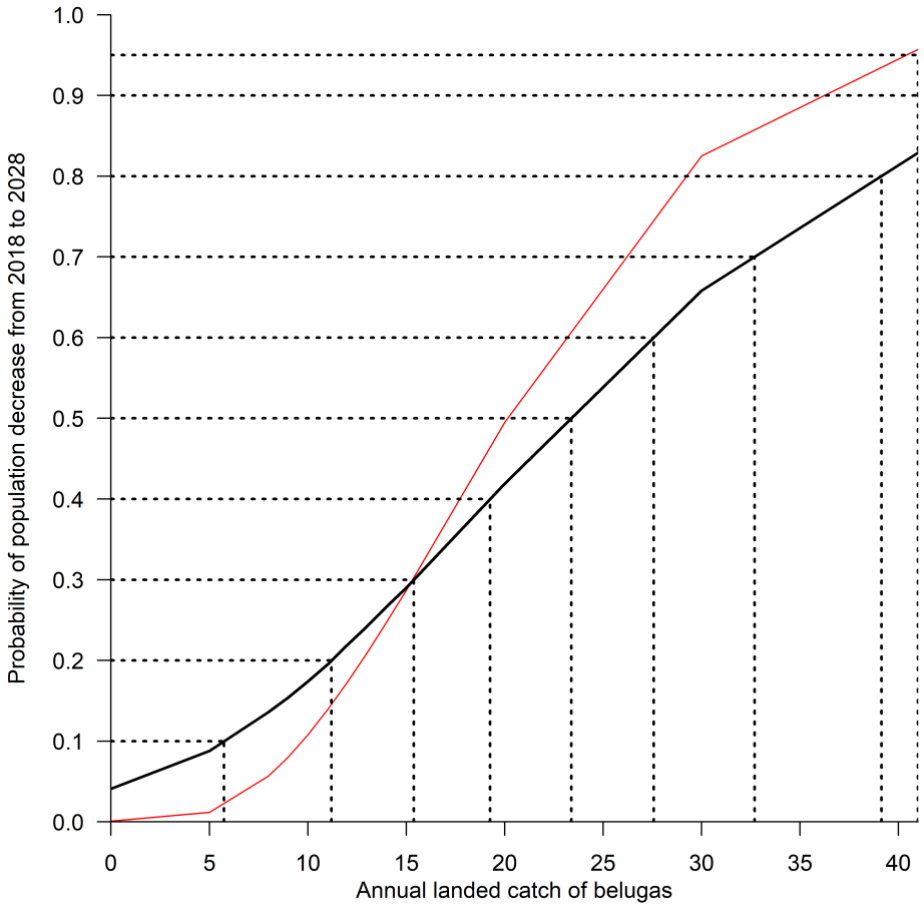

Figure 3.7 Probability of the CS beluga stock decreasing from the 2018 abundance estimate after 10 years of harvest, as a function of the number of reported beluga removed from the stock every year. Dotted lines indicate levels of harvest (x-axis) corresponding to the probability of decline (y-axis). Red line shows probability of CS beluga stock decrease from template model (Watt et al. 2020).

3.4 Discussion

Environmental variables ICE and SST were incorporated into the stock production model for CS beluga. The covariates ICE and SST acted on the process error, impacting the CS beluga population trajectory by contributing to some of the variability in population dynamics. The

positive coefficient for ICE means that following a year of above average ICE, the beluga population would increase, and after a below average year the beluga population would decrease. Similarly, the positive coefficient for SST reflects an upward trend in beluga population trajectory following a year of above average SST, and a downward trend after a year of below average SST. The coefficients for both covariates are small, reflecting a relatively small effect that ICE and SST have on population trajectory indirectly through process error. The inclusion of covariates did not increase model fit compared to the template model from Watt et al. (20202). Reduced model fit was expected because environmental covariates increased the number of parameters in the model and increased error (as they were modelled into the process error term). As such, our model should not become the preferred model for this population, but was created as a case study to explore methods for including the effects of environmental change when specific relationships with demographic parameters have not yet been identified. Compared to abundance estimates from the template model (Watt et al. 2020), the largest difference in any year was an increase of ~3000 individuals, the smallest was ~5 individuals. The greatest differences were in years at the beginning of the time series, this is likely because there are no available aerial surveys before 1990 to inform the trajectory, so during that period the covariates have more power to inform trends.

The posterior distributions for both ICE and SST coefficients spanned zero, and the probability of direction tests for B and C were both below 95%. These results suggest that the inclusion of covariates has a very limited effect on model trajectory, and as such, model results should be interpreted with this in mind. The relatively small effect of covariates via small coefficient estimates, the coefficient distributions spanning zero, and the lessened model fit with covariate inclusions (as per DIC) all suggest that, with the available data, inclusion of

environmental covariates is not yet notably beneficial for the estimation of CS beluga population dynamics. With the consideration of caveats associated with model fit, interpretation of our model will focus on dissecting model results as a case study on model structure, rather than as applicable management advice.

Although the coefficients allude to ICE and SST having similar effects on population trajectories, ICE and SST have low correlation, so there is an interactive effect between these covariates and how they affect the CS beluga population. The coefficient for ICE is three times larger than the coefficient for SST, therefore, in most years ICE will have a greater effect on population fluctuations than SST. In years where the value for either covariate has a high deviation from the mean, that covariate had a stronger effect on population fluctuations. The greatest uncertainty in the population estimate is at the peak in the 97.5^{th} quantile between 1970 – 1985. Aside from the lack of survey data in early years to bolster estimates, ICE trends were consistently high in CS in the early 1970's (Figure 3.3) and based on the results from the models where covariates were included separately, it appears ICE is driving the majority of this uncertainty. Sea ice is inherently variable; despite clear downward trends, annual values are found to commonly deviate from the trendline (Cavalieri & Parkinson 2012). The quantiles for SST alone are smaller, with less variation. SST is potentially more stable over time than sea ice, which is seasonally dependent and susceptible to short-term fluctuations (Cavalieri & Parkinson 2012, Carvalho & Wang 2020). The combination of consistently above average ICE values and relatively low harvest levels in the early-mid 1970's could have resulted in the model having increased uncertainty in population estimates for those years.

The final model contained both covariates, ICE and SST, but we also tested the independent effects of each covariate. While there was a positive effect from each environmental

covariate on the model trajectory, similar to our final model, the coefficient was lower for both ICE and SST when they were separate. Although they have a notable effect on the population trajectory alone, when ICE and SST are considered together coefficients for both are higher and thus, they have a greater effect on the re-creation of plausible population fluctuations, suggesting impacts are synergistic. There is also potential that the larger effect for each covariate when they are together is the result of their more extreme values dampening the effects of each other, as they are not correlated, or the effect of an unknown confounding variable acting on both. It is difficult to identify other temporally variable covariates that have known effects on beluga whale population dynamics because although important habitat features have been identified (Laidre et al. 2008), the effect that changes in those features has on population dynamics has not been quantified. The overall trajectories of the separate models have shallower fluctuations than our final model. In the final model the coefficients are greater and therefore have a larger effect on the process error, and thus create more fluctuations in trajectory. The inclusion of both covariates is ecologically plausible because there is likely interaction between these variables and how they are affecting beluga survival (Asselin et al. 2011, Hauser et al. 2017). Unfortunately, the data are still too sparse to identify these specific relationships in a population model context, but our model provides evidence that there is value in evaluating the effect of ICE and SST on beluga populations, with the opportunity to expand on these relationships as additional data become available.

Multiple studies recognize that the environmental changes occurring in the Arctic are affecting beluga whales (Laidre et al. 2008, Kovacs et al. 2011), but identifying the specific connections to reproduction and survival is challenging. Belugas are highly ice-associated; they prefer high ice cover (Asselin et al. 2011) and often use ice cover as refuge from predation

(Stewart & Stewart 1989, Shelden et al. 2003). Declining sea ice can make beluga whales more vulnerable to predation and reduce access to prey (Heide-Jørgensen & Laidre 2004, Kovacs et al. 2011), which explains why our model determined years of lower ICE had a negative effect on the CS beluga population trajectory. Beluga whales prefer to inhabit warmer water in the summer as it is believed to aid in skin molting (Watts et al. 1991). Calving also occurs in the summer and warmer water likely increases calf survival by aiding thermoregulation (Sergeant 1973, Blix & Steen 1979). The connection between warmer water and important aspects of beluga ecology could explain the positive relationship between SST and beluga population size determined by our model. There is a loose correlation between low SST years and higher ICE, although there is a lot of variability within this relationship (Hurrell et al. 2008), so the lack of correlation in our data between ICE in March and SST in August in Cumberland Sound is plausible.

Our model uses covariates that are one year autoregressive, and thus, focuses on the short-term effects of ICE and SST. The model could be altered to consider long-term effects by increasing the number of years the model is autoregressive to, resulting in model outputs being affected by years further in the past. Changing the temporal aspect of the covariate inclusion provides the potential to show how ICE and SST (or other covariates) affect the population after more than one year, which potentially varies from the initial impacts (Gilg et al. 2012). For example, low ICE may cause beluga whales to have reduced access to prey, but the result of a change in resources may not show up in the population for several years. Similarly, if summer SST is lower than average and negatively affects beluga molting, the effects tied to incomplete molting may take a number of years to become quantifiable or not even act on population parameters directly. At this time, a lack of data makes it difficult to speculate on the timeframe

over which impacts might occur. We started by evaluating a one-year time frame, but additional data may support increasing the time lag. Hammill et al. (2021)'s harp seal population model utilized mortality data to determine a one-year time lag for the effect that sea ice anomalies had on the survival of young of the year. Our model could be updated with a specific time lag relationship of this nature once more data are available.

The inclusion of environmental covariates into our model resulted in changes to multiple aspects of the previous CS beluga model from Watt et al. (2020). In comparison to the template CS stock production model (Watt et al. 2020), the model presented here had a higher starting population estimate, a slightly higher N_{2018} estimate, and a lower carrying capacity. The maximum growth rate increased slightly toward the accepted default for cetaceans (Wade 1998), and S&L increased by 3%. In the template model, the population decrease over time followed a relatively linear trajectory. However, in our model, there are more noticeable peaks and troughs in the population trend and wider credible intervals. The resulting increased starting population created a previously unobserved trend of steep population decrease early in the study period when both ICE and SST were below average for many years. This steep trend suggests that when the population abundance was higher it was quite vulnerable to environmental fluctuations. The higher starting population also suggests that pre-harvest abundance is potentially higher than was suggested in Watt et al. (2020), although carrying capacity is estimated to be lower by ~2,000 individuals. If model fit can be improved in future models these differences may need to be considered for future management goals if density dependence was to act on the population as it approached carrying capacity, but this is unlikely given its current population trend and endangered status (COSEWIC 2004).

We used a risk-based model approach to determine the probability of population decline under potential management scenarios. Compared to similar risk-based results from Watt et al. (2020), the inclusion of environmental covariates decreased the probability of decline for the three highest harvest scenarios and increased it for the two lowest scenarios. We speculate this is due to a more stable overall population trend in Watt et al.'s (2020) model (due to less variation in process error) allowing the population to remain stable at lower harvest levels. While a lower 2018 abundance estimate from Watt et al. (2020) may cause high harvest levels to have a more dramatic effect, bringing abundance so low that population stability is lost. In the template model, a harvest of 20 had a ~50% probability of decline, in our model a 50% probability of decline was reached at a harvest level of ~24. However, the recommended harvest suggested by our model is slightly more conservative than the harvest level suggested by Watt et al. (2020) when lower probabilities of decline are considered. Our model resulted in a 5% probability of decline over a 10-year period with a harvest of ~1, while Watt et al. (2020) found a suggested harvest of ~8 had a 5% probability of decline. Using the 2018 population estimate and the R_{max} of 0.038 from our model, the PBR threshold was 2. The PBR threshold calculated by Watt et al. (2020), using their 2018 estimate and an R_{max} of 0.04, had a value of 1. The slight difference between PBR thresholds is likely due to differences in estimated 2018 abundance. The goal of this work is to consider how environmental variables might change our interpretation of population trends and consider whether this ecosystem approach may be used for future assessments. In the face of uncertainty, a more conservative management strategy is beneficial because of the endangered status of CS beluga (COSEWIC 2020). Further research using a Bayesian stock production model could provide clarity on the effects of environmental covariates

on beluga population dynamics and provide increased confidence in sustainable management using a risk-based approach.

Hammill et al. (2021) proposed an age-structured harp seal population model with sea ice incorporated, where the specific relationship between sea ice cover anomalies and mortality of young of the year was defined. Compared to Arctic cetaceans, there are more data available on how covariates such as ice, which is used as a pupping platform, and prey availability affect specific aspects of harp seal population dynamics, such as mortality and reproductive rates (Stenson et al. 2020, Hammill et al. 2021). While the results of our model provide baseline knowledge on the effect of environmental variation on population fluctuations, there is potential for the inclusion of much more detail in models of this type in the future, as ICE and SST are only two of many variables that may affect beluga population dynamics. Other relevant variables may include: water depth, seafloor topography, and distance to important features such as shoreline (Asselin et al. 2011, Hauser et al. 2017). Belugas are thought to preferentially select for shallower water for increased prey availability, similarly they select for regions with a higher sea floor slope, likely due to the increased productivity resulting from increased upwelling in these regions (Asselin et al. 2011). Suspected selection for these static habitat features may change depending on changes in dynamic features, such as ICE, and the interplay between habitat change, prey availability, and the presence of predators. This model could further benefit from the inclusion of predator and prey dynamics, and the interactions these biotic variables might have with abiotic environmental variables. In this model the environmental covariates were introduced via process error, yet as beluga whale research progresses there is potential for more specific relationships between beluga population dynamics and changes in environmental parameters to be quantified. An understanding of the mechanistic relationships would allow

environmental covariates to be included into stock production models directly, rather than within the process error, which would create more certainty in resulting parameter estimates. For example, if new data allowed us to quantify the relationship between ICE and mortality from predation, the model could be modified to include that direct relationship. ICE and SST impacted the CS beluga population trajectory and thus inclusion of these variables in future models should be considered to aid in explaining population trajectories of beluga and other Arctic marine mammals.

CS beluga are a Threatened population under SARA (SARA 2017) and considered Endangered by COSEWIC (COSEWIC 2004), and it is important to consider this status when making decisions on modelling, management, and conservation. Including climate and habitat changes that are affecting endangered species is important for conservation research because in many cases, climate change is shifting the baselines that guide conservation goals (Wilkening et al. 2019, Hirsch 2020). Many endangered species are specialists, endemic to their habitat, making them likely to be disproportionately affected as their habitat changes (Preston et al. 2008, Gough et al. 2015, Wilkening et al. 2019). A certain level of uncertainty is almost always involved in endangered species management (Gregory & Long 2009), but incorporating different types of data into population modelling has the potential to reveal sources of uncertainty that should be considered for more informed management of species at risk.

3.5 References

Asselin NC, Barber DG, Stirling I, Ferguson SH, Richard PR (2011) Beluga (*Delphinapterus leucas*) habitat selection in the eastern Beaufort Sea in spring, 1975-1979. Polar Biol 34:1973-1988.

Aubin DJS, Smith TG, Geraci JR (1990) Seasonal epidermal molt in beluga whales, *Delphinapterus leucas*. Can J Zool 68:359-367.

Baker CS, Clapham PJ (2004). Modelling the past and future of whales and whaling. Trends Ecol Evol 19:365-371.

Best JK, Punt AE (2020) Parameterizations for Bayesian state-space surplus production models. Fish Res 222:105411.

Blix AS, Steen JB (1979) Temperature regulation in newborn polar homeotherms. Physiol Rev 59:285-304.

Bluhm BA, Gradinger R (2008) Regional variability in food availability for arctic marine mammals. Ecol Appl 18:S77-S96.

Brooks SP, Gelman A (1998) General Methods for Monitoring Convergence of Iterative Simulations. J Comput Graph Stat 7:434-455.

Burek KA, Gulland FM, O'Hara TM (2008) Effects of climate change on Arctic marine mammal health. Ecol Appl 18:S126-S134.

Burnham KP, Anderson DR (2002) Model Selection and Inference: A Practical Information-Theoretic Approach. Springer, New York.

Carvalho KS, Wang S (2020) Sea surface temperature variability in the Arctic Ocean and its marginal seas in a changing climate: Patterns and mechanisms. Glob Planet Change 193:103265.

Cavalieri DJ, Parkinson CL (2012) Arctic sea ice variability and trends, 1979-2010. The Cryosphere 6:881-889.

Chambault P, Albertsen CM, Patterson TA, Hansen RG, Tervo O, Laidre KL, Heide-Jørgensen MP (2018) Sea surface temperature predicts the movements of an Arctic cetacean: The bowhead whale. Sci Rep 8:9658.

Choy ES, Giraldo C, Rosenberg B, Roth JD, Ehrman AD, Majewski A, Swanson H, Power M, Reist JD, Loseto LL (2020) Variation in the diet of beluga whales in response to changes in prey availability: insights on changes in the Beaufort Sea ecosystem. MEPS 647:195-210.

Comiso JC (2012) Large decadal decline of the arctic multiyear ice cover. J Clim 25:1176-1193

COSEWIC (2004) COSEWIC assessment and update status report on the beluga whale *Delphinapterus leucas* in Canada. Committee on the Status of Endangered Wildlife in Canada, Ottawa.

de March B, Maiers L, Friesen M (2002) An overview of genetic relationships of Canadian and adjacent populations of belugas (*Delphinapterus leucas*) with emphasis on Baffin Bay and Canadian eastern Arctic populations. NAMMCO Scientific Publications 4:17-38.

de March B, Stern G, Innes S (2004) The combined use of organochlorine contaminant profiles and molecular genetics for stock discrimination of white whales (*Delphinapterus leucas*) hunted in three communities on southeast Baffin Island. J Cetacean Res Manag 6:241-250.

de Valpine P, Hastings A (2002) Fitting population models incorporating process noise and observation error. Ecol Monogr 72:57-76.

Geweke J (1996) Evaluating the accuracy of sampling-based approaches to the calculation of posterior moments. In: Bernardo JM, Berger JM, Dawid AP, Smith AFM (eds) Bayesian Statistics 4. Oxford University Press, Oxford.

Gilg O, Kovacs KM, Aars J, Fort J, Gauthier G, Grémillet D, Ims RA, Meltofte H, Moreau J, Post E (2012) Climate change and the ecology and evolution of Arctic vertebrates. Ann N Y Acad Sci 1249:166-190.

Gough LA, Sverdrup-Thygeson A, Milberg P, Pilskog HE, Jansson N, Jonsell M, Birkemoe T (2015) Specialists in ancient trees are more affected by climate than generalists. Ecol Evol 5:5632-5641.

Gregory R, Long G (2009) Using structured decision making to help implement a precautionary approach to endangered species management. Risk Anal 29:518-532.

Hammill MO, Stenson GB, Doniol-Valcroze T (2017) A management framework for Nunavik beluga. DFO Can Sci Advis Sec Res Doc 2017/060:v + 34 p.

Hammill MO, Stenson GB, Mosnier A, Doniol-Valcroz T (2021) Trends in Abundance of Harp Seals, *Pagophilus Groenlandicus*, in the Northwest Atlantic, 1952-2019. DFO Can Sci Advis Sec Res Doc 2021/006. iv + 30 p.

Hauser DDW, Laidre KL, Stern HL, Moore SE, Suydam RS, Richard PR (2017) Habitat selection by two beluga whale populations in the Chukchi and Beaufort seas. PLOS ONE 12:e0172755-e0172755.

Heide-Jørgensen MP, Laidre KL (2004) Declining extent of open-water refugia for top predators in Baffin Bay and adjacent waters. Ambio 33:487-494.

Hilborn R, Walters CJ (2013) Quantitative fisheries stock assessment: choice, dynamics and uncertainty. Springer Science & Business Media, Dordrecht.

Hilborn R, Amoroso RO, Anderson CM, Baum JK, Branch TA, Costello C, De Moor CL, Faraj A, Hively D, Jensen OP, Kurota H, Little LR, Mace P, McClanahan T, Melnychuk MC, Minto C, Osio GC, Parma AM, Pons M, Segurado S, Szuwalski CS, Wilson JR, Ye Y (2020) Effective fisheries management instrumental in improving fish stock status. PNAS 117:2218-2224.

Hirsch SL (2020) Anticipatory practices: Shifting baselines and environmental imaginaries of ecological restoration in the Columbia River Basin. Environ Plan E: Nature and Space 3:40-57.

Horbowy J (1996) The dynamics of Baltic fish stocks on the basis of a multispecies stock-production model. Can J Fish Aquat Sci 53:2115-2125.

Hurrell JW, Hack JJ, Shea D, Caron JM, Rosinski J (2008) A new sea surface temperature and sea ice boundary dataset for the community atmosphere model. J Clim 21:5145-5153

Jacobson EK, Boyd C, McGuire TL, Shelden KEW, Himes Boor GK, Punt AE (2020) Assessing cetacean populations using integrated population models: an example with Cook Inlet beluga whales. Ecol Appl 30: e02114.

Kovacs KM, Lydersen C, Overland JE, Moore SE (2011) Impacts of changing sea-ice conditions on Arctic marine mammals. Mar Biodivers 41:181-194.

Laidre KL, Heide-Jørgensen M P, Stern H, Richard P (2012) Unusual narwhal sea ice entrapments and delayed autumn freeze-up trends. Polar Biol 35: 149-154.

Laidre KL, Stern H, Kovacs KM, Lowry L, Moore SE, Regehr EV, Ferguson SH, Wiig Ø, Boveng P, Angliss RP (2015) Arctic marine mammal population status, sea ice habitat loss, and conservation recommendations for the 21st century. Conserv Biol 29:724-737.

Laidre KL, Stirling I, Lowry LF, Wiig O, Heide-Jorgensen MP, Ferguson SH (2008) Quantifying the sensitivity of arctic marine mammals to climate-induced habitat change. Ecol Appl 18:S97-S125.

Lowry LF, Frost KJ, Zerbini A, Demaster D, Reeves RR (2008) 201 Trend in aerial counts of beluga or white whales (*Delphinapterus leucas*) in Bristol Bay, Alaska, 1993-2005. J Cetacean Res Manage 10:201-207.

Marcoux M, Hammill MO (2016) Model estimates of Cumberland Sound beluga (*Delphinapterus leucas*) population size and total allowable removals. DFO Can Sci Advis Sec Res Doc 2016/077. iv + 35 p.

Maslanik J, Stroeve J, Fowler C, Emery W (2011) Distribution and trends in Arctic sea ice age through spring 2011. Geophys Res Lett 38:L13502.

Maunder MN, Piner KR (2014) Contemporary fisheries stock assessment: many issues still remain. ICES J Mar Sci 72:7-18.

Maunder MN, Punt AE (2013) A review of integrated analysis in fisheries stock assessment. Fish Res 142:61-74.

Mitchell E, Reeves RR (1981) Catch history and cumulative catch estimates of initial population size of cetaceans in the eastern Canadian Arctic. Report of the Intern Whaling Comm 31:645-682.

Mosnier A, Doniol-Valcroze T, Gosselin J-F, Lesage V, Measures L, Hammill MO (2014) An age structured Bayesian population model for St. Lawrence Estuary beluga (*Delphinapterus leucas*). DFO Can. Sci. Advis. Sec. Res. Doc. 2013/127. v + 39 p.

O'Corry-Crowe GM (2009) Beluga whale: *Delphinapterus leucas*. In: Perrin WF, Würsig B, Thewissen JGM (ed) Encyclopedia of Marine Mammals. Elsevier, San Diego.

Parkinson CL (2014) Spatially mapped reductions in the length of the Arctic sea ice season. Geophys Res Lett 41:4316-4322.

Pella JJ, Tomlinson PK (1969) A generalized stock production model. Inter-Am Trop Tuna Comm Bulletin 13:416-497.

Plummer M JAGS: A program for analysis of Bayesian graphical models using Gibbs sampling. In: Proceedings of the 3rd International Workshop on Distributed Statistical Computing. Vienna, Austria.

Plummer M, Best N, Cowles K, Vines K (2006) CODA: convergence diagnosis and output analysis for MCMC. R news 6:7-11.

Preston KL, Rotenberry JT, Redak RA, Allen MF (2008) Habitat shifts of endangered species under altered climate conditions: importance of biotic interactions. Glob Chang Biol 14:2501-2515.

R Core Team (2020) R: A language and environment for statistical computing. R Foundation for Statistical Computing, Vienna, Austria.

Rayner N, Parker DE, Horton E, Folland CK, Alexander LV, Rowell D, Kent E, Kaplan A (2003) Global analyses of sea surface temperature, sea ice, and night marine air temperature since the late nineteenth century. J Geophys Res 108:4407.

Richard P, Stewart DB (2008) Information relevant to the identification of critical habitat for Cumberland Sound belugas (*Delphinapterus leucas*). DFO Can Sci Advis Secr Res Doc 2008/085:iv + 24 p.

Richard PR, Pike DG (1993) Small whale co-management in the Eastern Canadian Arctic: a case history and analysis. Arctic 46:138-143.

SARA (2017) Species at Risk Act, SC 2002, c 29.

Schaefer MB (1954) Some aspects of the dynamics of populations important to the management of the commercial marine fisheries. Inter-Am Trop Tuna Comm Bulletin 1:23-56.

Sergeant DE (1973) Biology of White Whales (*Delphinapterus leucas*) in Western Hudson Bay. J Fish Res Board Can 30:1065-1090.

Shea DJ, Trenberth KE, Reynolds RW (1992) A global monthly sea surface temperature climatology. J Clim 5:987-1001.

Shelden KEW, Rugh DJ, Mahoney B, Dahlheim ME (2003) Killer whale predation on belugas in Cook Inlet, Alaska: Implications for a depleted population. Mar Mamm Sci 19:529-544.

Singh RK, Maheshwari M, Oza SR, Kumar R (2013) Long-term variability in Arctic sea surface temperatures. Polar Sci 7:233-240.

Stenson G, Hammill MO (2008) Incorporating the precautionary approach into the provision of advice on marine mammals. DFO Can Sci Advis Sec Res Doc 2008/079. iv + 12 p.

Stenson GB, Buren A, Sheppard G (2020) Updated estimates of reproductive rates in Northwest Atlantic harp seals and the influence of body condition. DFO Can Sci Advis Sec Res Doc 2020/057. iv + 22 p.

Stewart BE, Stewart REA (1989) *Delphinapterus leucas*. Mamm Species 336:1-8.

Stroeve JC, Kattsov V, Barrett A, Serreze M, Pavlova T, Holland M, Meier WN (2012) Trends in Arctic sea ice extent from CMIP5, CMIP3 and observations. Geophys Res Lett 39:L16502.

Su Y-S, Yajima M (2015) R2jags: Using R to Run 'JAGS'. R package version 0.5-7. Available: CRAN R-project org/package= R2jags.

Thomsen F, McCully SR, Weiss LR, Wood DT, Warr KJ, Barry J, Law RJ (2011) Cetacean stock assessments in relation to exploration and production industry activity and other human pressures: review and data needs. Aquat Mamm 37:1-93.

Turgeon J, Duchesne P, Colbeck GJ, Postma LD, Hammill MO (2012) Spatiotemporal segregation among summer stocks of beluga (*Delphinapterus leucas*) despite nuclear gene flow: implication for the endangered belugas in eastern Hudson Bay (Canada). Conserv Genet 13:419-433.

Vatcheva KP, Lee M (2016) Multicollinearity in Regression Analyses Conducted in Epidemiologic Studies. Epidemiology 6:227.

Wade PR (1998) Calculating limits to the allowable human-caused mortality of cetaceans and pinnipeds. Mar Mamm Sci 14:1-37.

Wade PR (2018) Stock Assessment. In: Würsig B, Thewissen JGM, Kovacs KM (ed) Encyclopedia of Marine Mammals (Third Edition). Academic Press.

Wade PR, Angliss RP (1997) Guidelines for assessing marine mammal stocks: report of the GAMMS workshop April 3-5, 1996, Seattle, Washington. U.S. Dep. Commer., NOAA Tech. Memo. NMFS-OPR-12, 93 pp.

Watt CA, Marcoux M, Ferguson SH, Hammill MO, Matthews CJD (2020) Population dynamics of the threatened Cumberland Sound beluga (*Delphinapterus leucas*) population. Arctic Sci 7:545-566.

Watts PD, Draper BA, Henrico J (1991) Preferential use of warm water habitat by adult beluga whales. J Therm Biol 16:57-60.

Wenzel GW (2009) Canadian Inuit subsistence and ecological instability—if the climate changes, must the Inuit? Polar Res 28:89-99.

Wilkening J, Pearson-Prestera W, Mungi NA, Bhattacharyya S (2019) Endangered species management and climate change: When habitat conservation becomes a moving target. Wildl Soc Bull 43:11-20.

Williams R, Lacy RC, Ashe E, Hall A, Plourde S, McQuinn I H, Lesage V (2021) Climate change complicates efforts to ensure survival and recovery of St. Lawrence Estuary beluga. Mar Pollut Bull 173:113096.

Yadav J, Kumar A, Mohan R (2020) Dramatic decline of Arctic sea ice linked to global warming. Nat Hazards 103:2617-2621.

Chapter 4

4 Estimating abundance of Eastern Canada-West Greenland bowhead whales using genetic mark-recapture analyses

Brooke A. Biddlecombe[1,2], Steven H. Ferguson[1,2], Mads Peter Heide-Jørgensen[3], Darren M. Gillis[2], Cortney A. Watt[1,2]

[1]Freshwater Institute

Fisheries and Oceans Canada

Winnipeg, Manitoba, Canada

[2]Department of Biological Sciences

University of Manitoba

Winnipeg, Manitoba, Canada

[3]Greenland Institute of Natural Resources

Nuuk, Greenland

Citation:

Biddlecombe BA, Ferguson SH, Heide-Jørgensen MP, Gillis DM, Watt CA (2023) Estimating abundance of Eastern Canada-West Greenland bowhead whales using genetic mark-recapture analyses. Global Ecology and Conservation 45:e02524

Abstract

The Eastern Canada-West Greenland (EC-WG) bowhead whale (*Balaena mysticetus*) population is widely distributed across the eastern Canadian Arctic and across Baffin Bay to the western coast of Greenland. Their vast distribution makes obtaining population estimates via aerial surveys difficult, as coverage over their entire range is not possible. Genetic mark recapture analyses address this issue, as biopsy samples can be collected at various locales across the EC-WG bowhead whale population's distribution and microsatellites can be analyzed to identify unique individuals. EC-WG bowhead whales were subject to intense commercial whaling pressure between the early 1700s and early 1900s, after which a moratorium on commercial whaling was put in place in 1915. We used available genetic samples from EC-WG bowhead whales in mark recapture models to estimate population abundance from 2012-2021 to gain insight on population dynamics ~100 years post commercial whaling. The preferred model, using a Jolly-Seber structure, estimated the total abundance as 5173 individuals (CI: 3436-7788). Since the cessation of commercial whaling, the population has been thought to be rebounding, which is reflected by gradually increasing abundance estimates, from the low hundreds in the 1970s and 1980s, to ~6000 in the early 2000s, but our present estimate suggests population abundance may be plateauing well below the pre-commercial whaling carrying capacity estimate. This population estimate for EC-WG bowhead whales is required to update the population dynamics for conservation efforts.

4.1 Introduction

The Eastern Canada-West Greenland (EC-WG) bowhead whale (*Balaena mysticetus*) population is widely distributed across the eastern Canadian Arctic and across Baffin Bay to the western coast of Greenland, covering approximately 179,000 km^2 (Heide-Jørgensen et al. 2003, Doniol-Valcroze et al. 2015, Doniol-Valcroze et al. 2020, Fortune et al. 2020). EC-WG bowhead whales were heavily harvested by commercial whaling from 1530 – 1915, and population abundance was severely depleted (Finley 2001, Higdon 2010). The population has recovered to an estimated ~6900 individuals in 2013 (Rekdal et al. 2015, Frasier et al. 2020), but the rate of population growth, especially in more recent years, is largely unknown due to difficulties in acquiring reliable population estimates. The vast distribution of EC-WG bowhead whales makes obtaining population estimates via aerial surveys and subsequent distance sampling analyses difficult, as coverage over their entire range is not possible (Frasier et al. 2020). Genetic mark recapture (MRC) analyses can address this issue, as biopsy samples can be collected at various locales across the population's distribution, and informed modelling decisions can address the constraints of spatially limited sample collection.

Estimating abundance is a critical step in population management, as it provides a current reference point for comparisons to past population dynamics and informs management. There is often added difficulty when estimating abundance for marine wildlife because of issues surrounding reliable detection and uncertainty in distribution (Taylor et al. 2007, Pace III et al. 2017). Direct counts are commonly used in marine settings, such as distance sampling via surveys for a fixed area, but for widespread populations accurate estimates can be difficult to obtain (Taylor et al. 2007, Booth et al. 2020, Frasier et al. 2020). Mark-recapture (MRC) analyses are also commonly used for marine populations and provide a method of estimating

abundance which bypasses concerns surrounding survey coverage (Jolly 1965, Seber 1965, Hammond 2009, Booth et al. 2020).

Mark-recapture analysis can use multiple data types to estimate various population parameters and population abundance. In its basic form, MRC analyses focus on estimating population abundance using two or more capture events, where all individuals in the first capture event are marked, then the proportion of recaptured animals are recorded in subsequent capture events (Jolly 1965, Seber 1965). The proportion of recaptures provides an estimate of total population size when compared to the number of initial captures (Jolly 1965, Seber 1965). Multiple capture events allow for more in-depth analyses, with the inclusion of parameters such as survival and age structure, as well as opportunities to monitor population growth or decline (Pollock et al. 1990). As MRC methods have progressed, the goals have shifted from estimating abundance as in the Jolly-Seber (JS) method (Jolly 1965, Seber 1965), to estimating apparent survival and probability of capture for each capture event as in the Cormack-Jolly-Seber (CJS) method (Cormack 1964, Lebreton et al. 1992, Schwarz & Arnason 2009). These methodologies evolved as goals surrounding population monitoring have changed, and although CJS primarily aims to estimate the aforementioned parameters, the results can also be used to estimate abundance for each capture period (Lindenmayer et al. 1998, Santos-Moreno & Hernández-Aguilar 2021). MRC analyses rely on all individuals having an equal probability of capture. Populations with small distribution can typically address this relatively easily by sampling throughout the distribution. However, individual and species wide traits may still present sampling challenges, or make some individuals more prone to sampling than others (Nichols & Pollock 1983). In situations where the entire range cannot be sampled, or populations are large, the CJS method is useful as it addresses the fact that sampling occurs only in a relatively small

portion of the populations' range, but still assumes probability of capture is equal (Lebreton et al. 1992, Schwarz & Arnason 2009).

Originally MRC analyses involved adding a physical mark to caught individuals using bands, tags, implants, etc. Alternative capture or marking methods have become more prevalent as analyses methods have progressed, such as genetic identification or using photography to identifying unique individuals via scars or colouration (Mace et al. 1994, Mills et al. 2000, Hammond 2009, Frasier et al. 2020). These newer methods can collect data remotely, reducing the need to handle individuals. Genetic data for MRC analyses are typically collected via remote biopsy, fecal samples, or hair snags, making data collection more accessible for animals that are difficult to capture (Mills et al. 2000, Citta et al. 2018).

With genetic data, individuals are often identified using microsatellite genotypes (Mowat & Strobeck 2000, Constantine et al. 2012), which are short sections of repeating base pairs that have a high mutation rate (Ellegren 2004). The high mutation rate leads to high genetic diversity, which can allow for comparisons across multiple microsatellite loci to identify distinct individuals within the same species (Taberlet & Luikart 1999, Ellegren 2004). Using microsatellite markers for MRC analyses provides the benefit of remote capture but is accompanied by the uncertainty of identifying unique individuals with potential errors in the amplified microsatellites. To overcome this, a certain number of mismatches are typically allowed when determining if multiple samples are from a single individual (Constantine et al. 2012, Frasier et al. 2015). Identifying individuals using genetic markers allows for the identification of "recaptures" within and across years so data can be analysed within an MRC framework.

The objective of this research was to use available genetic samples from EC-WG bowhead whales to estimate annual population abundance from 2012-2021 to determine population abundance ~100 years post commercial whaling. Analyses were accomplished by identifying unique individuals from microsatellite data and using those as capture/recapture events in two types of MRC models. CJS models were used to address potential temporal trends, and JS models estimated total abundance assuming temporal trends were not present. We hypothesized, due to EC-WG bowhead whales' previously observed trend of growth from commercial whaling abundance, that the current population estimate would be slightly higher than estimates from previous years. We do not, however, expect significant temporal trends as our time series is short relative to the life span of bowhead whales and because their reproductive rates are low (George et al. 2021). Thus, notable population dynamics are more likely to occur on a longer time scale.

4.2 Methods

4.2.1 Sampling

Community based sampling occurred in Igloolik, Pangnirtung, Kugaaruk, Taloyoak, and Arctic Bay in Nunavut Canada and Disko Bay, Greenland (Figure 4.1). From 2012 – 2021 a total of 1165 samples were collected, although there were no captures in 2015.

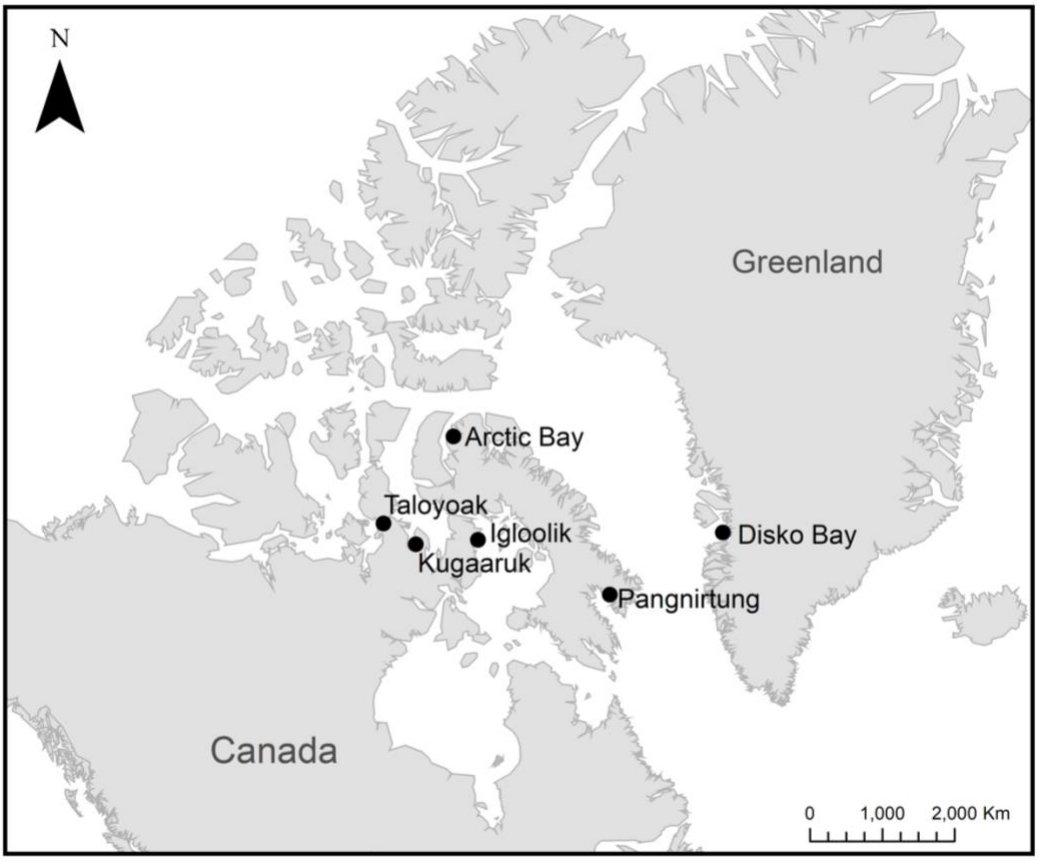

Figure 4.1 Locations of EC-WG bowhead whale biopsy samples.

The sampling protocol included the collection of small skin and blubber samples from free-swimming bowhead whales (*Balaena mysticetus*) using a 150 lb draw-weight cross bow (Excalibur Vixen) modified for tissue sample collection (from Ceta-DART, Denmark). Canadian biopsy samples were then preserved by flashing freezing in liquid nitrogen, or in a salt-saturated 20% DMSO solution (Seutin et al. 1991), RNAlater (Qiagen), or Allprotect (Qiagen), and frozen in the laboratory upon arrival. The Greenland biopsy samples were collected similarly, then placed in a 20% DMSO solution saturated with NaCl (Amos 1991) and frozen at -20°C.

4.2.2 Genetic Analyses

DNA extraction followed a modified version of the standard Qiagen extraction protocol (Wang et al. 2008). A μ Quant spectrophotometer (Bio-Tek) or NanoDrop spectrophotometer normalized to 10-100 ng/μl were used to quantify DNA. Amplification of 23 microsatellite loci was completed using multiple reactions (see Frasier et al. 2020 for details).

Pairwise comparisons were made between microsatellite genotypes from each sample to identify samples that were likely from the same individual. Matches were identified when there were differences in ≤ 3 of the 23 microsatellite loci (Frasier et al. 2020). Error in the assignment of recaptures is possible, and was not quantified, but ≤ 3 differences in microsatellite loci is an accepted threshold. Some samples did not have data for all 23 microsatellite loci; missing data were not counted as a difference as instances were relatively low. Pairwise matches were then compared to determine unique individuals and total number of captures for each, which resulted in a capture history from 2012-2012.

4.2.3 Estimating Abundance

Recaptures were first inspected by location to investigate a major assumption of both JS and CJS models: individuals must have equal probability of capture throughout their range. Recent research on EC-WG bowhead whale movement suggests that individuals make large scale movements across their range (Fortune et al. 2020), which suggests equal probability of capture. We aimed to confirm that recaptures were not isolated to a single location, as that would suggest individuals were not moving throughout their range and did not have equal probability of capture. Of the 90 total recaptures, 15 were in different locations, exclusively between Igloolik and Pangnirtung (the two most sampled locations), which are relatively far apart within EC-WG

bowheads' distribution (Figure 4.1). The separate capture locations suggest that individuals move to various locales within their range and capture across the EC-WG bowhead whale's range is possible. This should be considered with the caveat that EC-WG bowhead whales show segregation by sex and age throughout their range (Heide-Jørgensen et al. 2010, Fortune et al. 2020), and regions near Pangnirtung (in Cumberland Sound) appear to be primarily used by juveniles and sub-adults, while regions near Igloolik (in Foxe Basin) appear to be used by all age classes. As such, we assume equal catchability on a long-term scale, but this should be considered with scale of the EC-WG bowhead's range and their segregation in mind. Both CJS and JS models also assume the population is closed, with no migratory flow in or out. The vast size of this population's range combined with their genetic isolation from other bowhead populations (Baird & Bickham 2021) allows us to assume, on the short-term scale of this study, that the population is functionally closed.

To determine if captured individuals were age biased due to primary capture locations we analyzed body length, estimated in meters, or estimated as small, medium, or large during the time the biopsy was collected. Length is used as a proxy for age, where whales of both sexes <10m are identified as juveniles, and whales ≥10m are identified as sub-adults or adults (George et al. 2004, Higdon and Ferguson 2010, Fortune et al. 2020). Small and small/medium classified whales were assumed to be juveniles, and medium, medium/large, and large classifications were assumed sub-adult or adult. We did not have the resolution in our size data to differentiate between sub-adults and adults. We summarized ages of all captured individuals, as well as just those that had been recaptured. Because recaptures occurred exclusively near Pangnirtung and Igloolik, which are regions which may be juvenile biased, we wanted to determine if survival trends calculated from recaptures represented all age classes or were juvenile biased. Regions

near Pangnirtung have also been found to be used more by males than females (Heide-Jørgensen et al. 2010, Fortune et al. 2020), so we addressed potential sex biases in estimates by determining the proportion of males and females in both sub-adults/adults and juveniles.

Capture data were first analyzed with a CJS mark-recapture model (Lebreton et al. 1992) to estimate year-specific values for apparent survival rate (Φ) and probability of capture of marked individuals (*p*), which were then used to estimate annual population abundance. Within this model parameters can be constant or vary with each capture event (annual). Captures and recaptures were symbolized as a 1 in years where an individual was sampled, and 0 in a year where an individual was not sampled. For each individual capture history, in a year when the individual was sampled the probability of capture was estimated as p_t , where t is the capture year. When the individual was not sampled, probability of capture was estimated as 1- p_t . No probability of capture is estimated for the first capture period. The probability of apparent survival was estimated between capture periods as Φ_t, where t is the previous capture year. In a model where one or both parameters were set to vary annually, estimates from individuals are integrated to get annual Φ_t or p_t across all captures. In a model where one or both parameters were set to remain constant across years, estimates from individuals were integrated to estimate a single time series wide Φ or *p* value.

Four models were tested, all of which integrated capture histories from all individuals to achieve population estimates across the time series for 1) annual Φ_t and annual p_t, 2) annual Φ_t and constant *p*, 3) constant Φ and annual p_t, and 4) constant Φ and constant *p*.

Once a top model was selected (model selection described below) population abundance (N) was estimated for each year by taking the ratio of captured/recaptured individuals (n) to the probability of detection (*p*), N=n/p (Lindenmayer et al. 1998). Confidence intervals around

abundance estimates were estimated using the upper and lower confidence intervals the model estimated for *p*. Overlap of confidence intervals was inspected to determine if there was a significant temporal trend in abundance. A lack of temporal trend suggested that it is the same population of individuals throughout the time series because there were no significant additions or losses, and thus the abundance can be estimated with a single value.

To achieve a single abundance estimate, capture data were analyzed with a JS mark-recapture model. The JS model uses capture data to estimate four parameters. The first two are similar to the two estimated in the CJS model but include both marked and unmarked individuals: probability of capture for both marked and unmarked individuals (p), and the survival probabilities of both marked and unmarked animals (Φ). The final two parameters are super population size (N) which is the total number of individuals during the study period, and the probability of new individuals entering the super population (through births and immigration) at time t ($pent_t$). Parameter $pent_t$ is always estimated for each capture period, or annual time t, whereas, like the CJS model, p and Φ can be estimated annually or as constants. The general structure of how parameters are estimated is the same as described above for the CJS model except, in the JS model p is estimated for the first capture period. The JS model tested the same 4 model structures as the CJS model: 1) annual Φ_t and annual p_t, 2) annual Φ_t and constant p, 3) constant Φ and annual p_t, and 4) constant Φ and constant p. Each model also provided an estimate for N and annual estimates for $pent_t$.

The four models were first tested using all capture history data from all sample locations. Sampling effort for EC-WG bowhead whales is inconsistent across locations, so to test for potential spatial effects in the models, all four JS models were also run using only samples collected in Pangnirtung, the location with the greatest number of samples. Results for the top

model for full JS and the Pangnirtung JS models were compared for consistency, and to determine if sampling location had a potential effect on model estimates.

All model analyses were completed using package *marked* (*version 1.2.6;* Laake et al. 2013) in RStudio (*version 4.2.0;* RStudio Team 2020, R Core Team 2020) (see Appendix 3 for model code). Model fit was compared using AIC, where the top model had a ΔAIC of ≥ 2 compared to the next best model.

4.3 Results

Sampling intensity varied across locations with 877 from Pangnirtung, 273 samples from Igloolik, seven from Kugaaruk, six from Disko Bay, one from Taloyoak, and one from Arctic Bay (Table 4.1). Microsatellite loci comparisons identified 1068 unique individuals, of those, 88 were captured twice and 2 were captured three times from 2012-2021 (Table 4.1). The 877 samples from Pangnirtung which were isolated for the Pangnirtung JS models, consisted of 806 unique individuals and 65 recaptures.

Table 4.1 Total number of captures from EC-WG bowhead whales in each year and each capture location, with the number of those captures that were recaptures from a previous year in parentheses.

Year	Location	Number of Captures (Recaptures)
2012	Igloolik	114
	Pangnirtung	108
	Arctic Bay	1
	Taloyoak	1
2013	Igloolik	158(8)
	Pangnirtung	50(2)
2014	Pangnirtung	243(13)
	Disko Bay	6
2015	-	-
2016	Pangnirtung	85(8)
	Igloolik	1
2017	Pangnirtung	105(17)
2018	Pangnirtung	38(2)
2019	Pangnirtung	101(20)
2020	Pangnirtung	77(12)
	Kugaaruk	6
2021	Pangnirtung	70(10)
	Kugaaruk	1

Of the total 1165 biopsy samples, 51% had associated length estimates, of those 44% were classified as sub-adult or adults, and the remaining 56% were juveniles. 55% of recaptures were of sub-adult or adult whales. When the samples were subset to those collected near Pangnirtung, 67% had associated length estimates, of those, again, 56% were juveniles. Captured sub-adults/adults were 36% female, 55% male, and 9% were of unknown sex. Captured juveniles were 33% female, 53% males, and 14% were of unknown sex. This age breakdown allowed us to

move forward with the assumption that captures include the entire age structure of the EC-WG bowhead whale population, although the sample appears to be biased towards juveniles. The data did not allow us to separate sub-adults and adults, so the adult age class must be considered with the caveat that a portion of those whales are sub-adults and thus, not yet reproductive. The sex breakdown suggests that captures were slightly male biased, which was expected as most samples were collected near Pangnirtung, but there are no sex biases between adult and juvenile captures.

The top CJS model estimated constant Φ and annual *p* (Appendix 3. Table 1), the next best model, with a ΔAIC of 10.8 (Appendix 3. Table 2) estimated annual Φ and annual *p*. The subsequent abundance estimates from the top model are 4546, 7896, 6723, 4350, 14 961, 4094, 6096, and 6645 for 2013-2021 (excluding 2015), respectively (Figure 4.2). No estimates could be made for 2015 due to the absence of captures. The uncertainty around the 2018 estimate is higher than other years due to a smaller number of captures in that year. There is no clear temporal trend in abundance and no significant difference between abundance estimates in each year, as all confidence intervals overlap. The lack of trend suggests the population is largely the same individuals throughout the time period or there are equal amounts of gains and losses, thus, a single population estimate calculated in a JS model would more concisely show population status while accounting for minor fluctuations.

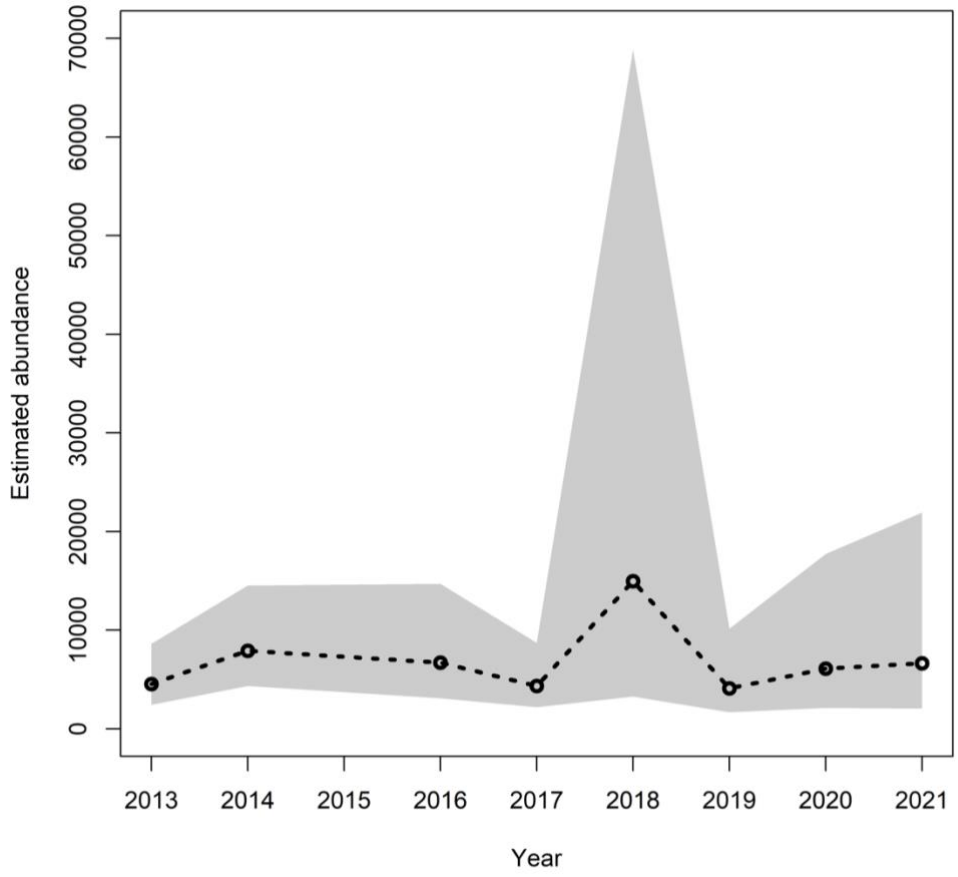

Figure 4.2 Annual abundance estimates for the EC-WG bowhead whale population from a Cormack-Jolly-Seber mark recapture model. Black points show annual abundance estimates, while the grey polygon indicates the confidence interval.

The JS model became the preferred model structure to achieve a single abundance estimate. The first JS models included samples from all sampling locations. The top JS model estimated constant Φ and annual *p* (Table 4.2), the next best model, with a ΔAIC of 9.7 (Appendix 3. Table 3) estimated annual Φ and annual *p*. The super population abundance estimate (*N*) was 5173 individuals (CI: 3436-7788). To address any potential spatial effects from inconsistent sampling, the JS models were also run using only samples collected from

Pangnirtung. The top Pangnirtung JS model also estimated constant Φ and annual *p* (Table 4.3), the next best model, with a ΔAIC of 12.9 (Appendix 3. Table 4) estimated annual Φ and annual *p.* The super population abundance estimate was 4227 individuals (CI: 2771-6447). The estimates from both JS models are not significantly different as they have overlapping confidence intervals (Figure 4.3).

Table 4.2 Estimated survival probability (Φ), probability of capture (*p*), super abundance estimate (*N*), and probability of individuals entering the super population (*pent*) from the top Jolly-Seber mark recapture model for EC-WG bowhead whales sampled from 2012-2021 from all sampling locations. No samples were taken in 2015.

Φ				
Year	**Estimated Survival Rate**	**SE**	**Lower Confidence Limit**	**Upper Confidence Limit**
All	0.9826	0.0586	0.0637	0.9999
p				
Year	**Estimated probability of capture**	**SE**	**Lower Confidence Limit**	**Upper Confidence Limit**
2012	0.0377	0.0074	0.0255	0.0553
2013	0.0355	0.0062	0.0252	0.0498
2014	0.0431	0.0071	0.0312	0.0593
2015	-	-	-	-
2016	0.0147	0.0029	0.0100	0.0216
2017	0.0185	0.0040	0.0121	0.0283
2018	0.0068	0.0019	0.0039	0.0118
2019	0.0182	0.0054	0.0102	0.0324
2020	0.0151	0.0052	0.0077	0.0295
2021	0.0130	0.0052	0.0060	0.0281

Cont.

pent				
Year	**Estimated probability of individuals entering population**	**SE**	**Lower Confidence Limit**	**Upper Confidence Limit**
Same for all years	0.0071	0.0315	$1.120x10^{-6}$	0.9785

N				
Year	**Estimated population size**	**SE**	**Lower Confidence Limit**	**Upper Confidence Limit**
All	5172.69	1079.87	3435.68	7787.90

Table 4.3 Estimated survival probability (Φ), probability of capture (*p*), super abundance estimate (*N*), and probability of individuals entering the super population (*pent*) from the top Jolly-Seber mark recapture model for EC-WG bowhead whales sampled from 2012-2021 from Pangnirtung. No samples were taken in 2015.

Φ				
Year	**Estimated Survival Rate**	**SE**	**Lower Confidence Limit**	**Upper Confidence Limit**
All	0.9999	0.0016	$4.98x10^{-30}$	1
p				
Year	**Estimated probability of capture**	**SE**	**Lower Confidence Limit**	**Upper Confidence Limit**
2012	0.0303	0.0107	0.0151	0.0601
2013	0.0131	0.0040	0.0072	0.0237
2014	0.0618	0.0133	0.0403	0.0937
2015	-	-	-	-
2016	0.0204	0.0039	0.0141	0.0296
2017	0.0244	0.0038	0.0180	0.0331
2018	0.0085	0.0017	0.0058	0.0125
2019	0.0217	0.0034	0.0159	0.0295
2020	0.0159	0.0030	0.0110	0.0229
2021	0.0139	0.0030	0.0091	0.0212
pent				
Year	**Estimated probability of individuals entering population**	**SE**	**Lower Confidence Limit**	**Upper Confidence Limit**
Same for all years	0.0366	0.0410	0.0039	0.2709
N				
Year	**Estimated population size**	**SE**	**Lower Confidence Limit**	**Upper Confidence Limit**
All	4226.64	910.32	2771.16	6446.57

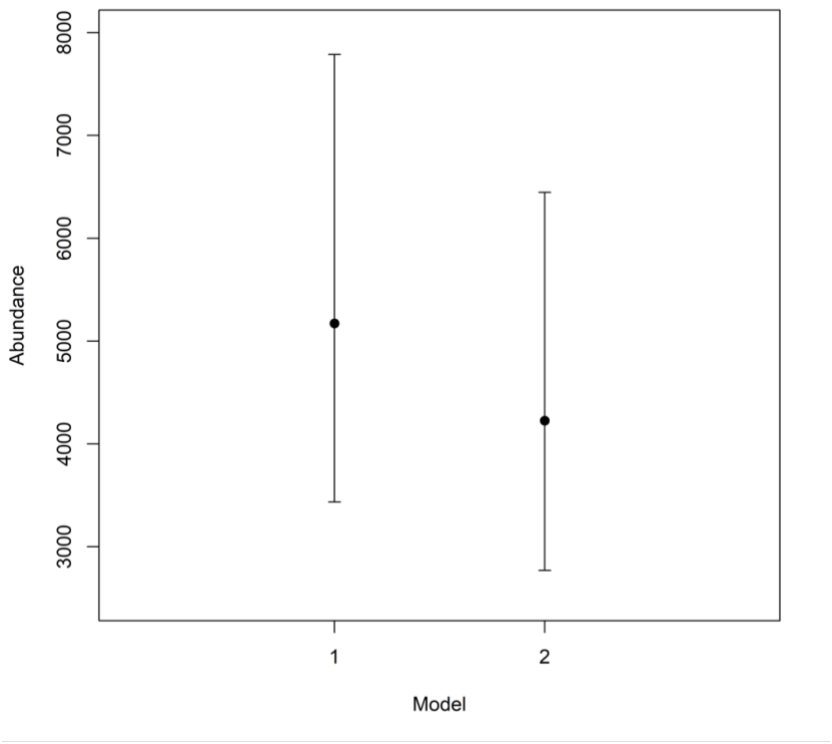

Figure 4.3 Comparison of abundance estimates with 95% confidence intervals from two Jolly-Seber mark recapture models for the EC-WG bowhead whale population sampled from 2012-2021. Model 1 includes samples from all locations, model 2 includes only samples collected in Pangnirtung.

4.4 Discussion

Our analyses estimated EC-WG bowhead whale (*Balaena mysticetus*) population abundance from 2012-2021 using genetic data collected via biopsy samples from various locales across their distribution. The vastness of the EC-WG bowhead population's range has historically presented challenges for population abundance estimates, as aerial surveys cannot cover their entire distribution, and segregated movement throughout their range made sample-based estimation methods difficult to analyze (Reeves et al. 1983, Finley 2001, Ferguson et al. 2010). The EC-WG bowhead population abundance has been estimated previously using a

genetic MRC model design that subdivided the samples by location and attempted to account for unsampled locations across their vast range (Frasier et al. 2020). We opted to analyze the population as one cohesive unit because recent research from Fortune et al. (2020) suggests that, while the intensity of use of different habitat regions varies based on age and sex, areas of predicted used for each group are spread throughout their distribution, thus on a long-term scale EC-WG bowheads have the potential to be captured throughout their range. This is supported by our inspection of recapture location, which occurred across their distribution for multiple individuals. Previous estimates used samples up to 2013 (Frasier et al. 2020), while our model updates the EC-WG bowhead whale abundance estimate by including samples up to 2021 (n=733 since 2013).

The age analysis of samples suggests that captures provide data for multiple age classes. Cumberland Sound is recognized as a high use area for juvenile bowhead whales (Fortune et al. 2020), and with much of the sampling occurring in Pangnirtung there was potential for the models to result in juvenile only estimates. 56% of the data being collected from juveniles does suggest our estimates are biased towards juveniles, but the included proportion of adults allows us to assume the estimates reflect something closer to a total population estimate than an exclusively juvenile one. Our inability to confidently separate the sub-adult and adult age classes, however, suggests that the mating proportion of the population may be underrepresented in our sample, as sub-adults are sexually immature. The current age distribution of EC-WG bowhead whales is unknown, but we can assume juveniles are overrepresented in our captures because adults are typically the largest group within the age structure of mysticete whales (Hamilton et al. 1998, Evans and Hindell 2004). The proportion of males and females also shows estimates are less biased than was expected based on previous EC-WG bowhead whale space use

analyses. Fortune et al. (2020) suggests that Cumberland Sound is not commonly used by adult female bowhead whales, and although our data shows a smaller proportion of adult females than adult males, the presence of multiple adult female samples from this region suggests more use than anticipated. This presence of adults in CS could also be driven by sub-adults within the sub-adult/adult group, thus maintaining that CS is primarily used by younger whales. The divisions of sex and age in captures suggest that, although an awareness of biases in our model estimates is necessary, the sample collection does not restrict model results to a single demographic group of the EC-WG bowhead whale population.

Results suggested that the JS model structure is preferred for the EC-WG bowhead whale population during our study period. The CJS model revealed no temporal trend in population abundance, which suggests that the individuals in this population from 2012-2021 have largely stayed the same. This temporal stability in abundance is novel because previous analyses of population dynamics for EC-WG bowhead whales show rapid increase (i.e., Ferguson et al. 2021), and our results suggest this trend of increase may be moving toward a plateau. To assess model robustness within the JS structure, we compared a model with all samples from all locations, and a reduced model with samples just from Pangnirtung, the primary sampling location. Both sampling regimes resulted in the same top model, which estimated constant Φ and annual *p*. Resulting abundance estimates were similar, with the estimate from all samples being ~900 individuals higher, and confidence intervals heavily overlapping. The similarities between the two models suggests there is likely not a spatial affect from sampling. We suspect the lower abundance estimate from the Pangnirtung model is the result of an overall reduced sample size, especially considering it removed all recaptures that occurred away from Pangnirtung, thus the model including all samples is the most preferred model. We also anticipated that the reduced

estimate from the Pangnirtung model would be due to samples being more juvenile biased, thus giving a juvenile only estimate. Conversely, the age distribution of Pangnirtung samples was the same as the full capture history, which for both is juvenile biased, but not exclusively juvenile. Although, the adult group in Pangnirtung could be more sub-adult biased than the adult group across all samples, potentially furthering the abundance estimate toward a non-reproductive whale bias. Previous observations suggest primarily young bowhead whales in CS, but it is difficult to confirm a sub-adult bias within the adult age class in our data as a large portion of our size estimates are vague.

Our estimates are within the range of what has been estimated by previous abundance analyses in similar time periods. Frasier et al. (2020) estimated a total abundance of 6877 whales after pooling samples from 2008-2013, although our estimate is lower, Frasier et al.'s (2020) estimate falls within our 95% confidence interval so the difference is not significant. Similarly, a 2013 aerial survey for EC-WG bowhead whales Doniol-Valcroze et al. (2015) estimated a total abundance of 6446, again our 2013 estimate is lower, but not significantly lower as the aerial survey results fall within our 95% confidence interval. Survival probability from our best model was 0.98 (closely matched by an estimate of 0.99 in the Pangnirtung JS model, and 0.98 in the CJS model). The exceptionally high estimated survival rates make sense because bowhead whales are the longest-lived mammal, waiting 25 years for first reproduction (George et al. 1999, Bockstoce 2008), so high survival between years is expected. That said, previous survival estimates from the Bering-Chukchi-Beaufort Sea bowhead whale population were marginally higher (Givens et al. 2017), which is likely a reflection of our captures being juvenile biased. This should be considered with the caveat that as we gain more knowledge of bowhead whale

population structure a greater understanding of juvenile mortality is still required, which will allow for the estimation of age specific survival probabilities.

EC-WG bowhead whales were subject to intense commercial whaling pressure between the early 1700s and early 1900s, after which a moratorium on commercial whaling was put in place in 1915 (Ross 1993, Higdon 2010). Since then, the population has been thought to be rebounding, which is reflected by gradually increasing abundance estimates, from the low hundreds in the 1970s and 1980s (Davis & Koski 1980, Zeh et al. 1993), to ~6000 in the early 2000s (IWC 2009), to our estimate of ~5200 in 2012-2021 which reflects a potential plateau in growth. This plateau is further supported by the lack of temporal trend in the CJS model. We think this estimate is robust because we tested multiple model types and sample groups, and we have an updated understanding of movement within the EC-WG bowhead population, but there are spatial and logistic constraints, and sampling biases that should be considered. The life span of bowheads is >200 years (George et al. 2021) and thus, population dynamics occur slowly, our nine year sample period does not allow for the observation of significant changes in population size which is reflected by the lack of temporal trend in our CJS model. The time series is short, providing short term insight, but making it difficult to extrapolate abundance into a long-term perspective. The similarity between our abundance estimate and the former estimates (Doniol-Valcroze et al. 2015, Frasier et al. 2020) suggests that EC-WG bowhead whales may be approaching a plateau in population growth rate. This plateau suggests that the EC-WG bowhead whale population may not approach the estimated pre-commercial whaling abundance of ~18,500 whales (Ferguson et al. 2021). This could be due to a change in the carrying capacity of the Arctic ecosystem, or other stressors that are affecting bowhead whale population growth (Laidre et al. 2008, Moore et al. 2021). The reduced carrying capacity could be explained by the

concept that large whales fertilize the oceans through a feedback loop, but the loss of baleen whales throughout human history could have broken this loop, thus reducing carrying capacity (Dufort et al. 2022). Continued sampling into the future is necessary for clarity on current abundance trends and changes in carrying capacity.

One of the constraints of this data set was unequal sampling effort across years. Samples ranged from 38-249 annually, with a standard deviation of 76.3. The lowest sampling effort occurred in 2018 with 38 samples (second lowest was 71 in 2021). The effect of unequal sampling is more evident in the CJS model, as 2018, the year with lowest number of samples, has the abundance estimate that differs most from the average, and the greatest amount of uncertainty surrounding that estimate. The JS models are less affected by unequal sampling, as all samples are included into a single abundance estimate.

The EC-WG bowhead whale population was analyzed as one group, with the assumption that individuals spend time in various parts of their distribution and are not explicitly segregated (Fortune et al. 2020), and molecular genetic analyses support this assumption as they suggest it is a single population (Postma et al. 2006). Previous work by Reeves et al. (1983), Finley (2001), Cosens & Blouw (2003), and Heide-Jørgensen et al. (2010) suggest there are seasonal age and sex segregations in the population. Frasier et al. (2020) worked with the evidence of spatial segregation throughout the population, estimating abundance for multiple regions separately and analyzing movement to account for unsampled regions. Even with these observed segregations, we opted to analyze the population as a whole. Although the timing of movement changes between individuals, from a sample of 43 individuals, over half were found to reside in Hudson Strait and Frobisher Bay over winter, and nearly 75% of individuals had locations in Foxe Basin (Fortune et al. 2020). The high use of these (and other) spatially separate regions suggests a

notable number of individuals are travelling across the population's range. This decision was further supported by our findings that multiple recaptures occurred between widespread sampling locations (i.e., Pangnirtung and Igloolik). We have quantified a bias towards juveniles within our samples, and behaviourally there may be some distinction between groups in the EC-WG bowhead population which may also lead to sampling bias, but for MRC analyses the large-scale interannual movement of sampled individuals and presence of all age-classes in captures allows the population to be analyzed as a whole.

This work provides a new, updated perspective on trends in abundance for the EC-WG bowhead whale population. The CJS model first allowed us to conclude that during the study period the population abundance was likely not changing a significant amount, suggesting for the first time, that population growth may be plateauing. The JS models allowed for a comparison in spatial sampling structure to determine that restricting samples to a single locale had only a minor effect on abundance estimates. The results from the best JS model also suggested that the abundance of EC-WG bowhead whales is no longer increasing at a steady rate, as was predicted, but rather, in reference to recent estimates (Doniol-Valcroze et al. 2015, Frasier et al. 2020), appears to be plateauing. Model results provide a short-term perspective of current abundance relative to a long-lived species; a longer time series of samples collected in the future could be valuable to uncover temporal trends using a CJS model and ensure that the population is not declining. Results can also be considered in a broader context when evaluating pre-commercial whaling abundance, and current management goals associated with ensuring a sustainable harvest since carrying capacity estimates may need to be reviewed. Our model provides a current, plausible abundance estimate that may be slightly lower than true abundance due to the high proportion of juveniles captured, which is valuable for managing a population like EC-WG

bowhead whales that incurs anthropogenic mortality and whose vast range has presented so many conservation challenges.

4.5 References

Amos W (1991) Long-term skin preservation of whale skin for DNA analysis. Rep Int Whaling Comm Spec Issue 13:99-103.

Baird AB, Bickham JW (2021) The stocks of bowheads. In: George JC, Thewissen JGM (ed) The Bowhead Whale. Academic Press, pp. 19-29.

Bockstoce JR (2008) Two historical weapon fragments as an aid to estimating the longevity and movements of bowhead whales. Polar Biol 31:751-754.

Booth CG, Sinclair RR, Harwood J (2020) Methods for Monitoring for the Population Consequences of Disturbance in Marine Mammals: A Review. Front Mar Sci 7:115.

Citta JJ, O'Corry-Crowe G, Quakenbush LT, Bryan AL, Ferrer T, Olson MJ, Hobbs RC, Potgieter B (2018) Assessing the abundance of Bristol Bay belugas with genetic mark-recapture methods. Mar Mamm Sci 34:666-686.

Constantine R, Jackson JA, Steel D, Baker CS, Brooks L, Burns D, Clapham P, Hauser N, Madon B, Mattila D (2012) Abundance of humpback whales in Oceania using photo-identification and microsatellite genotyping. MEPS 453:249-261.

Cormack RM (1964) Estimates of survival from the sighting of marked animals. Biometrika 51:429-438.

Cosens SE, Blouw A (2003) Size-and age-class segregation of bowhead whales summering in northern Foxe Basin: a photogrammetric analysis. Mar Mamm Sci 19:284-296.

Davis RA, Koski WR (1980) Recent observations of the bowhead whale in the eastern Canadian high Arctic. Rep Int Whaling Comm 30:439-444.

Doniol-Valcroze T, Gosselin J-F, Pike D, Lawson J, Asselin N, Hedges K, Ferguson S (2015) Abundance estimate of the Eastern Canada – West Greenland bowhead whale population

based on the 2013 High Arctic Cetacean Survey. DFO Can Sci Advis Sec Res Doc 2015/058:v + 27 p.

Doniol-Valcroze T, Gosselin J-F, Pike DG, Lawson JW, Asselin NC, Hedges KJ, Ferguson SH (2020) Distribution and Abundance of the Eastern Canada – West Greenland Bowhead Whale Population Based on the 2013 High Arctic Cetacean Survey. NAMMCO Scientific Publications 11.

Durfort A, Mariani G, Tulloch V, Savoca MS, Troussellier M, Mouillot D (2022) Recovery of carbon benefits by overharvested baleen whale populations is threatened by climate change. Proceed Royal Soc B 289: p.20220375.

Ellegren H (2004) Microsatellites: simple sequences with complex evolution. Nat Rev Genet 5:435-445.

Evans K, Hindell MA (2004) The age structure and growth of female sperm whales (*Physeter macrocephalus*) in southern Australian waters. J Zool 263:237-25.

Ferguson SH, Dueck L, Loseto LL, Luque SP (2010) Bowhead whale *Balaena mysticetus* seasonal selection of sea ice. MEPS 411:285-297.

Ferguson SH, Higdon JW, Hall PA, Hansen RG, Doniol-Valcroze T (2021) Developing a Precautionary Management Approach for the Eastern Canada-West Greenland Population of Bowhead Whales (*Balaena mysticetus*). Front Mar Sci 8.

Finley K (2001) Natural history and conservation of the Greenland whale, or bowhead, in the Northwest Atlantic. Arctic:55-76.

Fortune SME, Young BG, Ferguson SH (2020) Age- and sex-specific movement, behaviour and habitat-use patterns of bowhead whales (*Balaena mysticetus*) in the Eastern Canadian Arctic. Polar Biol 43:1725-1744.

Frasier TR, Petersen SD, Postma L, Johnson L, Heide-Jørgensen MP, Ferguson SH (2015) Abundance estimates of the Eastern Canada-West Greenland bowhead whale (*Balaena mysticetus*) population based on genetic capture-mark-recapture analyses. DFO Can Sci Advis Sec Res Doc 2015/008:iv + 21 p.

Frasier TR, Petersen SD, Postma L, Johnson L, Heide-Jørgensen MP, Ferguson SH (2020) Abundance estimation from genetic mark-recapture data when not all sites are sampled: An example with the bowhead whale. Global Ecol Conserv 22:e00903.

George JC, Bada J, Zeh J, Scott L, Brown SE, O'Hara T, Suydam R (1999) Age and growth estimates of bowhead whales (*Balaena mysticetus*) via aspartic acid racemization. Can J Zool 77:571-580.

George JC, Follmann E, Zeh J, et al (2004) Inferences from bowhead whale ovarian and pregnancy data: age estimates, length at sexual maturity and ovulation rates. Paper SC/56/BRG8 presented to the International Whaling Commission Scientific Committee.

George JC, Thewissen JGM, Von Duyke A, Breed GA, Suydam R, Sformo TL, Person BT, Brower Jr H (2021) Life history, growth, and form. In: George JC, Thewissen JGM (ed) The Bowhead Whale. Academic Press, pp 87-115.

Givens GH, Mocklin JA, Brattström LV, et al (2017) Survival rate and 2011 abundance of Bering–Chukchi–Beaufort Seas bowhead whales from photo-identification data over three decades. Paper SC/67a/AWMP09 presented to the Scientific Committee of the International Whaling Commission.

Hamilton PK, Knowlton AR, Marx MK, Kraus SD (1998) Age structure and longevity in North Atlantic right whales *Eubalaena glacialis* and their relation to reproduction. MEPS 171:285-292.

Hammond PS (2009) Mark–recapture. In: Perrin WF, Würsig B, Thewissen JGM (ed) Encyclopedia of marine mammals, 2nd edn. Academic Press, pp 705-709.

Heide-Jørgensen M, Laidre K, Wiig Ø, Jensen M, Dueck L, Maiers L, Schmidt H, Hobbs R (2003) From Greenland to Canada in ten days: Tracks of bowhead whales, *Balaena mysticetus*, across Baffin Bay. Arctic 56:21-31.

Heide-Jørgensen M, Laidre K, Wiig Ø, Postma L, Dueck L, Bachmann L (2010) Large-scale sexual segregation of bowhead whales. Endanger Species Res 13:73-78.

Higdon JW (2010) Commercial and subsistence harvests of bowhead whales (*Balaena mysticetus*) in eastern Canada and West Greenland. J Cetacean Res Manag 11:185-216.

Higdon JW, Ferguson SH (2010) Past, present, and future for bowhead whales (*Balaena mysticetus*) in northwest Hudson Bay. In: Ferguson SH, Loseto LL, Mallory ML (ed) A little less Arctic: Top predators in the world's largest northern inland sea, Hudson Bay. Springer, New York, pp 159–177.

IWC (2009) Annex F: Report of the Sub-Committee on Bowhead, Right and Gray Whales. J Cetacean Res Manag 11:168.

Jolly GM (1965) Explicit estimates from capture-recapture data with both death and immigration-stochastic model. Biometrika 52:225-247.

Laake J, Johnson D, Conn P (2013) marked: An R package for maximum-likelihood and MCMC analysis of capture-recapture data. Methods Ecol Evol 4:885-890.

Laidre KL, Stirling I, Lowry LF, Wiig O, Heide-Jorgensen MP, Ferguson SH (2008) Quantifying the sensitivity of arctic marine mammals to climate-induced habitat change. Ecol Appl 18:S97-S125.

Lebreton J-D, Burnham KP, Clobert J, Anderson DR (1992) Modeling Survival and Testing Biological Hypotheses Using Marked Animals: A Unified Approach with Case Studies. Ecol Monogr 62:67-118.

Lindenmayer D, Lacy R, Viggers K (1998) Modelling survival and capture probabilities of the mountain brushtail possum (*Trichosurus caninus*) in the forests of south-eastern Australia using trap-recapture data. J Zool 245:1-13.

Mace RD, Minta SC, Manley TL, Aune KE (1994) Estimating grizzly bear population size using camera sightings. Wildl Soc Bull:74-83.

Mills LS, Citta JJ, Lair KP, Schwartz MK, Tallmon DA (2000) Estimating animal abundance using noninvasive DNA sampling: promise and pitfalls. Ecol Appl 10:283-294

Moore SE, George J, Reeves RR (2021) Bowhead whale ecology in changing high-latitude ecosystems. In: George JC, Thewissen JGM (ed) The Bowhead Whale. Academic Press, pp 417-427.

Mowat G, Strobeck C (2000) Estimating Population Size of Grizzly Bears Using Hair Capture, DNA Profiling, and Mark-Recapture Analysis. J Wildl Manag 64:183.

Nichols JD, Pollock KH (1983) Estimation Methodology in Contemporary Small Mammal Capture-Recapture Studies. J Mammal 64:253-260.

Pace III RM, Corkeron PJ, Kraus SD (2017) State–space mark–recapture estimates reveal a recent decline in abundance of North Atlantic right whales. Ecol Evol 7:8730-8741

Pollock KH, Nichols JD, Brownie C, Hines JE (1990) Statistical inference for capture-recapture experiments. Wildl Monogr 107:3-97.

Postma LD, Dueck LP, Heide-Jørgensen MP, Cosens SE (2006) Molecular genetic support of a single population of bowhead whales (*Balaena mysticetus*) in Eastern Canadian Arctic and Western Greenland waters. DFO Can Sci Advis Sec Res Doc 2006/051.

R Core Team (2020) R: A language and environment for statistical computing. R Foundation for Statistical Computing, Vienna, Austria. URL https://www.R-project.org/.

Reeves R, Mitchell E, Mansfield A, McLaughlin M (1983) Distribution and migration of the bowhead whale, *Balaena mysticetus*, in the eastern North American Arctic. Arctic 36:5-64.

Rekdal SL, Hansen RG, Borchers D, Bachmann L, Laidre KL, Wiig Ø, Nielsen NH, Fossette S, Tervo O, Heide-Jørgensen MP (2015) Trends in bowhead whales in West Greenland: Aerial surveys vs. genetic capture-recapture analyses. Mar Mamm Sci 31:133-154.

Ross WG (1993) Commercial whaling in the North Atlantic sector. In: Burns JJ, Montague JJ, Cowles CJ (ed) The Bowhead Whale. Society for Marine Mammalogy Special Publication Number 2, Lawrence, Kansas, pp 511–561.

RStudio Team (2020) RStudio: Integrated Development for R. RStudio, PBC, Boston, MA URL http://www.rstudio.com/.

Santos-Moreno A, Hernández-Aguilar I (2021) Estimation of bat colony size even with low recapture rates: an example based on the Cormack-Jolly-Seber model in Oaxaca, México. Rev Biol Tropical 69:231-244.

Schwarz CJ, Arnason AN (2009) Jolly-Seber models in MARK. In: Cooch E, White G (ed) MARK: A gentle introduction, 8th edn. Available: http://www.phidot.org/software/mark/docs/book.

Seber GA (1965) A note on the multiple-recapture census. Biometrika 52:249-259.

Seutin G, White BN, Boag PT (1991) Preservation of avian blood and tissue samples for DNA analyses. Can J Zool 69:82-90.

Taberlet P, Luikart G (1999) Non-invasive genetic sampling and individual identification. Biol J Linn Soc 68:41-55.

Taylor BL, Martinez M, Gerrodette T, Barlow J, Hrovat YN (2007) Lessons from monitoring trends in abundance of marine mammals. Mar Mamm Sci 23:157-175.

Wang J, Frasier T, Yang S, White B (2008) Detecting recent speciation events: the case of the finless porpoise (genus *Neophocaena*). Heredity 101:145-155.

Zeh JE, Clark CW, George JC, Withrow D, Carroll GM, Koski WR (1993) Current population size and dynamics. In: Burns JJ, Montague JJ, Cowles CJ (ed) The Bowhead Whale. Society for Marine Mammalogy Special Publication Number 2, Lawrence, Kansas, pp 409-489.

Chapter 5

5 Combining multiple data sources to extrapolate population estimates and model population dynamics of Eastern Canada-West Greenland bowhead whales

Brooke A. Biddlecombe[1,2], Mads Peter Heide-Jørgensen[3], Steven H. Ferguson[1,2], Darren Gillis[2], Cortney A. Watt[1,2]

[1]Freshwater Institute

Fisheries and Oceans Canada

Winnipeg, Manitoba, Canada

[2]Department of Biological Sciences

University of Manitoba

Winnipeg, Manitoba, Canada

[3]Greenland Institute of Natural Resources

Nuuk, Greenland

Citation:

Biddlecombe BA, Heide-Jørgensen MP, Ferguson SH, Gillis D, Watt CA (2023) Combining multiple data sources to extrapolate population estimates and model population dynamics of Eastern Canada-West Greenland bowhead whales. Ecological Modelling. *Submitted*

Abstract

The Eastern Canada-West Greenland (EC-WG) bowhead whales (*Balaena mysticetus*) were heavily harvested from 1530 – 1915, and the population was depleted to commercial extinction. The Committee on the Status of Endangered Wildlife in Canada has classified this population as "Special Concern" due to increased vulnerability to killer whale predation as a result of reduced ice coverage, despite indications of growth since the end of commercial whaling. Obtaining reliable estimates of abundance through aerial surveys can be challenging due to the vast area that needs to be covered. To overcome this, a Brownian bridge movement model (BBMM) was used with data obtained from satellite-tagged bowhead whales. The BBMM was employed to generate a map displaying the probability density of occupancy of whales within the range of EC-WG bowhead whale population. The BBMM also allowed the calculation of the probability of occupancy both inside and outside areas surveyed during aerial surveys conducted in 1981, 2002 and 2013. By applying a Quasi-Poisson regression, the relationship between the probability of occupancy and abundance in the surveyed areas was established. This relationship was then used to extrapolate survey estimates into unsurveyed areas. Extrapolated estimates were included with genetic mark-recapture abundance estimates from 2013 and 2017 and harvest history into a Bayesian stock production model to recreate population dynamics post-commercial whaling, 1915-2022, and project 10 years into the future under various harvest levels (0, 10, 20, 30 whales). The model estimated a 2022 population of 8243 (95% CI 5201-14,950) whales, and an initial population (N_{1915}) estimate of 1028 (95% CI 213-4758) whales. By computing the likelihood of population decline, the determination of a sustainable harvest indicated probabilities of decline ranging from 24-53% after a 10-year period across all harvest levels. The findings of the model suggest that EC-WG bowhead whales have been consistently recovering

following the cessation of commercial whaling and have already surpassed the point of maximum productivity, leading to a slowdown in growth in recent years. This model provides updated insights into the population dynamics of the EC-WG bowhead whale population, utilizing a variety of available data sources in an attempt to generate the most informed estimates possible.

5.1 Introduction

Bowhead whales (*Balaena mysticetus*) are the only Arctic resident mysticete whale; they are an ice-associated filter feeder with a near circumpolar distribution (Finley 2001, Rugh and Shelden 2009). Similar to the two Arctic odontocetes (beluga whale (*Delphinapterus leucas*) and narwhal (*Monodon monoceros*)), bowhead whales migrate annually, moving further north as the ice retreats in the summer, and using sea ice as cover from killer whale predation (Matthews et al. 2020, Reinhart et al. 2013). Due to their association with sea ice, they have adapted the ability to break through up to 60 cm of ice to create breathing holes (Rugh and Shelden 2009). There are two defined bowhead whale populations in the Canadian Arctic, the Eastern Canada-West Greenland (EC-WG) population and the Bering-Chukchi-Beaufort (BCB) population.

The Eastern Canada-West Greenland (EC-WG) bowhead whale population spends summers in Gulf of Boothia and Prince Regent Inlet and migrates to Hudson and Davis Straits in the winter (Ferguson et al. 2010, Fortune et al. 2020) . The EC-WG bowhead whales were heavily harvested from 1530 – 1915, and population abundance was depleted (Higdon 2010). The population has rebuilt in recent years (Ferguson et al. 2021), but past details on population dynamics are lacking to inform management and conservation action. EC-WG bowhead whales are currently harvested at an average of three whales per year by multiple Inuit communities in Nunavut, Nunavik, and Greenland (Higdon 2010). This population has been assessed as “Special Concern” by the Committee on the Status of Endangered Wildlife in Canada because the population cannot yet be deemed sustainable due to a lack of data, although there is evidence via multiple abundance estimations of increase since the termination of commercial whaling (COSEWIC 2009, Frasier et al. 2020, IWC 2009, Koski et al. 2007.

Monitoring is essential for marine mammal management. Population estimates are a major component of management, and for marine mammals these often take the form of distance sampling via aerial surveys (Richard et al. 2010, Watt et al. 2020b). Reliable aerial survey estimates can be difficult to obtain, as they require extensive coverage over a population's range (Booth et al. 2020, Taylor et al. 2007). The EC-WG bowhead whale population exemplifies these challenges with aerial surveys because this population has a wide distribution covering approximately 179,000 km^2 (Doniol-Valcroze et al. 2020, Heide-Jørgensen et al. 2003) and extensive aerial survey coverage in the Arctic is expensive and logistically challenging (Koski et al. 2013). Mark recapture (MRC) population estimates have the potential to overcome the challenges surrounding aerial surveys; while physically capturing bowhead whales is generally unfeasible, using genetic samples collected via remote biopsy across their range to "capture" individuals allows for the estimation of abundance (Biddlecombe et al. 2023, Frasier et al. 2020). An updated understanding of movement and behaviour can also aid in increasing the accuracy of abundance estimates, by providing context for where animals exist versus where they are observed.

Utilization distribution (UD) mapping is useful for understanding animal occupancy, typically used to identify individual or population home ranges (Van Winkle 1975, Worton 1987). Kernel density uses a probability density estimation to provide the probability of occupancy (Worton 1989). Kernel density models use telemetry location points to estimate space use, but this method can be updated with a Brownian Bridge movement model (BBMM), which estimates UD using paths between consecutive telemetry locations, or steps (Horne et al. 2007). BBMMs estimate the probability of an animal's presence in any given location based on the frequency and duration of stay within paths (Horne et al. 2007), this means the UD is based on

movement, instead of simply location. UD from BBMM analysis provides a map showing probability density of occupancy within an individual's or a population's range, which can determine the probability that individuals in a population exist outside of areas where aerial surveys occurred. Many unsurveyed regions could have initially been included in survey plans but missed due to time constraints or logistical issues. Comparison of BBMM probability density values in surveyed regions and the corresponding abundance estimates from those surveys allows a relationship between abundance and UD to be determined. This relationship could then be used for extrapolation of an abundance estimate into unsurveyed areas using BBMM values from unsurveyed areas, potentially increasing the accuracy of an abundance estimate and, as a result, better informing management action.

Stock production models are a common management method for determining stock status for fisheries (Hilborn et al. 2020, Maunder and Punt 2013). Data that are often available for aquatic populations, such as abundance estimates and harvest records, are incorporated into stock production models to calculate temporal population dynamics (Hilborn et al. 2020, Pella and Tomlinson 1969). Recreating past trajectories allows for visualization of how a population is changing over time and how it has responded to stressors, such as overharvesting and effects of climate change. Managers of marine mammal populations often lack biological data, such as age structure, fecundity, mortality, and population growth rate to be included in stock production models, so the models are generally relatively simple in structure, relying on abundance estimates and harvest history (Biddlecombe and Watt 2022, Hilborn et al. 2020, Watt et al. 2020a).

Population dynamics of EC-WG bowhead whales are of interest because the population was near extirpated from commercial whaling, which resulted in a moratorium in 1915 (Higdon

2010, Ross 1993). Although commercial whaling has ceased, this population is still harvested by northern communities in Canada and Greenland for subsistence, so understanding population dynamics is useful in determining sustainable harvest levels. A model that estimated pre-commercial whaling abundance and included a catch history from 1530 to 2019 was created by Ferguson et al. (2021). However, an updated abundance estimate for 2012-2021 is now available (Biddlecombe et al. 2023), and available telemetry location data can be used to adjust past aerial survey estimates thereby providing the opportunity to update the model. The first objective of this research is to estimate abundance from past aerial surveys using BBMMs built from telemetry data to extrapolate abundance estimates into unsurveyed areas. The second objective is to use a stock production model to recreate the population dynamics of EC-WG bowhead whales using updated abundance estimates and harvest history after the cessation of commercial whaling (1915). The updated abundance estimates may inform previously undetected dynamics in more recent decades. The third objective is to predict trajectories 10 years into the future under various harvest scenarios. The focus is on the EC-WG bowhead whale's population trajectory after the commercial whaling moratorium to present day, which follows their rebound approximately 100 years after commercial whaling pressure was removed.

5.2 Methods

5.2.1 Location Data

To track EC-WG bowhead whale movement, we used data from 145 whales equipped with long-term satellite telemetry tags (Wildlife Computers SPOT and SPLASH MK10) from 2005-2019. Tags were deployed from boats using an 8m fibre glass tagging pole and ARTS method in Greenland (Heide-Jørgensen et al. 2003). Tagging occurred in Foxe Basin,

Cumberland Sound, and Admiralty Inlet in Canada, and in Disko Bay in Greenland. Tags provided data on date, time, and location up to 400 times per day in summer and 100 times per day in winter (see Fortune et al. 2020 for details on temporal resolution of telemetry data collection).

The raw Argos location data was filtered for speed, distance, and angle using sdafilter in the argosfilter package (Freitas et al. 2008) in RStudio (R Core Team 2020). The sdafilter used the default velocity threshold of 2 m/s, and removed outliers by removing "spikes" or acute angles in the movement path (using default thresholds of angles <15° when 2.5 km from the previous location and angles <25° when 5 km from the previous location).

Locations were subset to those in March and those in August, as abundance estimates to be extrapolated using location data were from aerial surveys conducted in March or August. March locations were from 29 tagged individuals from 2007-2017, and August locations were from 105 tagged individuals from 2005-2019 (see Appendix 4. Figure 1 to visualize location points).

5.2.2 Utilization distribution mapping

Two utilization distribution maps were created to extrapolate aerial survey estimates using BBMMs. A BBMM is an extension of the kernel density method for estimating home range, taking both the position and the path travelled into consideration, by placing a kernel function over the step (the line connecting two successive locations), rather than over a single location (Bullard 1991, Calenge 2011). The Brownian Bridge process models the stochastic variance of paths between locations based on starting and ending location and time between those locations/speed movement. This process refines utilization distribution by incorporating

probable movement between locations, rather than solely basing utilization on recorded locations. The 1981 survey was completed in March, thus locations from March were used for one BBMM, while the 2002 and 2013 surveys were completed in August and therefore, a second BBMM used August locations.

The BBMM method has been further developed to create a dynamic Brownian bridge movement model (dBBMM) which separates tracks into behavioural types (Kranstauber et al. 2012). A dBBMM is useful if there are multiple behavioural movement types in the telemetry data, or for providing more detail when movement is being predicted (Kranstauber et al. 2012). A dBBMM model was not necessary for our analyses as we used data exclusively from March and August, which are not migratory periods for bowhead whales, thus differences in movement type are less likely.

The locations were first converted into trajectories for each individual bowhead whale, which were then resampled into a series of bursts, where all consecutive locations within a burst must be <24 hours apart. Two smoothing parameters were set for the BBMM, sig1 is related to the speed of the animal between locations, and influences the width of the bridge connecting successive location points (see Horne et al. 2007 for details). The longer the time between locations (i.e., larger sig1), the wider the bridge, which represents less certainty in the animal's path between locations. We used function liker in the adehabitatHR package (Calenge 2011) in RStudio (R Core Team 2020) to identify a sig1 value for each individual. The second required parameter is sig2, which is derived from the imprecision of locations. We used a sig2 value of 1910m, which is the median error of all locations in pinnipeds at sea from Costa et al. (2010), the most in-depth review quantifying distances of Argos location accuracy ratings in marine mammals available. The BBMM was run with function kernelbb in package adehabitatHR

(Calenge 2011) in RStudio (R Core Team 2020), with all individuals included in one model, and grid value of 120 (grid value is unitless and is defined in reference to coverage of telemetry locations; see Calenge (2011) for details on how grid value determines resolution of BBMM output), where each pixel had a calculated relative probability density of occupancy. Both BBMM maps (March and August) were then clipped to a 100% minimum convex polygon for all locations.

5.2.3 Extrapolation of Survey Estimates

Three aerial survey abundance estimates, from 1981, 2002, and 2013, were extrapolated using BBMM maps. Existing aerial survey estimates were 1549 whales (CI: 589-4072) in 1981 (Koski et al. 2007), 6344 whales (CI: 3119-12906) in 2002 (IWC 2009), and 6446 whales (CI: 3722-11200) in 2013 (Doniol-Valcroze et al. 2020). To attain more precision in the relationship between observed abundance and probability of occupancy the aerial surveys were subdivided into the strata reported in each survey design, each with separate abundance estimates (Figure 5.1, Table 5.1). The 2002 aerial survey data were analyzed multiple ways, with the most confidence in the estimate from the International Whaling Committee (IWC) in 2009, which was informed by aerial survey results from Dueck et al. (2008), but the IWC analysis provides only a single abundance estimate for all 2002 strata combined (IWC 2009). Dueck et al. (2008) presented results from two strata, Eclipse Sound and Gulf of Boothia/Prince Regent Inlet, providing surface estimates where 28.7% of the total surface estimate was from Eclipse Sound, and 71.3% was from Gulf of Boothia/Prince Regent Inlet. To stratify the IWC estimate, the ratio from Dueck et al. (2008) was used to separate the 6,344 whales into 1821 whales in Eclipse Sound, and 4523 whales in Gulf of Boothia/Prince Regent Inlet. For each survey, polygons of

each stratum within the surveyed area were used to clip the BBMM map, and the BBMM values from the resulting strata clipped rasters were averaged to give mean probability density of occupancy within each stratum in each survey (referred hereafter as mean BBMM), standard deviation (SD), and standard error (SE). Area of each stratum was also recorded.

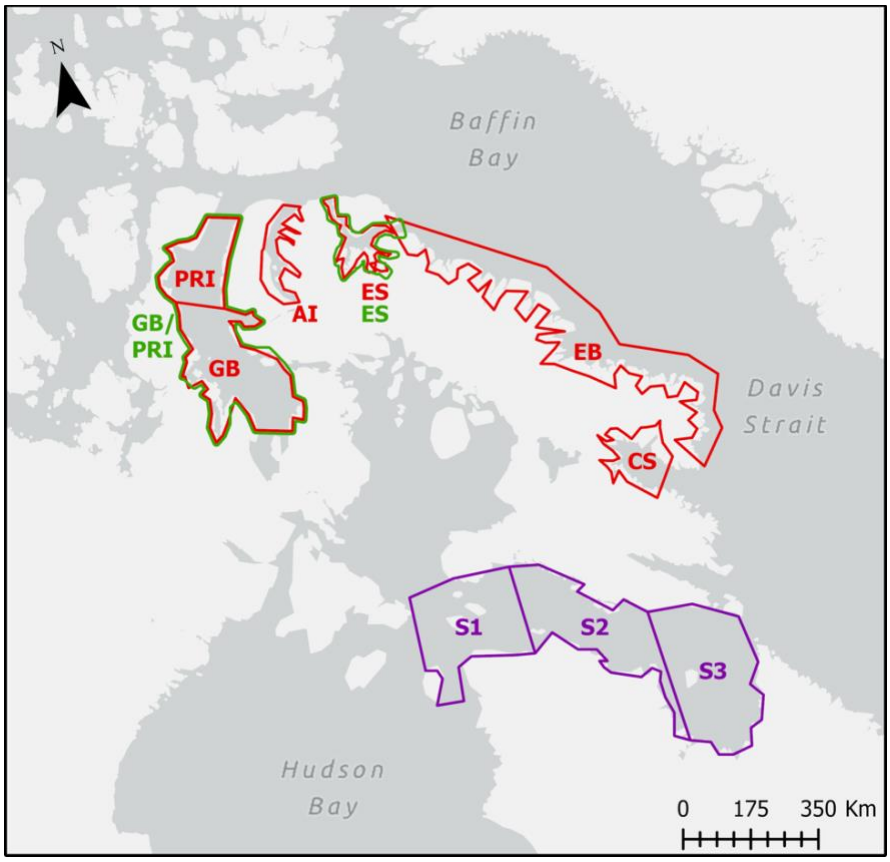

Figure 5.1 Strata for EC-WG bowhead whale aerial surveys conducted in 1981 (purple; S1: strata 1, S2: strata 2, S3: strata 3), 2002 (green; GB/PRI: Gulf of Boothia/ Prince Regent Inlet, ES: Eclipse Sound), and 2013 (red; PRI: Prince Regent Inlet, GB: Gulf of Boothia, AI: Admiralty Inlet, ES: Eclipse Sound, EB: East Baffin Island, CS: Cumberland Sound).

Table 5.1 Data used for Poisson regression analysis from EC-WG bowhead whale aerial surveys. See Figure 5.1 for strata: S1: strata 1, S2: strata 2, S3: strata 3, ES: Eclipse Sound, GB: Gulf of Boothia, PRI: Prince Regent Inlet, AI: Admiralty Inlet, CS: Cumberland Sound, and EB: East Baffin Island. Mean BBMM refers to the mean probability density of occupancy from BBMM analyses, and estimated abundance refers to reported aerial survey estimates.

Year	Strata	Mean BBMM	Area (km^2)	Estimated abundance
1981	S1	5820.69	64951.55	1236
	S2	1752.13	65016.49	113
	S3	193.28	77381.99	0
2002	ES	124.58	11777.72	1821
	GB/PRI	2404.95	98435.95	4523
2013	AI	1971.4	13588.85	82
	CS	5942.18	21201.43	2696
	EB	2688.47	108659.57	2090
	ES	124.58	11777.72	32
	GB	2711.65	63423.81	660
	PRI	1503.11	31133.4	886

To determine the relationship between probability of occupancy from BBMM analyses and estimated abundance, and determine if the area of the strata had an effect, a Quasi-Poisson multiple regression analysis was completed. Available abundance estimates from aerial survey data are limited and based on large, strata-wide generalizations, so a relatively simple regression model was used to distill down the data heavy BBMM results and combine them with the restrictive abundance data in a relatively straightforward way. Various regression models were

considered to model the relationship between BBMM means and estimated abundance, including linear, polynomial, Poisson, and Quasi-Poisson. The distribution of the abundance estimates most closely reflected count data, and data are also required to be integer-valued, thus Poisson and Quasi-Poisson models were preferred *a priori*. The Poisson model showed the response variable was overdispersed so the Quasi-Poisson model was chosen to account for increased variance. Mean BBMM probability density value and strata area were the independent variables, and abundance was the dependent variable for all strata. Area was found to have no effect on abundance (see results), so a Quasi-Poisson regression was run with mean BBMM value as the sole independent variable acting on abundance. Model assumptions were validated by plotting residuals against fitted values and inspecting for absence of residual patterns. Comparisons for best fit between Quasi-Poisson, linear, and polynomial models was difficult as comparison across different model family structures is restrictive. We plotted all three regression lines for visual comparison, and compared model fit between the two Gaussian models using AIC, where a $\Delta AIC > 2$ is evidence of a better model fit.

The resulting regression line from the regression analysis was used to estimate abundance from mean BBMM values for regions outside of aerial surveyed areas. We opted to separate regions of high probability of occupancy from regions of low probability in unsurveyed areas to better extrapolate abundance because a large portion of the unsurveyed areas had a very low probability of occupancy, which could potentially artificially lower the estimated abundance. To separate regions of high and low expected use we calculated the mean BBMM value in the total unsurveyed area for each survey year, then separated the raster into BBMM values above the mean, and BBMM values below the mean. This effectively isolated regions of high expected occupancy. We then calculated mean BBMM values for unsurveyed regions of high expected

use, and mean BBMM values for regions of low expected use. Those means were used in the regression equation to estimate abundance in high occupancy and low occupancy unsurveyed regions for each survey year.

Estimates for unsurveyed and surveyed regions were then summed to give an updated abundance estimate for each survey separately. Standard errors (SE) for abundance estimates were also updated (SE_{Total}) by combining the variance of BBMM values outside each survey (Var_B) and the variance from the abundance estimate for each aerial survey (Var_S) (Eqn. 1).

$$SE_{Total} = \sqrt{Var_B + Var_S} \quad (1)$$

5.2.4 Population model specifications

To estimate population trajectory after the cessation of commercial whaling for EC-WG bowhead whales, we used a stochastic stock production model with density dependence acting on population growth. Hierarchical Bayesian inference was used to fit the model, and the Markov Chain Monte Carlo (MCMC) method was used to sample parameter posteriors. We used a hierarchical state-space model, which has two separate stochastic processes, observation process and state process (de Valpine and Hastings 2002). Observation process reflects observation error related to data collection, as is defined by the relationship between observed data (S_t) and true population size (N_t), linked with a multiplicative error term (ε_{S_t}) (Eqn. 2). This is a log-normal model where the logarithm of the median true population estimate (N_t) is applied to the second stochastic process, the state process.

$$\ln(S_t) = \ln(N_t) + \varepsilon_{S_t} \quad (2)$$

The state process estimates annual population abundance using various population parameters and an error term related to random variation in population dynamics. The state

process is a discrete formulation of the Pella and Tomlinson stock production model (Innes et al. 2002, Pella and Tomlinson 1969), which describes dynamics as true population size over time. Population size at time *t* is a function of the previous year's population estimate (Eqn. 3).

$$N_t = N_{t-1} * \left(1 + (R_{max}) * \left(1 - \frac{N_{t-1}}{K}\right)^{\theta}\right) * \varepsilon_{p_t} - R_t \quad (3)$$

Where: R_{max} is the maximum growth rate or rate of population increase,

K is the environmental carrying capacity,

θ (theta) defines the shape of the density-dependent function which determines how abruptly population growth declines with increasing abundance,

ε_{pt} is a stochastic term for the process error estimated annually,

R_t are the removals for that year, calculated as reported catches, C_t , that are corrected for the proportion of animals that were struck and lost, $S\&L$ (Eqn. 4):

$$R_t = C_t \cdot (1 + S\&L) \quad (4)$$

S&L is used to account for under-reporting in catch histories, although S&L data themselves are often associated with a high level of uncertainty. This type of stock production model has the potential to include age and sex structure, but these data are not available for association with population parameters in EC-WG bowhead whales. Telemetry studies have provided information on age and sex in EC-WG bowhead whales (i.e., Cosens and Blouw 2003, Fortune et al. 2020), and there is potential to uncover relationships relevant to stock production modelling as this type of work progresses.

Harvest history data and population estimates from both aerial surveys and mark-recapture population analyses were used to fit the model. Harvest data for EC-WG bowhead whales are available dating back to 1530 (Higdon 2010), although our model only used harvest history starting from the cessation of commercial whaling in 1915. Ferguson et al. (2021)

modeled the historical population trajectory of EC-WG bowhead whales starting in 1530, so our updated goals for the population model are to focus on trends in abundance post-commercial whaling, with updated abundance estimates. The aerial survey abundance estimates used for the model were those updated using the BBMMs from 1981, 2002, and 2013. Mark recapture abundance estimates for EC-WG bowhead whales were also included (similar to the use of aerial survey estimates with a single MRC estimate in Ferguson et al. 2021), an estimate of 11747 whales (CI: 8169-20043) from 2013 (Frasier et al. 2020), and an estimate of 5173 whales (CI: 3436-7788) from 2012-2021 (Biddlecombe et al. 2023), where we used 2017 as the representative year for input into the model.

5.2.5 Priors

Prior distributions were informed by previous cetacean models (i.e., Ferguson et al. 2021, Wade 1998) and existing ecological knowledge on cetaceans generally and bowhead whales specifically. Maximum population growth rate (R_{max}) for cetaceans is estimated to be 4% annually, or 0.04 (Wade 1998), so we set the prior to a uniform distribution ranging from 0.025 – 0.045 as this includes what is accepted as ecologically plausible. Theta (θ), the parameter responsible for shaping the effect of density dependence ranges from 1 to 7 in marine mammal populations (Taylor and Demaster 1993), where higher values refer to the growth rate declining more abruptly as abundance approaches carrying capacity. Therefore, at higher θ values, maximum productivity occurs closer to carrying capacity. The prior for θ was set as a uniform distribution ranging from 1-5 following Ferguson et al. (2021), as values from 1-5 represent a range in density dependence that results in maximum sustainable yield levels assumed for baleen whales (Witting 2013). Starting population size in 1915 was assumed to be relatively low

(~1000) based on trends from Ferguson et al. (2021), and Higdon and Ferguson (2016) stated that based on the rebound trend the population in 1915 could not have been higher than the mid-thousands. So, we assigned starting population a uniform prior distribution from 100 to 5,000. Carrying capacity (K) was assigned a uniform distribution ranging from 5,000 to 25,000, based on Ferguson et al.'s (2021) K estimate of 18,500 individuals in 1530, while also anticipating a potential decrease in carrying capacity since the 1500's (Table 5.2). For this population, pre-commercial whaling abundance is assumed to reflect carrying capacity, and this value was extensively modelled by Higdon and Ferguson (2016). They found with varying values for S&L and R_{max} the range for carrying capacity had to be between 15,000 and 20,000 to prevent extinction but still result in the extent of decline that occurred during commercial whaling. We used this information to further justify our upper limit for carrying capacity. Different priors for starting population size and carrying capacity were not explored as they were informed by existing knowledge on EC-WG bowhead whales but remained relatively wide to give our model space to update the parameter estimate.

Table 5.2 Prior distributions, parameters and hyper-parameters used in the population model for EC-WG bowhead whales. “dist.” denotes a hyper-parameter with its own prior distribution. Dashes indicate parameters that do not apply to the model.

Parameters	**Notation**	**Prior distribution**	**Hyper-parameters**	**Values**
Survey error (t)	ε_{st}	Log-normal	μ_s	0
			τ_s	*dist.*
Precision (survey)	τ_s	*Gamma*	α_s	*2.5*
			β_s	*0.8*
Process error (t)	ε_{pt}	Log-normal	μ_p	0
			τ_p	*dist.*
Precision (process)	τ_p	Gamma	α_p	1.5
			β_p	0.001
Density dependence	θ	*Uniform*	N_{upp}	5
			N_{low}	1
Struck-and-lost	*S&L*	-	-	0.28
Initial population	N_{1960}	Uniform	N_{upp}	5,000
			N_{low}	100
Carrying capacity	K	Uniform	K_{upp}	25,000
			K_{low}	5,000
Max growth rate	R_{max}	Uniform	N_{upp}	0.045
			N_{low}	0.025

A S&L adjustment is necessary for harvest removals, as harvest alone underestimates the number of removals from a population because animals can be wounded or killed but not recovered by hunters. The data included in model fitting do not provide information to update a S&L parameter estimate, so reported struck and lost data were used to set S&L. From 1918-

1988, 36 whales were killed from Inuit harvest, with an additional 14 reported S&L (Higdon 2010), which equates to a S&L value of 0.28 (Table 5.2).

Process error was given a log-normal distribution with a location parameter of zero. The precision parameter for process error had an informative prior gamma (1.5, 0.0001) distribution (Table 5.2). Gamma distributions are typical for random error precision hyperparameters (Plummer 2003), and the resulting process error term had quartiles of 0.99 and 1.01. Bowhead whales are an extremely long-lived species (>200 years) (Bockstoce 2008, George et al. 2021), so the narrow stochastic process error range reflects the assumption that their stock dynamics have low interannual variability which corresponds with their longevity (Le Coeur et al. 2021, Morris et al. 2008).

Similar to process error, observation error was also given a log-normal distribution with a location parameter of zero. The precision parameter for observation process error or survey error was given an informative prior gamma (2.5, 0.8) distribution, which results in quartiles of 0.49 – 0.77 (Table 5.2). The survey error precision prior reflects error higher than coefficients of variation calculated for each aerial survey or MRC population estimate (where mean CV = 0.43), to allow more space for error around the survey estimates to account for increased error from the extrapolation of estimates using BBMMs and the variation within the Quasi-Poisson regression model.

5.2.6 Parameter Estimation and Model Diagnostics

Posterior estimates for the model parameters were obtained using a Gibbs sampler algorithm implemented in JAGS (Plummer 2003) via RStudio (R Core Team 2020; *version 1.2.5033*) using packages *R2jags* (Su and Yajima 2015; *version 0.6-1*) and *coda* (Plummer et al.

2006; *version 0.19-3*). A MCMC simulation method was used to sample parameter values which were then checked for convergence by comparing to a stationary distribution. Model convergence, mixing, and autocorrelation within parameters were investigated after initial and final model runs.

Geweke's Diagnostic and Geweke plots were used to test similarity between different sections of the chains and to test for mixing within each chain (Geweke 1996). The Brooks-Gelman-Rubin (BGR) diagnostic test was used to test for convergence between chains by comparing the width of the 80% credible interval of the chains pooled with the mean widths of the 80% credible interval for each of the chains individually (Brooks and Gelman 1998).

Initial model runs to investigate convergence used three chains and had the number of iterations corrected to equal 10,000 after a burn in of 6,000 and thinning value of 60. Initial runs were done with θ as described above (uniform (1,5) distribution) and with $\theta=1$, as there was uncertainty around the model's ability to estimate θ, and the robustness of model results to changing θ. We assessed outputs from initial runs by visually inspecting diagnostics for model validation, combined with consideration of biological relevance, to determine if the model was suitable. The final preferred model was run using five chains, and 100,000 iterations after a burn-in of 60,000, with thinning at 100.

5.2.7 Future Projections and Harvest Scenarios

To address the potential effects of harvest on the EC-WG bowhead whale population's post-commercial whaling rebound, the model was extended 10 years into the future under four potential annual harvest scenarios: 0, 10, 20, and 30 bowhead whales per year. Harvest has not surpassed 6 individuals per year since 1915, so the higher harvest values are largely hypothetical.

However, totals represent all anthropogenic mortality and would include deaths from vessel strikes which are expected to increase with resource development activities such as iron ore mining (Halliday et al. 2022, Reeves et al. 2012). Harvest quotas for marine mammals are re-assessed on a short-term basis, ideally every 5 years, so a short projection time of 10 years was chosen to account for this. The probability of decline over 10 years was also calculated to assess potential impacts of harvest over time. This method of calculating probability of decline is known as the risk-based approach to assessing harvest levels, typically used for populations considered data-rich in Canada (Hammill et al. 2017), and was preceded by the calculation of Potential Biological Removal (PBR), which is still utilized for data-poor populations.

5.3 Results

The BBMM UD maps for EC-WG bowhead whales revealed regions where probability density of occupancy is highest in March and August (Figure 5.2). For the 1981 survey in March, survey coverage encompassed ~32% of high occupancy regions, with highest BBMM values within areas that were included in the surveys. The August 2002 survey encompassed ~33% of high occupancy regions, and the August 2013 survey encompassed ~77% of high occupancy regions including regions with the highest BBMM values (Figure 5.2).

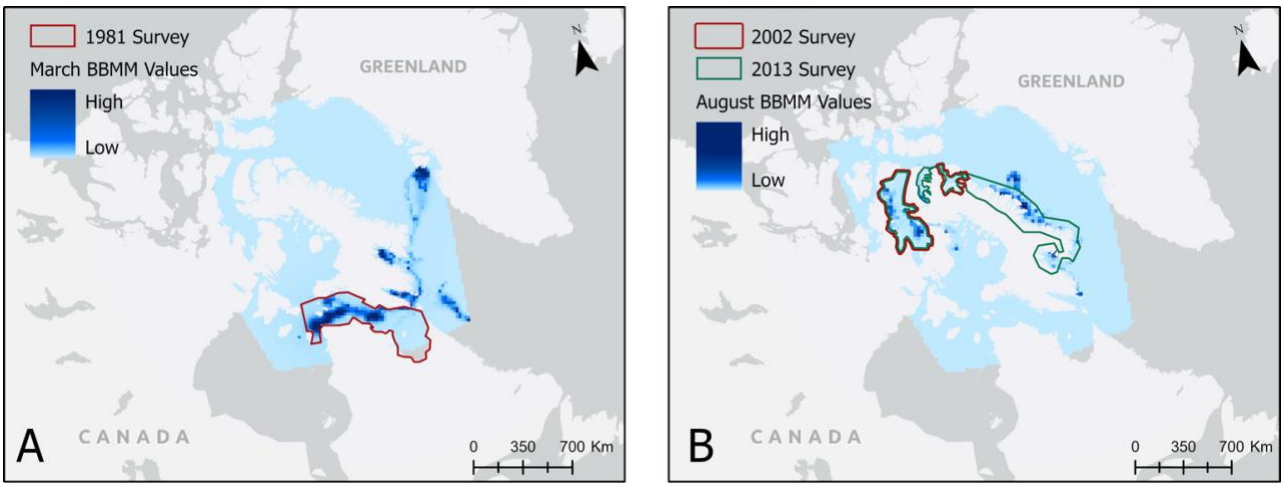

Figure 5.2 BBMM probably of occupancy results for EC-WG bowhead whales in A) March with 1981 aerial survey coverage and B) August with 2002 and 2013 aerial survey coverage. BBMM values are relative probability density of occupancy values, and thus, have been presented as relative high and low probabilities.

When aerial survey estimated abundance was plotted against the mean BBMM value in each survey strata, the Gulf of Boothia/Prince Regent Inlet stratum from the 2002 survey was determined to be an outlier by visual inspection, with a survey abundance estimate nearly double the next highest abundance estimate. This was likely related to the Gulf of Boothia and Prince Regent Inlet strata not being subdivided into separate abundance estimates in 2002. The outlier was initially included in trial regression model runs, but regardless of model type the outlier remained >2 standard deviations outside of regression line, so it was removed from the regression analyses (Figure 5.3). The multiple regression determined no significant relationship between estimated abundance and mean BBMM value and no significant relationship between estimated abundance and strata area (Intercept: 6.20, SE: 0.81, t-value: 7.67, p-value<0.001; BBMM: 2.36×10^{-4}, SE: 1.51×10^{-4}, t-value: 1.57, p-value: 0.161; area: 4.14×10^{-8}, SE: 1.11×10^{-5},

t-value: 0.004, p-value: 0.997). Due to a very high p-value, area was removed from the model, and it was re-run with BBMM as the sole predictor, as the p-value for BBMM was much lower and could be of marginal significance. The resulting regression determined no significant relationship between estimated abundance and mean BBMM value under a strict 0.05 p-value significance threshold. The p-value for mean BBMM was 0.132, which, based on the sparsity of the available data set, was deemed of enough significance to be used for extrapolation (Intercept: 6.20, SE: 0.57, t-value: 10.87, p-value<0.001; BBMM: 2.36×10^{-4}, SE: 1.41×10^{-4}, t-value: 1.68, p-value: 0.132). Comparison of the Quasi-Poisson regression with linear and polynomial regressions showed very little difference between the three models (Figure 5.3). The Quasi-Poisson and polynomial regressions were nearly identical, and the linear regression differed slightly. The linear regression found a nearly significant relationship between estimated abundance and mean BBMM (p-value: 0.09), and the polynomial regression found a similar significance between estimated abundance and mean BBMM for the linear term (p-value: 0.10), and no significance for the quadratic term (p-value: 0.61). The ΔAIC between the linear and polynomial models was <2. There was very little difference between model fits, but Quasi-Poisson was the preferred model due to our *a priori* identification of the response variable as count data. The equation for the Quasi-Poisson regression line between estimated abundance and mean BBMM value for survey strata is $y = \exp(6.203+2.363\times10^{-4}x)$ (Figure 5.3). Plotted residuals were random with no trend (Linear regression p-value: 0.976), so model fit was accepted. Plotted residuals for linear and polynomial models also lacked a trend, but upon visual inspection residuals from the linear model showed slightly more non-random clumping.

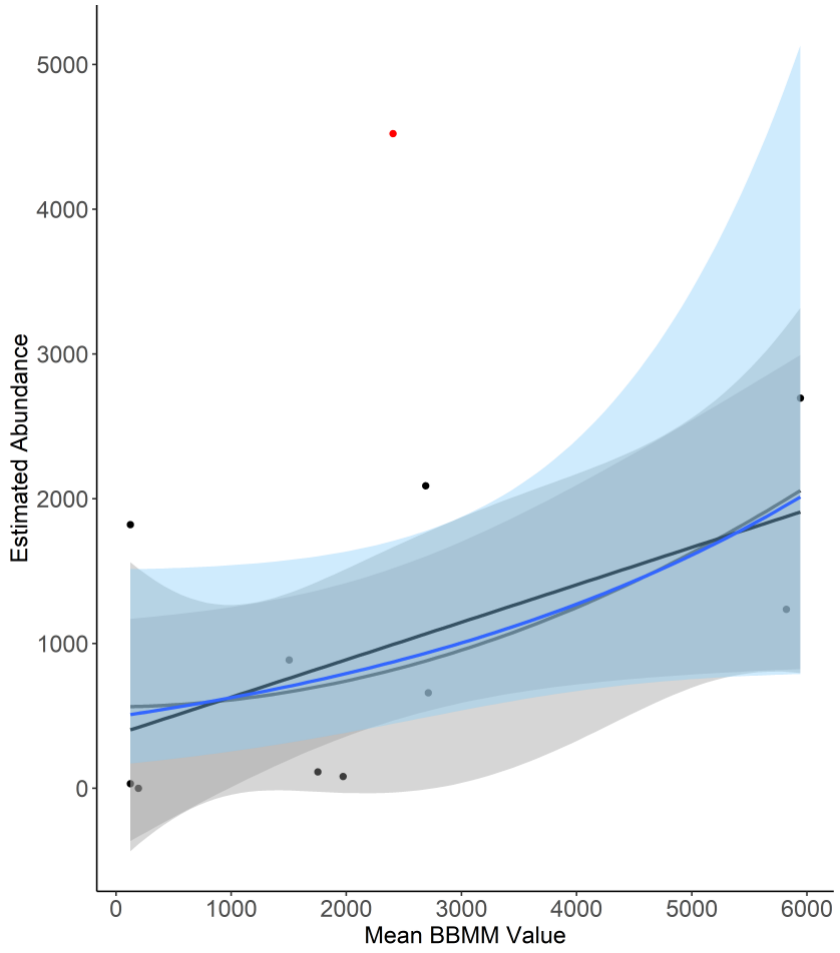

Figure 5.3 Quasi-Poisson regression (blue regression line, light blue 95% confidence interval) comparing mean Brownian Bridge movement model probability density value to estimated abundance in each EC-WG bowhead whale aerial survey strata (from surveys conducted in 1981, 2002, and 2013). Linear regression shown in black, with dark grey 95% confidence interval, and polynomial regression shown in grey, with light grey 95% confidence interval. Outlier removed from regression analyses shown in red.

Extrapolation of aerial survey estimates using the regression equation resulted in the 1981 estimate increasing from 1549 to 2898 individuals, the 2002 estimate increasing from 6344 to

7822 individuals, and the 2013 estimate increasing from 6446 to 7592 individuals (Table 5.3). The unsurveyed high-use region abundance estimates were 1.7, 1.9 and 1.3 times greater than the unsurveyed low-use region abundance estimates for 1981, 2002, and 2013, respectively (Table 5.3). SE adjustment factors were 1.036, 1.009, and 1.012 for 1981, 2002, and 2013 survey SEs respectively.

Table 5.3 Results of extrapolation of EC-WG bowhead whale aerial survey estimates using probability of occupancy from BBMM analyses. Unsurveyed areas were separated into high-use and low-use regions based on BBMM values, and abundance was extrapolated separately using Poisson regression results (see text for details).

Survey year	Survey abundance estimate	Unsurveyed high-use abundance estimates	Unsurveyed low-use abundance estimate	Total adjusted abundance estimate
1981	1549	851	498	2898
2002	6344	981	497	7822
2013	6446	650	496	7592

The EC-WG bowhead whale stock production model recreated the population trajectory from 1915-2022, using adjusted aerial survey estimates from 1981, 2002, and 2013, and genetic mark recaptures estimates from 2013 and 2017 (plotted with log-normal confidence intervals derived from SEs and updated SEs for adjusted survey estimates) (Figure 5.4A). All model diagnostics indicated suitable model fit, with rapid convergence of all chains for all estimated parameters, and BGR statistics <1.05 (Table 5.4, see Appendix 4. Figure 2 for detailed diagnostics). The models with differing priors for θ, a uniform (1,5) distribution and θ=1,

resulted in similar population trends, and little change in parameter estimates and future projections (Table 5.4, Figure 5.4 and 5.5, Appendix 4. Table 1 and Appendix 4. Figure 3 and 4). We chose to use the model with the uniform (1,5) distribution prior for θ as our preferred model as we expected that a baleen whale population would exhibit some level of density dependence (Witting 2013). Estimates of model parameters are presented as the median from the posterior distribution. The starting population in 1915 was estimated as 1028 whales (95% CI 213-4758), and the estimate for 2022 was 8243 whales (95% CI 5202-14,950) (Figure 5.4A). Carrying capacity (K) was estimated as 9045 (95% CI 5295-23,645), and the estimated maximum growth rate (R_{max}) was 1.033 (95% CI 0.025-0.044) or 3.3%. The density dependence shaping parameter (θ) was estimated as 2.79 (95% CI 1.071-4.886) (Table 5.4). State process (prec.process) (11,812.77, 95% CI 1070.62-46,675.81) and observation process (prec.surv) (3.51, 95% CI 1.12-8.23) error are presented as precision, which is defined as the inverse of variance, as such the standard deviation (SD) for state process is 0.009, and SD for observation process is 0.534 (Table 5.4).

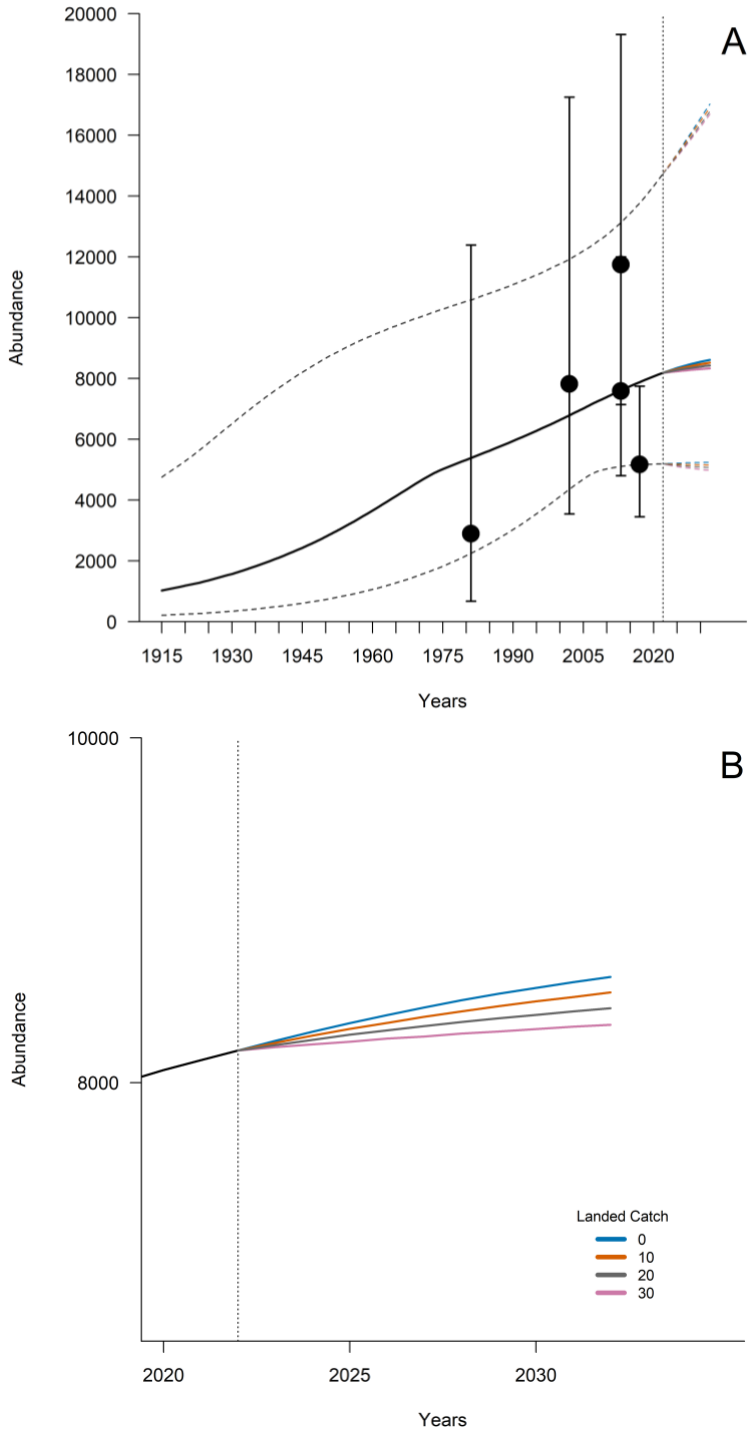

Figure 5.4 Future population projections for EC-WG bowhead whales under four different harvest scenarios based on population estimates from a stochastic stock production model fitted to extrapolated aerial survey estimates flown in 1981, 2002, and 2013, and genetic mark

recapture estimates from 2013 and 2017 (black dots ± 95% log-normal CI). The solid line indicates the posterior median estimates and dashed lines show 95% credible intervals. A) Full model trajectory with future predictions, B) Plot enlarged to show future predictions.

Table 5.4 Model output for the EC-WG bowhead whale stock model. The mean, standard deviation (SD), median (50^{th} Q), 25^{th} and 75^{th} quantiles (25^{th} Q, 75^{th} Q), 95% credibility intervals (2.5%CI, 97.5%CI) are given for the following model parameters: carrying capacity (K), process error (process), survey precision (surv), starting population (startpop), struck and loss (S&L), and population size in 2022 (N_{2022}). $\widehat{R}$ is the Brooks-Gelman-Rubin statistics; values < 1.05 indicate convergence of chains. N.eff is the number of effective chains after considering autocorrelation.

Parameters	Mean	SD	2.5% CI	25% Q	50% Q	75% Q	97.5% CI	$\widehat{R}$	n.eff
K	10972.133	5208.201	5294.891	7003.831	9045.006	13745.254	23645.312	1.001	500000
theta	2.857	1.177	1.071	1.804	2.791	3.873	4.886	1.001	440000
deviance	94.573	2.251	90.885	93.003	94.521	95.693	99.844	1.001	500000
Rmax	0.034	0.006	0.025	0.029	0.033	0.039	0.044	1.001	500000
prec.process	14983.43	12234.799	1070.617	6046.261	11812.773	20517.749	46675.809	1.001	220000
prec.surv	3.815	1.849	1.116	2.467	3.514	4.836	8.228	1.001	500000
startpop	1660.017	1405.367	213.302	530.062	1027.509	2666.445	4758.201	1.001	500000
struck.and.lost	0.28	0	0.28	0.28	0.28	0.28	0.28	1	1
N_{2022}	8717.397	2594.156	5201.601	6769.966	8243.134	10148.752	14950.329	1.001	500000

The probability of population decline 10 years into the future (i.e., $N_{2022} > N_{2032}$) for four harvest scenarios was estimated and plotted (Figure 5.4B). A landed catch of 0, 10, 20, and 30 bowhead whales annually had 24%, 36%, 46%, 53% probability of population decline, respectively (Figure 5.5). This also means, a landed catch of 0, 10, 20, and 30 bowhead whales annually had 76%, 64%, 54%, 47% probability of increase over 10 years.

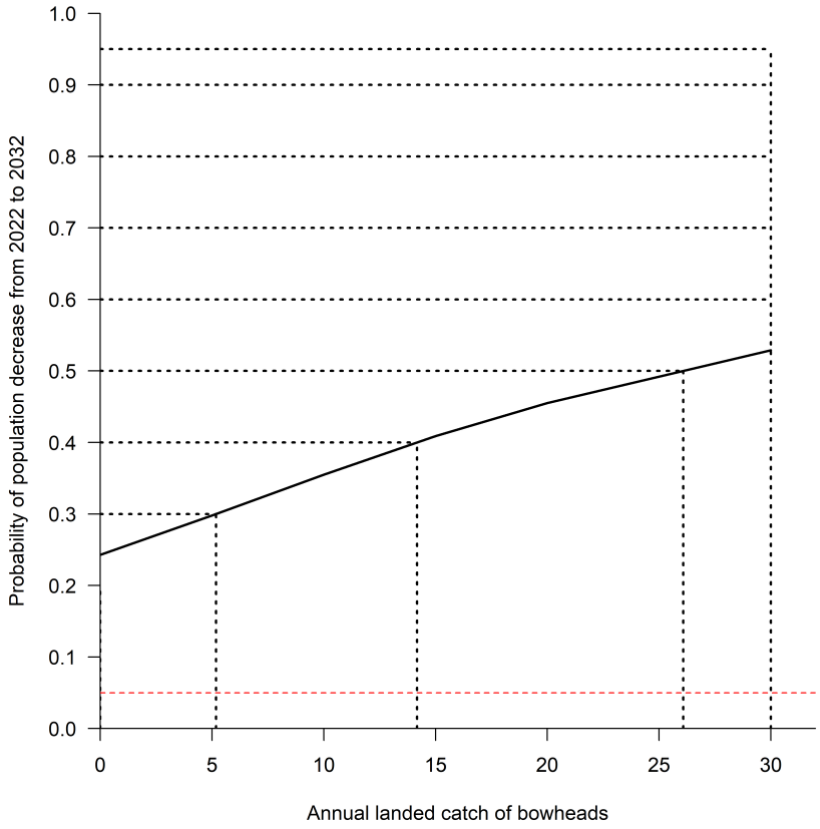

Figure 5.5 Probability of EC-WG bowhead whale stock decreasing from the 2022 abundance estimate after 10 years of harvest, as a function of the number of reported bowhead whales removed from the stock every year. Dotted lines indicate levels of harvest (x-axis) corresponding to the probability of decline (y-axis). Red dotted line indicates low risk of decline.

5.4 Discussion

Utilization distribution (UD) was determined for EC-WG bowhead whales using a BBMM, which showed the majority of probable occupancy was covered by the most recent aerial survey in 2013, while the two earlier surveys had more than half of the higher expected use areas outside their survey coverage. Aerial survey estimates were extrapolated to account for the probability of individuals outside survey areas; the maximum abundance increase from

extrapolation was nearly 1500 individuals in 2002, but proportionally the greatest increase was nearly doubling the 1981 estimate by adding 1349 individuals to the existing estimate of 1549 individuals. The addition of over 1000 whales for each of the three aerial survey estimates suggests that although the surveys focus within high occupancy regions, there is still a considerable amount of high-use area that was not covered by aerial surveys. Most notably, the two earlier surveys had lower coverage, and thus missed more high occupancy area, resulting in greater extrapolation estimates. The addition of over 1000 whales to each survey estimate also supports the argument that aerial surveys are lacking in their ability to estimate the total abundance of EC-WG bowhead whales due to the vastness of their range (Doniol-Valcroze et al. 2020, Frasier et al. 2020).

The occupancy data that the BBMMs provided was useful in abundance extrapolation when applied in conjunction with a spatial breakdown of aerial survey estimates into separate strata. Survey strata allowed for multiple relationships between mean BBMM values and estimated abundance to be analyzed together with a regression model. Regression model selection was mildly indeterminate, as the small data set reduced the strength of model fit for all model types. The Quasi-Poisson regression was preferred due to the distribution of the data, but other models closely matched the Quasi-Poisson results. The greatest disparity between two models resulted in an estimated abundance difference of <200 individuals. This difference is negligible in the scope of the confidence intervals, and the error surrounding survey estimates built into the population dynamics model.

Using occupancy as a proxy for abundance has been done for many species (i.e., Fuller et al. 2022, Stauffer et al. 2021), but it is important to consider that occupancy and abundance are different approaches to understanding a population, and as such, may not directly correspond

(Trenkel et al. 2013). Combining these two data types was done in an effort to use available data, from this very data limited population, to address restrictions in estimating abundance through aerial surveys alone. The EC-WG bowhead whale population presents challenges with both abundance estimation and space use analyses. Issues surrounding aerial surveys are related to their vast distribution, as discussed above. The telemetry data presents biases as tagging effort is not population wide, and likely is not representative of complete population movement or occupancy. The biases from restricted survey coverage and the biases in occupancy modelling both underestimate true population abundance. As such, when extrapolation combines these data sources, resulting estimates are likely to be underestimates. In the case of harvest management, underestimates are preferable to overestimates, and thus our extrapolated abundance estimates are conservative and useful in management modelling.

The 2002 survey presented a challenge with the analysis, as the survey abundance estimate was for the entire survey, not for individual strata (IWC 2009). We were able to utilize previous reports of the 2002 aerial survey results (Dueck et al. 2008), to separate the 2002 estimate into the two reported strata. The larger of these strata encompassed Gulf of Boothia and Prince Regent Inlet (GB/PRI), while the same region from 2013 separated GB/PRI into two strata. The 2002 GB/PRI abundance estimate was almost two times larger than the next highest abundance estimates from any other stratum in both 1981 and 2013, which resulted in the 2002 GB/PRI data point being an outlier in the regression model. If the 2002 GB/PRI strata could have been separated into two strata, as the region was in 2013, this issue likely would have been avoided. The PRI strata has notably lower BBMM values than the GB strata (Figure 5.2B, Table 5.1), so combining both strata increased abundance but decreased mean BBMM value relative to the 2013 GB strata. Separation of the 2002 GB/PRI strata could not confidently be done, because

separate surface estimates from these strata were not reported in any previous analyses of the 2002 survey data and therefore, a ratio of abundance between these two strata could not be determined. Hypothetically, the 2002 GB/PRI strata could have been separated using the proportions from the 2013 GB and PRI strata, similar to how we separated the 2002 survey into two strata using proportions from 2002 surface abundance estimates. But this would assume that the distribution of bowhead whales in the GB/PRI region was the same in 2002 and 2013 which is not necessarily true, and thus separation of the 2002 GB/PRI strata was not possible. If we were to assume bowhead distribution in the GB/PRI strata was the same in 2002 and 2013, and thus the 2002 GB/PRI strata was separated, the relationship between mean BBMM value and abundance of these two strata would not directly follow the results of our regression trend line. In 2013 the GB strata has a higher BBMM value but a slightly lower abundance estimate when compared to the PRI strata, whereas our trend line assumes higher BBMM values are connected to higher abundance estimates. If the separated 2002 GB and PRI points were included in the regression model, they may slightly alter the shape of the curve, making abundance estimates associated with BBMM values of ~2000 (refer to Figure 5.3) marginally higher, but overall, the trend would likely stay the same. Keeping survey strata and analyses of abundance within those strata consistent in the future will be beneficial for increasing certainty in the relationship between probability of occupancy and bowhead abundance, and thus increase certainty of population abundance extrapolation.

The extrapolation curve was not separated by year, although separation of points based on survey years was considered due to the temporal trend in estimated abundance. As abundance increased over time, the association between observed abundance and probability of occupancy was potentially changing. The low number of strata in both 1981 and 2002, three and two strata

respectively, restricted creating extrapolation curves for each survey year separately. The resulting extrapolations from our Quasi-Poisson regression curve lacked temporal trends related to population growth over time, but including all strata into a single regression model provided more confidence in an already relatively data sparse model. Similarly, the telemetry data used for the BBMMs combined multiple years to maximize a limited sample size, so BBMM values could not be separated by year, although variation in occupancy between years likely exists.

Using multiple surveys across years is accompanied by uncertainties surrounding differences in methodological approaches. The 1981 survey was conducted as a systematic strip transect survey, adjusted for availability and perception bias *post hoc* (Koski et al. 2006). No data was available for availability bias, so the adjustment value was calculated from time-depth recorders deployed on bowhead whales near Disko Bay, Greenland ~15 years later (Koski et al. 2006). The 2002 survey was flown as a double platform line transect survey, but results were associated with a great deal of uncertainty and data were re-analyzed multiple times before the preferred estimate was achieved by the IWC (2009) using distance sampling methods. The multiple re-analyses were driven by the small number of whales observed on transect lines in one of the strata, creating uncertainty in estimated abundance. This survey estimate was corrected for perception and availability bias, where availability bias was estimated using the same time-depth recorder data as was used for the 1981 survey. Finally, the 2013 survey was conducted as a double platform line transect survey, analyzed using mark recapture distance sampling methods (Doniol-Valcroze et al. 2020). This survey was also adjusted for perception and availability bias, where the availability bias adjustments were calculated using time-depth recorder data from bowhead whales tagged near Pangnirtung and Igloolik in 2015. Comparing across surveys, there is a notable issue with availability bias adjustments used for 1981, as the time-depth data was

collected with a large temporal disparity to the conduction of the aerial survey. Further, the time-depth recorders were not deployed on whales within the winter survey area, thus if diving behaviour differs spatially or temporally the adjustments are not accurate. Our model structure allowed for estimation of higher than typical survey error, which accommodated for error in the extrapolation of survey estimates using BBMMs, but also accommodated the uncertainty associated with differences in survey design and adjustments.

Comparing occupancy and survey coverage of the most recent survey in 2013 suggests that survey coverage could be altered to better cover areas of probable density (Figure 5.2B). Survey coverage generally covers high-use areas but could be expanded along the northeastern coast of Baffin Island, and reduced coverage of Eclipse Sound. Surveying all high occupancy areas would increase the confidence of the resulting abundance estimates and make the extrapolation of abundance estimates unnecessary. However, relying solely on complete survey coverage is unlikely due to logistic constraints that commonly arise while surveys are being performed, such as inclement weather and unpredictable sea ice cover. Further, whale movement may change year-to-year and past telemetry data may not reflect current movement patterns or completely encompass occupancy.

Previous work on EC-WG bowheads suggests that since the cessation of commercial whaling abundance has been rebounding, which is supported by our model trajectory. The starting population estimate of 1028 individuals in 1915 reflects the potential starting point of rebound immediately after the moratorium on commercial whaling, although total landed catch was below 100 individuals for ~60 years before the moratorium (Higdon 2010). Ferguson et al. (2021) estimates rebound to have begun ~1880, around the same time commercial harvest was greatly reduced, so the 1915 start time for the model reflects post-commercial whaling trends

opposed to rebound specifically. Before the first abundance estimate in 1981, the model is being informed by harvest history alone, this is evident by the credible intervals widening until the first abundance estimate. In 2013, there was both an aerial survey and a MRC estimate, and our model estimate more closely reflects the adjusted aerial survey estimate. The 2013 MRC estimate was determined by projecting abundance into unsampled regions (Frasier et al. 2020), which could be an overestimation due to overestimating the number of individuals in unsampled regions, or because the estimate was a result of combining multiple years of data.

Our model made use of multiple types of data, with population dynamics being informed by abundance estimates from both aerial surveys and MRC estimates. Stock production models typically make use of abundance estimates from one type of data collection method, mainly aerial survey estimates (Biddlecombe and Watt 2022, Kingsley et al. 2013, Watt et al. 2020a). However, because the aerial surveys are collected over a long-term period, usually multiple decades, there are often discrepancies between how data is collected and analyzed resulting in inconsistencies between abundance estimates, which can be accounted for by increased error in the model. Utilizing abundance estimates from other data analysis methods, such as mark-recapture, relies on the model accommodating abundance estimates with similar discrepancies as might exist between temporally disparate aerial surveys. Previous work by Ferguson et al. (2021) modelled EC-WG bowhead whale population dynamics using much of the same available data that was used in this study, using the 2013 aerial survey estimate and the 2013 MRC estimate. Authors compared the sensitivity of the model using the two 2013 estimates separately, and found the overall trend stayed the same. We opted to include both 2013 estimates in our model so the model trajectory could be informed by both valid, but methodologically differing,

population estimates, even so, extrapolation adjustments to the 2013 aerial survey resulted in highly overlapping confidence intervals for the two estimates.

The aerial survey estimates were conducted in different seasons, winter in 1981 and summer in 2002 and 2013. Due to the difference in season, the areas surveyed differ, and because space use differs seasonally for EC-WG bowhead whales (Finley 2001, Fortune et al. 2020) the extent of coverage is difficult to directly compare. Extrapolation methods aimed to address the seasonal difference in surveys by creating two separate BBMMs, subsetting telemetry data to locations exclusively in March to extrapolate the survey conducted in March, and subsetting data to August to extrapolate surveys conducted in August. There could be bias as satellite tags were deployed at only four sites across the EC-WG bowheads' range, and because EC-WG bowhead whales are segregated by sex and age (Fortune et al. 2020, Heide-Jørgensen et al. 2010) the location data used for population-wide extrapolation could be biased to certain demographic groups. Although we cannot account for this bias, missing portions of demographic groups would result in an underestimation of whales in unsurveyed areas in our model, which is preferable to an overestimate for management applications.

Aerial survey and MRC estimates suggest a plateau in population growth from the 2002 survey onwards, and the estimated trajectory from our model suggests a levelling off of abundance, although up to 2022 growth is still evident. The population trend is similar to one of the model results from multiple models presented in Ferguson et al. (2021), which also estimates steady increase from the cessation of commercial whaling in 1915 with slowed growth near the end of the time series. The closest matching model result from Ferguson et al. (2021) reduced the rate of rebound by accounting for a 26-year delay in reproduction at the start of rebound to represent the age of maturation in bowhead whales. Our model time series starts at the cessation

of commercial whaling, which is shortly after whaling had declined and rebound had already begun, thus it was not necessary to consider this 26-year reproductive delay at the beginning of our time series. Ferguson et al.'s (2021) model trend shows a gradual decline in population growth toward the end of their time series, near 2013. Similarly, our model shows a gradual decline in population growth near the end of the time series, but the slowed growth is much more apparent in the future projections. In our model we truncated harvest history to post-commercial whaling as we have no new data to inform changes in the precommercial whaling population dynamics estimated by Ferguson et al. (2021). The addition of another abundance estimate reduces uncertainty in modelled population trends in recent decades, providing more confidence in the estimated trajectory of continued increase during the period of rebound.

The maximum annual population growth rate for bowhead whales or other closely related whale species is estimated somewhere between 4-7% (Romero et al. 2022, Wade 2018, Witting 2013). Our model estimated a maximum growth rate of 3.3%, slightly below expected maximum growth rate, but ecologically plausible as long-lived marine species typically show low rates of population growth (Heppell et al. 1999, Wade 2018). Theta (θ), representing the effect of density dependence, was estimated as 2.8, which means that EC-WG bowhead whales exhibit non-linear density dependence, which is also common for long-lived marine mammal species (Taylor and Demaster 1993). As population abundance approaches carrying capacity the growth rate will begin to decline. The θ value of 2.8 translates to maximum growth occurring at 62% of carrying capacity. The 2022 estimate of 8243 is 91% of estimated carrying capacity (9045 whales), which suggests that the EC-WG bowhead population has passed a period of maximum productivity. An expected high level of productivity at a lower abundance explains the large amount of growth from the 1981 survey estimate to the 2002 survey estimate, as maximum productivity would be

reached at an abundance of 5611 individuals, which occurred between these aerial surveys. The slowed growth post maximum productivity explains the risk of decline near a moderate level with a harvest of zero in our future projections. All harvest levels resulted in similar probabilities of decline, within ~30%, which suggests that although growth is slowing, continued growth is potentially consistent regardless of harvest, but that the population may not yet be stable. The Fisheries and Oceans Canada Precautionary Approach (DFO 2009) quantifies a 25-50% probability of decline as moderate; all projected harvest levels in this study fall within or very near to this moderate probability of decline. A moderate probability of decline at low harvest levels suggests that the population faces a risk of decline not associated with harvest which may suggest population instability or that the population is approaching a plateau in growth, potentially associated with declining growth rate or density dependence effects. Conversely, moderate probability of decline at higher harvest levels, even those 10-fold greater than reported harvest in recent years, suggests that the population has reached an abundance that is relatively robust to harvest. This potential robustness to harvest should be considered in comparison to the harvest levels during commercial harvest, for which a harvest of 30 whales (our maximum modelled harvest level) is vastly lower than peak whaling numbers, which were well over 1000 (Higdon 2010). The effect of harvest would also be variable based on the sex and age class of whales being harvested, but demographics of harvested whales are not available to inform harvest effects in that amount of detail. The Precautionary Approach (DFO 2009) categorizes 5% as very low risk of decline, and our model suggests that a very low risk of decline cannot be achieved even when harvest is zero. A harvest of zero falls within the low risk (5-25%) category, but very close to moderate at a risk of 24%. The lack of a very low risk of decline presents challenges for management, as a 5% risk of decline is the preferred level of risk within a

decision-making framework, and our model suggests this is not achievable. We infer that the inability for the model to achieve the preferred low risk is due to the slowed growth that is estimated with the current population abundance and future projections being so close to carrying capacity. Little is available in the literature concerning how management goals or frameworks may differ as a population reaches carrying capacity, largely because few marine mammal populations are near carrying capacity due to histories of exploitation, so little is known about how populations at high densities respond to harvest (Stenson et al. 2012). Trends for all harvest levels suggest that the driving factor behind the modelled probability of decline is that the population is approaching carrying capacity, although the effects of harvest become more apparent as harvest increases. As a population approaches carrying capacity, density dependence effects result in population growth slowing and plateauing, leading to a possibility of population decline, regardless of harvest, but high harvest levels may exacerbate this trend.

We compared a model that estimated θ, and a model where θ was set at 1. The overall trend for both models was similar with highly comparable posterior distributions, but there were notable differences between the probabilities of decline under various harvest scenarios. Our chosen model, where θ is estimated, showed a higher risk of decline under all harvest levels, whereas when the effect of density dependence was not included in the model harvest appeared to have less of an effect on abundance. This difference is likely attributed to the effect of density dependence in our preferred model dampening growth near the end of the time series as carrying capacity is approached, thereby flattening the curve regardless of harvest. When the effect of density dependence is removed there are not intrinsic factors reducing growth, so growth is more sustained, especially in scenarios with little to no harvest. The $\theta=1$ model remains less

ecologically plausible, as baleen whales typically exhibit density dependence that would affect population growth as abundance approaches carrying capacity.

The rebound for the EC-WG bowhead whale population appears steady since the cessation of commercial whaling, but this trend will likely not be sustained. As mentioned above, the population has moved past a period of maximum productivity, and as the population continues to approach carrying capacity, population growth will likely continue to slow due to the effects of density dependence. Our estimated carrying capacity is more than 9000 individuals less than the estimated pre-commercial whaling carrying capacity of 18 500 whales from Ferguson et al. (2021). Carrying capacity is a non-stationary population parameter, and continued decline would impact population growth, potentially making the population more prone to harvest induced decline. Climate change and anthropogenic stressors have been modelled or observed to reduce the carrying capacity of various species in multiple ecosystems (i.e., Baby et al. 2014, Calizza et al. 2017, Goyert et al. 2018, Woodworth-Jefcoats et al. 2017). Bowhead whales are predicted to be highly sensitive to changes in macroplankton prey species abundance and distribution (Laidre et al. 2008), and changes in the distribution of zooplankton species in the Arctic have been recorded in response to warming water (Abe et al. 2020, Balazy et al. 2018, Blachowiak-Samolyk et al. 2008). Similarly, declining sea ice cover, particularly in regions of shallow water and over continental shelf are predicted to have negative effects on bowhead whales (Chambault et al. 2022, Laidre et al. 2008). There has also been an exponential increase killer whale presence in the Arctic since the mid-1900s, which has resulted in increased killer whale predation on bowhead whales (Ferguson et al. 2010). Changes in zooplankton distribution, sea ice cover, and presence of predation since pre-commercial whaling could explain the decline in carrying capacity. Data concerning the direct effects of these habitat

changes are lacking, making it difficult to identify specific relationships. The effects of bowhead whale habitat change in the Arctic not only impacts the EC-WG population, but also the BCB population, which was also severely depleted by commercial whaling but has shown a more successful rebound than the EC-WG population (Rugh et al. 2003).

The BCB bowhead whale population faces similar data challenges as the EC-WG population. Extensive, high confidence abundance estimates are lacking, but other data sources, including opportunistic sightings, acoustic recordings, and photographic mark-recapture have been used to estimate abundance (Koski et al. 2010, Givens et al. 2013). Telemetry data for BCB bowheads are also available (Citta et al. 2021), which could address uncertainty in existing abundance estimates using the extrapolation methods presented in this study. A model structure similar to the one presented in this study could also be built to utilize the types of data available for BCB bowhead whales to model population trajectory and create a more informed understanding of population dynamics. Bowhead whales are not the sole mysticete species lacking data and confidence in abundance estimation (i.e., Bradford et al. 2021, Stevick et al. 2003, Williams et al. 2006). Many species have variable types of available data, collected with varying methods, often opportunistically or with partial coverage, and as such, may not be easily combined to acquire long term trends and future predictions. As mentioned above, the analyses presented in this work provide an example of how pieces of data can be combined to model population dynamics. This type of approach is not exclusive to bowhead whales, or even to cetaceans, but rather could be applied to many species that have presented challenges in data collection.

The challenge in attaining accurate abundance estimates for EC-WG bowhead whales has contributed to uncertainty surrounding the population's response to the suspension of

commercial whaling (Finley 2001). After commercial whaling of the EC-WG bowhead population ceased, the details concerning the extent of growth or rebound had low certainty because of the minimal abundance estimates available during this period (Finley 2001, Koski et al. 2007). Our model provides an estimated trajectory that has more certainty than previous models, due to an added abundance estimate and BBMM adjustments applied to previous survey estimates informing the model. Increasing mean Arctic temperatures and associated ecosystem effects are a potential threat to both our parameter estimates and the population they represent. Aerial surveys to achieve abundance estimates should continue being performed, and survey design will ideally utilize UD maps to increase certainty that occupied regions are surveyed. With updated abundance estimates, stock production models can be updated to increase certainty in population dynamics and future projections. An estimated reduction in carrying capacity when compared to the past could also be a problem for this population, and as such, could present challenges for population stability and sustainable harvest. Subsistence harvest from the EC-WG bowhead whale population was low in recent years (mean of 3 landed catches per year), but the population should continue to be monitored to track its stability as it approaches carrying capacity and patterns in growth and sustainable harvest potentially change.

5.5 References

Abe Y, Matsuno K, Fujiwara A, Yamaguchi A (2020) Review of spatial and inter-annual changes in the zooplankton community structure in the western Arctic Ocean during summers of 2008–2017. Prog Oceanogr 186:102391.

Baby S, Nathawat MS, Al-Sarawi MA (2014) Major Impacts from Anthropogenic Activities on Landscape Carrying Capacity of Kuwaiti Coast. Pol J Environ Stud 23:7-17.

Balazy K, Trudnowska E, Wichorowski M, Błachowiak-Samołyk K (2018) Large versus small zooplankton in relation to temperature in the Arctic shelf region. Polar Res 37:1427409.

Biddlecombe BA, Ferguson SH, Heide-Jørgensen MP, Gillis DM, Watt CA (2023) Estimating abundance of Eastern Canada-West Greenland bowhead whales using genetic mark-recapture analyses. Global Ecol Conserv 45:e02524.

Biddlecombe BA, Watt CA (2022) Modeling population trajectory and probability of decline in northern Hudson Bay narwhals (*Monodon monoceros*). Mar Mamm Sci 38:1357-1370.

Blachowiak-Samolyk K, Søreide JE, Kwasniewski S, Sundfjord A, Hop H, Falk-Petersen S, Hegseth EN (2008) Hydrodynamic control of mesozooplankton abundance and biomass in northern Svalbard waters (79–81 N). Deep Sea Res Part II 55:2210-2224.

Bockstoce JR (2008) Two historical weapon fragments as an aid to estimating the longevity and movements of bowhead whales. Polar Biol 31:751-754.

Booth CG, Sinclair RR, Harwood J (2020) Methods for Monitoring for the Population Consequences of Disturbance in Marine Mammals: A Review. Front Mar Sci 7.

Bradford AL, Oleson EM, Forney KA, Moore JE, Barlow J (2021) Line-transect abundance estimates of cetaceans in U.S. waters around the Hawaiian Islands in 2002, 2010, and

2017. U.S. Dept. of Commerce, NOAA Technical Memorandum NMFS-PIFSC-115, 52 p. doi:10.25923/daz4-kw84.

Brooks SP, Gelman A (1998) General Methods for Monitoring Convergence of Iterative Simulations. J Comput Graphical Stat 7:434-455.

Bullard F (1991) Estimating the home range of an animal: a Brownian bridge approach. University of North Carolina, Chapel Hill.

Calenge C (2011) Home range estimation in R: the adehabitatHR package. Office national de la classe et de la faune sauvage: Saint Benoist, Auffargis, France.

Calizza E, Costantini ML, Careddu G, Rossi L (2017) Effect of habitat degradation on competition, carrying capacity, and species assemblage stability. Ecol Evol 7:5784-5796.

Chambault P, Kovacs KM, Lydersen C, Shpak O, Teilmann J, Albertsen CM, Heide-Jørgensen MP (2022) Future seasonal changes in habitat for Arctic whales during predicted ocean warming. Sci Adv 8:eabn2422.

Citta JJ, Quakenbush L, George JC (2021) Distribution and behavior of Bering-Chukchi-Beaufort bowhead whales as inferred by telemetry. In The Bowhead Whale, Academic Press, pp. 31-56.

Cosens SE, Blouw A (2003) Size-and age-class segregation of bowhead whales summering in Northern Foxe Basin: A photogrammetric analysis. Mar Mamm Sci 19:284-296.

COSEWIC (2009) COSEWIC assessment and update status report on the Bowhead Whale Balaena mysticetus, Bering–Chukchi–Beaufort population and Eastern Canada–West Greenland population,in Canada. Committee on the Status of Endangered Wildlife in Canada. Ottawa, vii + 49 pp.

Costa DP, Robinson PW, Arnould JPY, Harrison A-L, Simmons SE, Hassrick JL, Hoskins AJ, Kirkman SP, Oosthuizen H, Villegas-Amtmann S, Crocker DE (2010) Accuracy of ARGOS Locations of Pinnipeds at-Sea Estimated Using Fastloc GPS. PLOS ONE 5:e8677.

de Valpine P, Hastings A (2002) Fitting population models incorporating process noise and observation error. Ecol Monogr 72:57-76.

DFO (2009) A fishery decision-making framework incorporating the precautionary approach. Government of Canada. https://www.dfo-mpo.gc.ca/reports-rapports/regs/sff-cpd/precaution-back-fiche-eng.htm.

Doniol-Valcroze T, Gosselin J-F, Pike DG, Lawson JW, Asselin NC, Hedges KJ, Ferguson SH (2020) Distribution and Abundance of the Eastern Canada – West Greenland Bowhead Whale Population Based on the 2013 High Arctic Cetacean Survey. NAMMCO Sci Pub 11.

Dueck L, Richard P, Cosens SE (2008) A review and re-analysis of Cosens et al. (2006) aerial survey assessment of bowhead whale abundance for the eastern Canadian Arctic. Can. Sci. Adv. Res. Secretar. Res. Doc. 2007:33.

Ferguson SH, Dueck L, Loseto LL, Luque SP (2010) Bowhead whale *Balaena mysticetus* seasonal selection of sea ice. MEPS 411:285-297.

Ferguson SH, Higdon JW, Hall PA, Hansen RG, Doniol-Valcroze T (2021) Developing a Precautionary Management Approach for the Eastern Canada-West Greenland Population of Bowhead Whales (*Balaena mysticetus*). Front Mar Sci 8.

Finley K (2001) Natural history and conservation of the Greenland whale, or bowhead, in the Northwest Atlantic. Arctic 54:55-76.

Fortune SME, Young BG, Ferguson SH (2020) Age- and sex-specific movement, behaviour and habitat-use patterns of bowhead whales (*Balaena mysticetus*) in the Eastern Canadian Arctic. Polar Biol 43:1725-1744.

Frasier TR, Petersen SD, Postma L, Johnson L, Heide-Jørgensen MP, Ferguson SH (2020) Abundance estimation from genetic mark-recapture data when not all sites are sampled: An example with the bowhead whale. Global Ecol Conserv 22:e00903.

Freitas C, Lydersen C, Fedak MA, Kovacs KM (2008) A simple new algorithm to filter marine mammal Argos locations. Mar Mamm Sci 24:315-325.

Fuller AK, Augustine BC, Morin DJ, Pigeon K, Boulanger J, Lee DC, Bisi F, Garshelis DL (2022) The occupancy-abundance relationship and sampling designs using occupancy to monitor populations of Asian bears. Glob Ecol Conserv 35:e02075.

George J, Thewissen J, Von Duyke A, Breed GA, Suydam R, Sformo TL, Person BT, Brower Jr H (2021) Life history, growth, and form. In: The Bowhead Whale. Academic Press, Cambridge, MA, pp. 87-115.

Geweke J (1996) Evaluating the accuracy of sampling-based approaches to the calculation of posterior moments. In: Bernardo JM, Berger JM, Dawid AP, Smith AFM (eds.), Bayesian Statistics 4. Oxford University Press, Oxford, pp. 169-193.

Givens GH, Edmondson SL, George JC, Suydam R, Charif RA, Rahaman A, Hawthorne D, Tudor B, DeLong RA, Clark CW (2013) Estimate of 2011 abundance of the Bering-Chukchi-Beaufort Seas bowhead whale population. Scientific Committee of the International Whaling Commission 65a, Paper SC/65a/BRG01, Jeju Island, Korea.

Goyert HF, Garton EO, Poe AJ (2018) Effects of climate change and environmental variability on the carrying capacity of Alaskan seabird populations. The Auk: Ornithol Adv 135:975-991.

Halliday WD, Le Baron N, Citta JJ, Dawson J, Doniol-Valcroze T, Ferguson M, Ferguson SH, Fortune S, Harwood LA, Heide-Jørgensen MP (2022) Overlap between bowhead whales (*Balaena mysticetus*) and vessel traffic in the North American Arctic and implications for conservation and management. Biol Conserv 276:109820.

Hammill MO, Stenson GB, Doniol-Valcroze T (2017) A management framework for Nunavik beluga. DFO Can. Sci. Advis. Sec. Res. Doc. 2017/060., v + 34 p.

Heide-Jørgensen MP, Laidre K, Wiig Ø, Jensen M, Dueck L, Maiers L, Schmidt H, Hobbs R (2003) From Greenland to Canada in ten days: Tracks of bowhead whales, *Balaena mysticetus*, across Baffin Bay. Arctic 56:21-31.

Heide-Jørgensen MP, Laidre K, Wiig Ø, Postma L, Dueck L, Bachmann L (2010) Large-scale sexual segregation of bowhead whales. Endang Spec Res 13:73-78.

Heppell SS, Crowder LB, Menzel TR, Musick J (1999) Life table analysis of long-lived marine species with implications for conservation and management. American Fisheries Society Symposium, pp. 137-148.

Higdon JW (2010) Commercial and subsistence harvests of bowhead whales (*Balaena mysticetus*) in eastern Canada and West Greenland. J Cetacean Res Manag 11:185-216.

Higdon JW, Ferguson SH (2016) Historical abundance of Eastern Canada - West Greenland (EC-WG) bowhead whales (*Balaena mysticetus*) estimated using catch data in a deterministic discrete-time logistic population model. DFO Can. Sci. Advis. Sec. Res. Doc. 2016/023. v + 26 p.

Hilborn R, Amoroso RO, Anderson CM, Baum JK, Branch TA, Costello C, De Moor CL, Faraj A, Hively D, Jensen OP, Kurota H, Little LR, Mace P, McClanahan T, Melnychuk MC, Minto C, Osio GC, Parma AM, Pons M, Segurado S, Szuwalski CS, Wilson JR, Ye Y (2020) Effective fisheries management instrumental in improving fish stock status. PNAS 117:2218-2224.

Horne JS, Garton EO, Krone SM, Lewis JS (2007) Analyzing animal movements using Brownian bridges. Ecology 88:2354-2363.

Innes S, Heide-Jørgensen MP, Laake JL, Laidre KL, Cleator HJ, Richard P, Stewart RE (2002) Surveys of belugas and narwhals in the Canadian high Arctic in 1996. NAMMCO Sci Pub 4:169-190.

IWC (2009) Annex F: Report of the Sub-Committee on Bowhead, Right and Gray Whales. J Cetacean Res Manag 11:168.

Kingsley MCS, Asselin NC, Ferguson SH (2013) Updated stock-dynamic model for the Northern Hudson Bay narwhal population based on 1982–2011 aerial surveys. DFO Canadian Science Advisory Secretariat Research Document 2013/011.

Koski WR, da-Silva CQ, Zeh J, Reeves RR (2013) Evaluation of the potential to use capture-recapture analyses of photographs to estimate the size of the Eastern Canada–West Greenland bowhead whale (*Balaena mysticetus*) population. Can Wildl Biol Manage 2:23-35.

Koski WR, Heide-Jorgensen MP, Laidre KL (2007) Winter abundance of bowhead whales, *Balaena mysticetus*, in the Hudson Strait, March 1981. J Cetacean Res Manag 8:139.

Koski WR, Zeh J, Mocklin J, Davis AR, Rugh DJ, George JC, Suydam R (2010) Abundance of Bering-Chukchi-Beaufort bowhead whales (*Balaena mysticetus*) in 2004 estimated from photo-identification data. J Cetacean Res Manag 1:89-99.

Kranstauber B, Kays R, LaPoint SD, Wikelski M, Safi K (2012) A dynamic Brownian bridge movement model to estimate utilization distributions for heterogeneous animal movement. J Anim Ecol 81:738-746.

Laidre KL, Stirling I, Lowry LF, Wiig O, Heide-Jorgensen MP, Ferguson SH (2008) Quantifying the sensitivity of arctic marine mammals to climate-induced habitat change. Ecol Appl 18:S97-S125.

Le Coeur C, Storkey J, Ramula S (2021) Population responses to observed climate variability across multiple organismal groups. Oikos 130:476-487.

Matthews CJ, Breed GA, LeBlanc B, Ferguson SH (2020) Killer whale presence drives bowhead whale selection for sea ice in Arctic seascapes of fear. PNAS 117:6590-6598.

Maunder MN, Punt AE (2013) A review of integrated analysis in fisheries stock assessment. Fish Res 142:61-74.

Morris WF, Pfister CA, Tuljapurkar S, Haridas CV, Boggs CL, Boyce MS, Bruna EM, Church DR, Coulson T, Doak DF, Forsyth S, Gaillard J-M, Horvitz CC, Kalisz S, Kendall BE, Knight TM, Lee CT, Menges ES (2008) Longevity can buffer plant and animal populations against changing climatic variability. Ecology 89:19-25.

Pella JJ, Tomlinson PK (1969) A generalized stock production model. Inter-American Tropical Tuna Commission Bulletin 13:416-497.

Plummer M (2003) JAGS: a program for analysis of Bayesian graphical models using Gibbs sampling. In: Hornik K, Leisch F, Zeileis A (eds.) Proceedings of the 3rd International

Workshop on Distributed Statistical Computing (DSC 2003), Technische Universität, Vienna.

Plummer M, Best N, Cowles K, Vines K (2006) CODA: convergence diagnosis and output analysis for MCMC. R News 6:7-11.

R Core Team (2020) R: A language and environment for statistical computing. R Foundation for Statistical Computing, Vienna, Austria.

Reeves R, Rosa C, George JC, Sheffield G, Moore M (2012) Implications of Arctic industrial growth and strategies to mitigate future vessel and fishing gear impacts on bowhead whales. Marine Policy 36:454-462.

Reinhart N, Ferguson S, Koski W, Higdon J, LeBlanc B, Tervo O, Jepson P (2013) Occurrence of killer whale *Orcinus orca* rake marks on Eastern Canada-West Greenland bowhead whales *Balaena mysticetus*. Polar Biol 36:1133-1146.

Richard P, Laake J, Hobbs R, Heide-Jørgensen M, Asselin N, Cleator H (2010) Baffin Bay narwhal population distribution and numbers: aerial surveys in the Canadian High Arctic, 2002-04. Arctic 63:85-99.

Romero MA, Coscarella MA, Adams GD, Pedraza JC, González RA, Crespo EA (2022) Historical reconstruction of the population dynamics of southern right whales in the southwestern Atlantic Ocean. Sci Rep 12:3324.

Ross WG (1993) Commercial whaling in the North Atlantic sector. In: Burns JJ, Montague JJ, Cowles CJ (eds.) The Bowhead Whale. Society for Marine Mammalogy Special Publication Number 2, Lawrence, Kansas, pp. 511–561.

Rugh DJ, Demaster D, Rooney A, Breiwick J, Shelden K, Moore S (2003) A review of bowhead whale (Balaena mysticetus) stock identity. J Cetacean Res Manage 5:267-79.

Rugh DJ, Shelden KE (2009) Bowhead whale: *Balaena mysticetus*. In: Perrin WF, Würsig B, Thewisssen JGM (eds.) Encyclopedia of Marine Mammals. Academic Press, San Diego, pp.129-131.

Stauffer GE, Roberts NM, Macfarland DM, Van Deelen TR (2021) Scaling occupancy estimates up to abundance for wolves. J Wildlife Manage 85:1410-1422.

Stenson GB, Hammill M, Ferguson S, Stewart R, Doniol-Valcroze T (2012) Applying the Precautionary Approach to Marine Mammal Harvests in Canada. DFO Can. Sci. Advis. Sec. Res. Doc. 2012:15.

Stevick PT, Allen J, Clapham PJ, Friday N, Katona SK, Larsen F, Lien J, Mattila DK, Palsbøll PJ, Sigurjónsson J, Smith TD (2003) North Atlantic humpback whale abundance and rate of increase four decades after protection from whaling. MEPS 29:263-73.

Su Y-S, Yajima M (2015) R2jags: Using R to Run 'JAGS'. R package version 0.5-7. Available: CRAN. R-project. org/package= R2jags.(September 2015).

Taylor BL, Demaster DP (1993) Implications of non-linear density dependence. Mar Mamm Sci 9:360-371.

Taylor BL, Martinez M, Gerrodette T, Barlow J, Hrovat YN (2007) Lessons from monitoring trends in abundance of marine mammals. Mar Mamm Sci 23:157-175.

Trenkel VM, Beecham JA, Blanchard JL, Edwards CT, Lorance P (2013) Testing CPUE-derived spatial occupancy as an indicator for stock abundance: application to deep-sea stocks. Aquat Living Resources 26:319-332.

Van Winkle W (1975) Comparison of Several Probabilistic Home-Range Models. J Wildl Manag 39:118-123.

Wade PR (1998) Calculating limits to the allowable human-caused mortality of cetaceans and pinnipeds, Mar Mamm Sci 14:1-37.

Wade PR (2018) Population Dynamics. In: Würsig B, Thewissen JGM, Kovacs KM (eds.), Encyclopedia of Marine Mammals (Third Edition). Academic Press, pp. 763-770.

Watt CA, Marcoux M, Ferguson SH, Hammill M, Matthews C (2020a) Population dynamics of the threatened Cumberland Sound beluga (*Delphinapterus leucas*) population. Arctic Sci 7:545-566.

Watt CA, Hornby C, Hudson J (2020b) Narwhal (*Monodon monoceros*) abundance from the 2018 aerial survey of the Northern Hudson Bay population. DFO Can. Sci. Advis. Sec. Res. Doc. 2020/nnn., iv + p.

Williams R, Hedley SL, Hammond PS (2006) Modeling distribution and abundance of Antarctic baleen whales using ships of opportunity. Ecol and Soc 1:11.

Witting L (2013) Selection-delayed population dynamics in baleen whales and beyond. Pop Ecol 55:377-401.

Woodworth-Jefcoats PA, Polovina JJ, Drazen JC (2017) Climate change is projected to reduce carrying capacity and redistribute species richness in North Pacific pelagic marine ecosystems. Global Chang Biol 23:1000-1008.

Worton BJ (1987) A review of models of home range for animal movement. Ecol Model 38:277-298.

Worton BJ (1989) Kernel methods for estimating the utilization distribution in home-range studies. Ecology 70:164-168.

Chapter 6

6 Conclusion

Monitoring population dynamics is essential for effective management, although for many marine mammal species there are notable challenges associated with population monitoring. In this thesis I focused on three populations of Arctic cetacean: Northern Hudson Bay (NHB) narwhal, Cumberland Sound (CB) beluga, and Eastern Canada-West Greenland (EC-WG) bowhead whales, and the unique challenges each population poses for management and informing sustainable harvest. Three of the four research-based chapters utilize population dynamics modelling, while one chapter (Chapter 4) addresses acquiring reliable population estimates, an important prerequisite for population dynamics modelling. Chapter 4 and 5 together show the important steps required to build a reliable population dynamics model.

When results from this thesis are considered together, it is difficult to make large scale conclusions about the status of cetaceans in the Canadian Arctic. Each population of focus is experiencing something very different in terms of current population dynamics. It was expected that each population would show different trends, because population trends in Arctic cetaceans are highly variable, even within the same species (COSEWIC 2004, 2009, 2020). As such, it is common for multiple populations of the same species to have different Committee on the Status of Endangered Wildlife in Canada (COSEWIC) or Species at Risk Act (SARA) ratings, as is the case with beluga whale populations in the Canadian Arctic (COSEWIC 2020). When considering how my findings could be applicable to management of other populations or species in the Arctic, the population trends themselves are not particularly enlightening. Rather, the more general species specific parameters, such as maximum growth rate, can help inform future

models, and more broadly my work sets a foundation for how to include more data, combine seemingly incongruent data streams, and improve on data-limited population models.

Chapters 2 -5 each address a different concern associated with assessing marine mammal populations in the Arctic. The NHB narwhal population presented challenges with using historical data that had inconsistencies with data collection/analysis over time. Discrepancies within historical data are a common issue for most long-term datasets. As science progresses, methodologies for data collection and analyses also progress, this is evident in the temporal difference in aerial survey analysis methods discussed in Chapter 2. An awareness of these differences is crucial, and adjusting for them can be relatively straight forward, by comparing analyses and adjustments between surveys, allowing for increased confidence in model results. The CB beluga population posed a different challenge, of a more exploratory nature. The intent was to create a way that the effects of environmental change on population dynamics could be quantified within a population model. Chapter 3 provides a framework from which environmental covariates could contribute to a population model, but there is room here for progress, pending further information on relationships between environmental covariates and specific population parameters. This general framework could be implemented with modifications for other populations that may have more research regarding specific population wide responses to environmental variables, allowing environmental covariates to be connected to specific model parameters. Chapter 4 redirects away from a population dynamics approach, though not entirely, as the presence of a short-term temporal trend is inspected via the Cormack Jolly-Seber model. Having multiple years of "capture" data (biopsy data for EC-WG bowhead whales) presents an opportunity to investigate population trends, while achieving abundance estimates. The MRC methodology addresses the constraints of achieving abundance estimates

via aerial surveys. Having a high degree of confidence in an abundance estimate creates more confidence for use in subsequent population dynamics modelling. Though, MRC analyses do not rid a population of all issues surrounding abundance estimates, as was evident in the sampling bias present in the Chapter 4 analysis. As with abundance estimates for virtually all marine mammal populations, uncertainties will be present due to the number of constraints surrounding data collection. Finally, Chapter 5 delves into trying to increase confidence in population modelling by collating multiple data types, to effectively utilize the limited data that is available. Building a model that incorporates many data types will be specific to the population of focus and the available data, but Chapter 5 provides a case study of how management issues specific to a population can be addressed using available data.

As the effects of climate change progress, the fate of wildlife in the Arctic is becoming a greater concern (Burek et al. 2008, Laidre et al. 2015, Descamps et al. 2017, Bruno et al. 2018). Understanding population dynamics is often one of the primary goals involved with management or population monitoring, as it provides a valuable baseline view of population status (Stenson et al. 2012, Hammill et al. 2017, Watt et al. 2020). There are many species and populations in the Arctic where data collection is difficult, or that have a variety of data types that may not typically work together to answer questions about population dynamics. The work in this thesis provides a framework on how multiple data types can be utilized for population dynamics modelling, or how challenges surrounding limited data availability can be addressed. It is important to note that, as per each of the research chapters in this thesis, populations each pose unique challenges and goals. Thus, although this work addresses issues with population modelling, the larger application is providing examples of structures from which models can be constructed to incorporate available information. It is unlikely that other Arctic marine mammal populations

will have the same types of data, or the same questions associated with management, but the work presented here could serve as a steppingstone to building a solution to many management questions.

To increase the effectiveness of population modelling and thus, management, the collection of specific types of data should be a priority. For the scope of the work in this thesis, the type of data that is potentially the most valuable is data that can quantify relationships between environmental variables and demographic parameters. There are many expected effects of environmental change on Arctic marine mammals (Burek et al. 2008, Laidre et al. 2008, Moore & Huntington 2008, Kovacs et al. 2011), but the indirect nature of these effects or the lack of data to solidify relationships makes postulating those effects tenuous. There are a number of potential methods that could be used to collect useful data, although, as with most Arctic research, the cost of acquiring this data would be high, as well as the accompanying logistic challenges. Collecting thermoregulatory data and reproductive success in female Arctic marine mammals, alongside ambient ocean temperatures, could uncover the effects of increased Arctic Ocean temperatures on recruitment, and thus, population growth rate. Continuing to monitor killer whale presence in the Arctic (Ferguson et al. 2010, Lefort et al. 2020) would also be valuable. Using killer whale data alongside changes in sea ice extent and Inuit Qaujimajatuqangit (Inuit traditional knowledge) surrounding killer whale predation on marine mammals could quantify a relationship between sea ice and predation, informing a mortality parameter within a population model. Another avenue would be analyzing energetics of an Arctic marine mammal species, then analyzing range shifts in prey species, such as Arctic cod for beluga and narwhal (Marcoux et al. 2012, Watt & Ferguson 2015), or zooplankton species for bowhead whales (Pomerleau et al. 2011). Identifying relationships between presence and abundance of prey and

predator energetics could be used to model temporal variation in carrying capacity within a population model. While the types of data discussed (alongside many other types of data) would be valuable to understanding Arctic marine mammal dynamics, it is important to consider that collecting these types of data is challenging and it is unlikely all (or potentially any) of this data will be available in the near future. As such, being able to alter population models, and use available data to inform these models (such as achieving abundance estimates through genetic MRC analyses) are tools that can be used in the present to meaningfully contribute to monitoring population dynamics, providing information that can be confidently used to inform management action.

Continuing to progress population monitoring methodologies will provide better insight for managers and stakeholders of Arctic cetacean populations. Current methods provide information on population dynamics with the intent of achieving enough confidence in results to be used by managers, using as much data as is available for these populations, as many are still considered data deficient (Stenson & Hammill 2008, Magera et al. 2013). Results such as those achieved in this thesis provide an early step in management action, from which decisions must be made considering the communities that rely on these populations for subsistence, and prioritizing sustainability so subsistence harvest and the health of cetacean populations can be maintained indefinitely.

6.1 References

Bruno JF, Bates AE, Cacciapaglia C, Pike EP, Amstrup SC, van Hooidonk R, Henson SA, Aronson RB (2018) Climate change threatens the world's marine protected areas. Nat Clim Change 8:499-503.

Burek KA, Gulland FM, O'Hara TM (2008) Effects of climate change on Arctic marine mammal health. Ecol Appl 18:S126-S134.

COSEWIC (2004) COSEWIC assessment and update status report on the narwhal Monodon monoceros in Canada. Committee on the Status of Endangered Wildlife in Canada Ottawa vii + 50 pp.

COSEWIC (2009) COSEWIC assessment and update status report on the Bowhead Whale Balaena mysticetus, Bering–Chukchi–Beaufort population and Eastern Canada–West Greenland population,in Canada. Committee on the Status of Endangered Wildlife in Canada Ottawa:vii + 49 pp.

COSEWIC (2020) COSEWIC assessment and status report on the Beluga Whale Delphinapterus leucas, Eastern High Arctic - Baffin Bay population, Cumberland Sound population, Ungava Bay population, Western Hudson Bay population, Eastern Hudson Bay population and James Bay population in Canada. Committee on the Status of Endangered Wildlife in Canada Ottawa xxxv + 84 pp.

Descamps S, Aars J, Fuglei E, Kovacs KM, Lydersen C, Pavlova O, Pedersen AO, Ravolainen V, Strom H (2017) Climate change impacts on wildlife in a High Arctic archipelago - Svalbard, Norway. Glob Chang Biol 23:490-502.

Ferguson SH, Higdon JW, Chmelnitsky EG (2010) The Rise of Killer Whales as a Major Arctic Predator. In: Ferguson SH, Loseto LL, Mallory ML (eds) A Little Less Arctic. Springer, Dordrecht.

Hammill MO, Stenson GB, Doniol-Valcroze T (2017) A management framework for Nunavik beluga. DFO Can Sci Advis Sec Res Doc 2017/060:v + 34 p.

Kovacs KM, Lydersen C, Overland JE, Moore SE (2011) Impacts of changing sea-ice conditions on Arctic marine mammals. Marine Biodiv 41:181-194.

Laidre KL, Stern H, Kovacs KM, Lowry L, Moore SE, Regehr EV, Ferguson SH, Wiig Ø, Boveng P, Angliss RP, Born EW, Litovka D, Quakenbush L, Lydersen C, Vongraven D, Ugarte F (2015) Arctic marine mammal population status, sea ice habitat loss, and conservation recommendations for the 21st century. Conserv Biol 29:724-737.

Laidre KL, Stirling I, Lowry LF, Wiig O, Heide-Jorgensen MP, Ferguson SH (2008) Quantifying the sensitivity of arctic marine mammals to climate-induced habitat change. Ecol Appl 18:S97-S125.

Lefort KJ, Matthews CJD, Higdon JW, Petersen SD, Westdal KH, Garroway CJ, Ferguson SH (2020) A review of Canadian Arctic killer whale (*Orcinus orca*) ecology. Can J Zool 98:245-253.

Magera AM, Mills Flemming JE, Kaschner K, Christensen LB, Lotze HK (2013) Recovery trends in marine mammal populations. PLoS One 8:e77908.

Marcoux M, McMeans BC, Fisk AT, Ferguson SH (2012) Composition and temporal variation in the diet of beluga whales, derived from stable isotopes. MEPS 471:283-291.

Moore SE, Huntington HP (2008) Arctic marine mammals and climate change: Impacts and resilience. Ecol Appl 18:S157-S165.

Pomerleau C, Ferguson SH, Walkusz W (2011) Stomach contents of bowhead whales (*Balaena mysticetus*) from four locations in the Canadian Arctic. Polar Biol 34:615-620.

Stenson G, Hammill M (2008) Incorporating the precautionary approach into the provision of advice on marine mammals. DFO Can Sci Advis Sec Res Doc 2008/079. https://waves-vagues.dfo-mpo.gc.ca/Library/337968.pdf.

Stenson GB, Hammill M, Ferguson S, Stewart R, Doniol-Valcroze T (2012) Applying the precautionary approach to marine mammal harvests in Canada. DFO Can. Sci. Advis. Sec. Res. Doc. 2012:15.

Watt C, Marcoux M, Ferguson SH, Hammill M, Matthews C (2020) Population dynamics of the threatened Cumberland Sound beluga (*Delphinapterus leucas*) population. Arctic Sci 7:545-566.

Watt CA, Ferguson SH (2015) Fatty acids and stable isotopes (δ13C and δ15N) reveal temporal changes in narwhal (*Monodon monoceros*) diet linked to migration patterns. Mar Mamm Sci 31:21-44.

Appendices

Appendix 1

Appendix 1. Table 1. Reported harvests for Northern Hudson Bay narwhal from 1951 – 2018. Data for 1951 – 1953 are from Stewart (2008), data for 1953 – 2018 are from Mansfield (1975), Kemper (1980), Strong (1989), and DFO harvest statistics 1988-2018 (unpublished data).

Year	Reported catch	Year	Reported catch	Year	Reported catch
1951	0	1974	0	1997	45
1952	0	1975	0	1998	0
1953	0	1976	8	1999	28
1954	0	1977	0	2000	157
1955	0	1978	6	2001	45
1956	0	1979	31	2002	108
1957	175	1980	1	2003	67
1958	35	1981	26	2004	43
1959	15	1982	41	2005	120
1960	0	1983	23	2006	86
1961	0	1984	11	2007	94
1962	0	1985	27	2008	88
1963	0	1986	16	2009	29
1964	0	1987	7	2010	118
1965	23	1988	16	2011	103
1966	100	1989	38	2012	92
1967	73	1990	16	2013	56
1968	2	1991	17	2014	115
1969	0	1992	36	2015	96
1970	0	1993	20	2016	47
1971	5	1994	14	2017	73
1972	14	1995	6	2018	113
1973	1	1996	14		

Detailed outputs from the model to examine population abundance trends of Northern Hudson Bay narwhal using catch history data from 1951-2018, and aerial abundance observations from 1982, 2000, 2011, and 2018.

Appendix 1. Table 2. Model outputs for NHB narwhal stock using 1951–2018 catch history and 1982–2018 adjusted abundance observations. The mean, standard deviation (SD), 2.5^{th} , 25^{th}, 50^{th}, 75^{th} and 97.5^{th} quantiles are given for the following model parameters and their priors: carrying capacity (K), shaping parameter (theta), process error (prec.process), survey precision (prec.survey), starting population (startpop), struck and lost (S&L), and population size in 2019 (N2019). $\widehat{R}$ is the Brooks-Gelman-Rubin statistic; values near one indicate convergence of chains. N.eff is the number of effective runs after considering autocorrelation.

Parameter	mean	sd	2.50%	25%	50%	75%	97.50%	Rhat	n.eff
K	18,043.963	4,847.476	11,365.241	14,331.783	16,780.341	21,062.227	28,925.174	1.001	5.00E+05
theta	2.959	1.161	1.091	1.944	2.94	3.964	4.897	1.001	260,000
deviance	77.471	1.77	74.762	76.155	77.519	78.303	81.61	1.001	5.00E+05
Rmax	0.039	0.016	0.012	0.025	0.038	0.052	0.068	1.001	440,000
prec.process	14,9993.867	12,2593.316	10,618.713	60,502.855	118,498.246	205,393.797	467,150.492	1.001	44,000
prec.surv	10.566	5.499	2.681	6.547	9.632	13.571	23.768	1.001	230,000
startpop	8,342.42	5,241.543	1,447.335	3,881.599	7,160.237	12,205.5	19,144.186	1.001	5.00E+05
struck.and.lost	0.25	0	0.25	0.25	0.25	0.25	0.25	1	1
N2019	14,625.173	2,595.859	10,257.97	12,762.376	14,381.192	16,221.802	20,381.804	1.001	5.00E+05

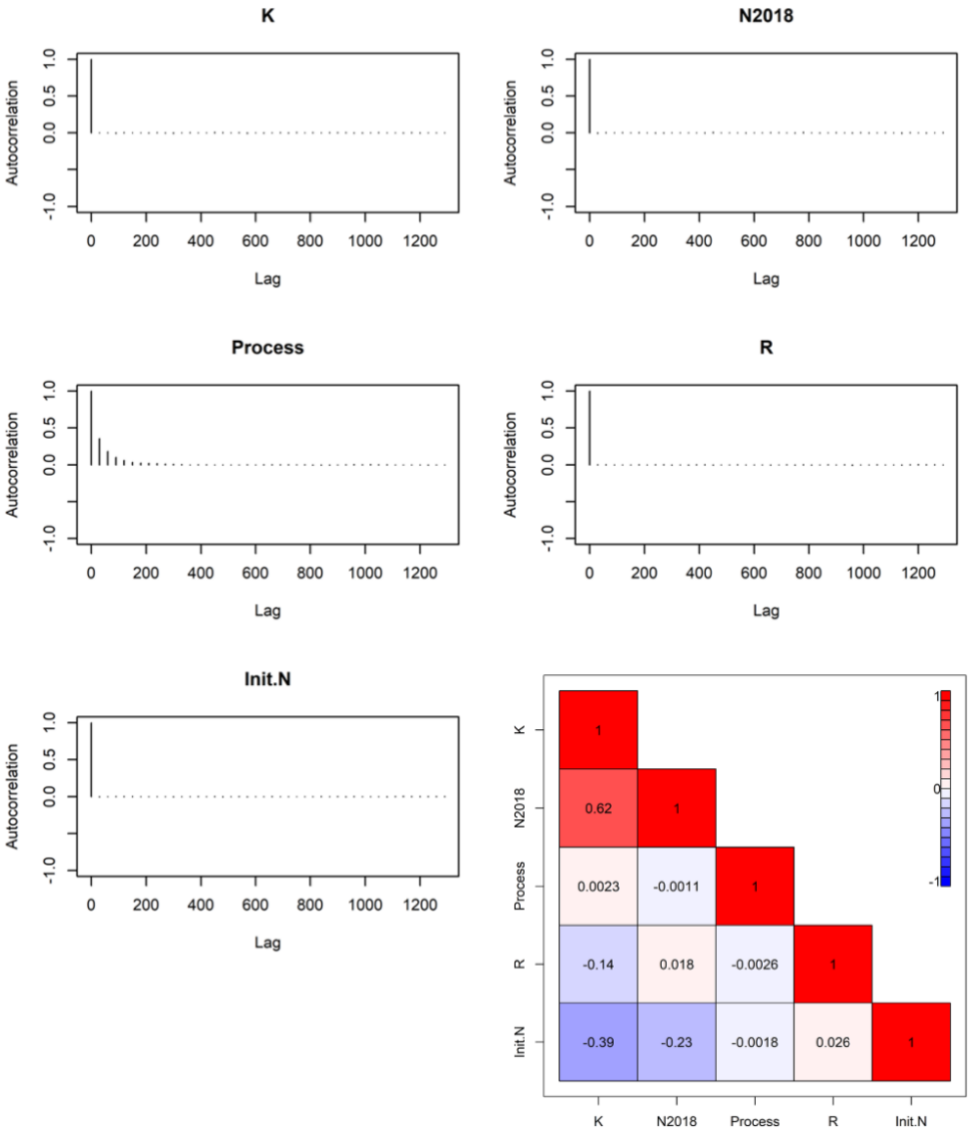
K
N2018
Process
R
Init.N
Autocorrelation
Lag
0
200
400
600
800
1000
1200
-1.0
0.0
0.5
1.0
K
N2018
Process
R
Init.N
1
0.62
1
0.0023
-0.0011
1
-0.14
0.018
-0.0026
1
-0.39
-0.23
-0.0018
0.026
1
0
-1

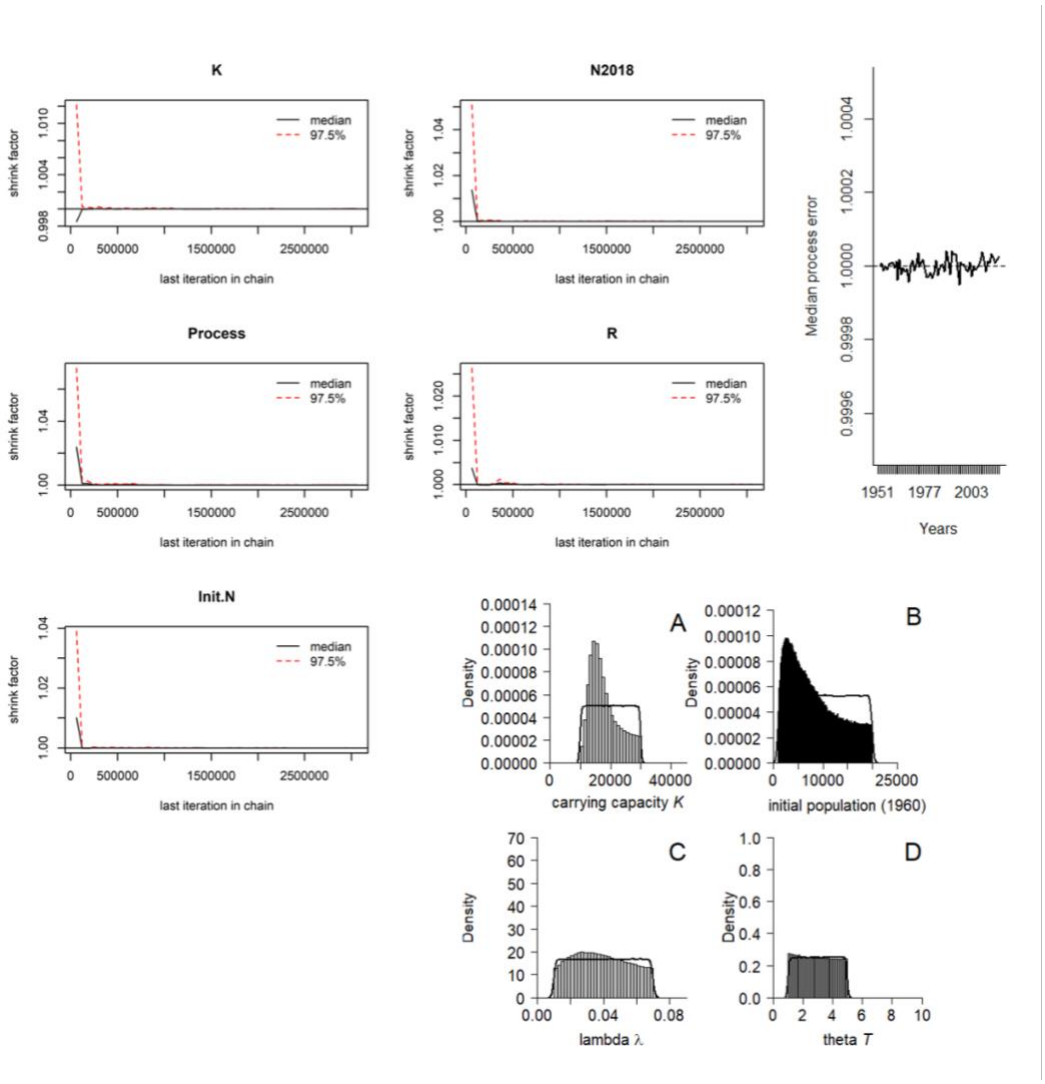

Appendix 1. Figure 1. The model was fit to harvest data (1951–2018) and adjusted aerial survey data (1982-2018). Plots show change in autocorrelation (first page, 5 figures in top left), cross correlation (first page, bottom right), BGR test results (second page, 5 figures in top left), priors (lines) and posteriors (histograms) for A) carrying capacity, B) initial population, C) lambda (R_{max} -1), and D) theta, and median process error (second page, top right).

Appendix 2

Evidence of model convergence for a stochastic stock production model for Cumberland Sound (CS) beluga with sea ice concentration (ICE) and sea surface temperature (SST) covariates included in the state process.

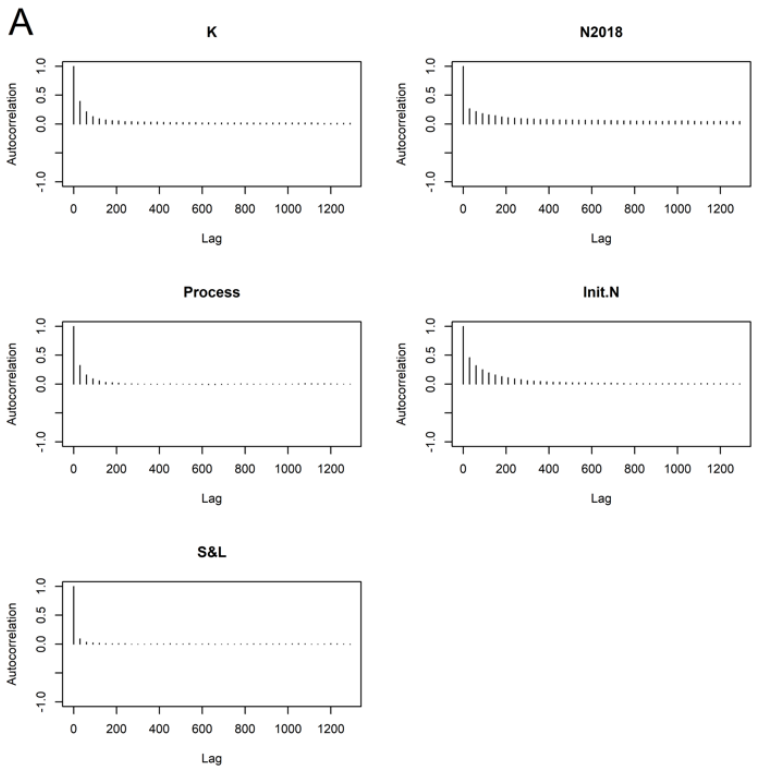

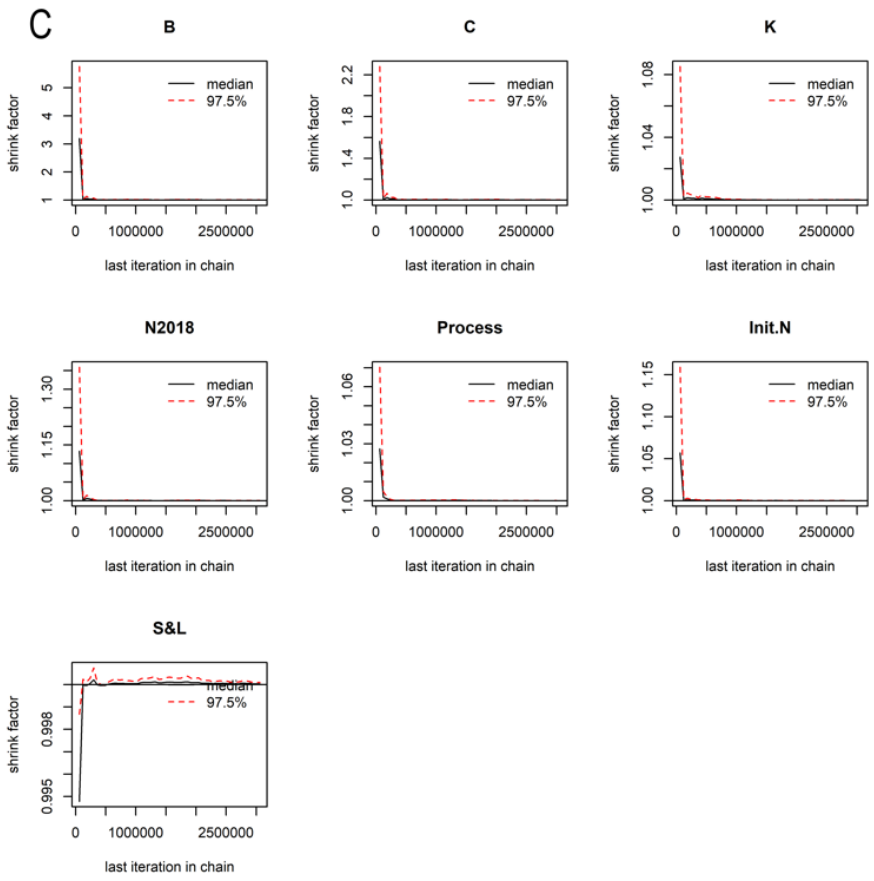
C
B
C
K
N2018
Process
Init.N
S&L
shrink factor
median
97.5%
last iteration in chain
0
1000000
2500000

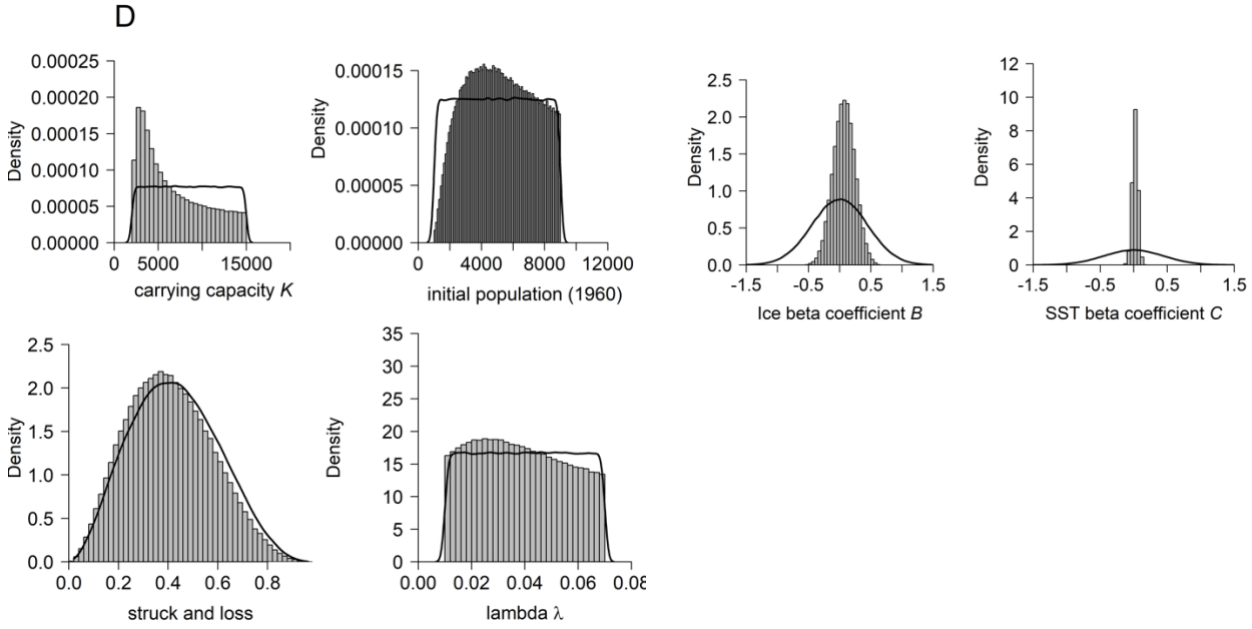
D
Density
carrying capacity K
initial population (1960)
Ice beta coefficient B
SST beta coefficient C
struck and loss
lambda λ

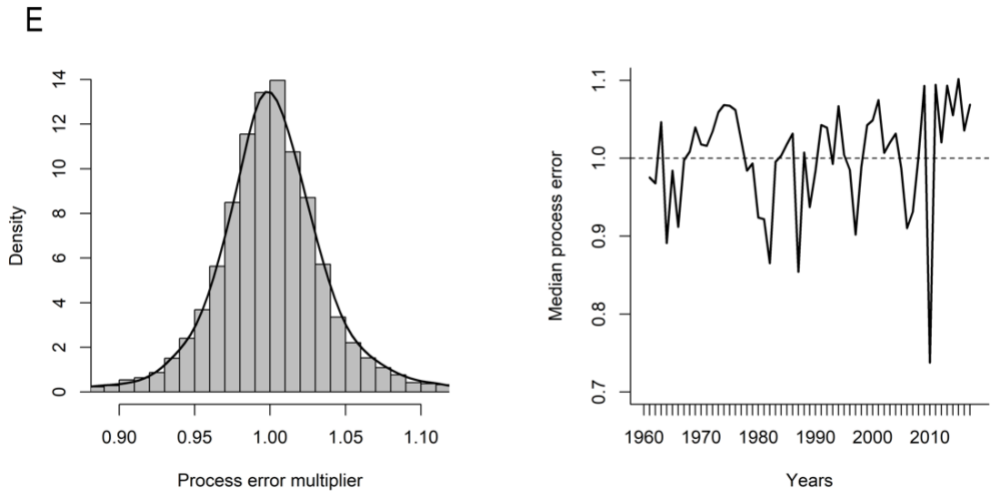

Appendix 2. Figure 1. Model fitted to harvest data (1960–2017) and adjusted aerial survey data (1990-2017). Plots are: A) autocorrelation plots showing correlation in successive lags of the chain, B) cross correlation showing correlation between variables within the model, C) Gelman plots showing convergence by comparing between and within chain variance, D) priors (lines), posterior (histograms) for B (coefficient for ICE), C (coefficient for SST), K (carrying capacity), lambda (maximum growth rate), initial population and S&L (struck and lost), and E) process error plots showing prior and posterior distributions and time series of median process errors.

Results and evidence of convergence for stochastic stock production models for CS beluga with ICE and SST included in the state process in separate models.

Appendix 2. Table 1. Model outputs for the CS beluga stock model incorporating environmental covariate ICE (see Table 2). The mean, standard deviation (SD), median (50^{th} Q), 25^{th} and 75^{th} quantiles (25^{th} Q, 75^{th} Q), 95% credibility intervals (2.5%CI, 97.5%CI) are given for the following model parameters and their priors: beta coefficient for ICE (B), carrying capacity (K), process error (process), survey precision (surv), starting population (startpop), struck and loss

(S&L), and population size in 2018 (N_{2018}). $\widehat{R}$ is the Brooks-Gelman-Rubin statistics; values near 1 indicate convergence of chains. N.eff is the number of effective chains after considering autocorrelation.

Parameter	Mean	SD	2.5%CI	25th Q	50th Q	75th Q	97.5% CI	$\widehat{R}$	n.eff
B	0.006	0.134	-0.241	-0.088	0.002	0.095	0.282	1.002	5100
B.prior	0.001	0.448	-0.874	-0.301	0	0.303	0.88	1.001	$5.00x10^5$
K	6083.121	3653.788	2192.64	3072.364	4659.816	8572.63	14275.88	1.001	160000
K.prior	8493.125	3752.272	2326.881	5238.804	8489.796	11740.05	14677.06	1.001	$5.00x10^5$
R	1	0	1	1	1	1	1	1	1
deviance	77.29	2.477	73.722	75.584	76.85	78.522	83.404	1.001	28000
$Lambda_{max}$	0.041	0.017	0.012	0.027	0.041	0.055	0.068	1.001	$2.00x10^5$
$Lambda_{max}$.prior	0.04	0.017	0.012	0.025	0.04	0.055	0.068	1.001	$5.00x10^5$
prec.process	1530.532	1228.798	130.051	634.398	1212.79	2087.254	4717.411	1.001	160000
prec.process.prior	1497.837	1225.425	107.891	605.272	1179.835	2048.927	4679.145	1.001	$5.00x10^5$
prec.surv	6.271	3.165	1.714	3.956	5.745	8.008	13.852	1.001	110000
prec.surv.prior	6.25	3.952	1.038	3.347	5.436	8.282	16.035	1.001	$5.00x10^5$
startpop	4706.804	2028.681	1695.155	3017.37	4376.688	6275.048	8690.19	1.001	69000
startpop.prior	5001.598	2308.393	1200.535	3003.504	5004.486	7002.356	8799.419	1.001	$5.00x10^5$
struck.and.lost	0.403	0.17	0.109	0.275	0.393	0.521	0.752	1.001	250000
struck.and.lost.prior	0.429	0.175	0.118	0.297	0.421	0.553	0.777	1.001	$5.00x10^5$
N_{2018}	1199.382	382.113	615.955	948.894	1148.242	1387.115	2087.789	1.001	150000

A

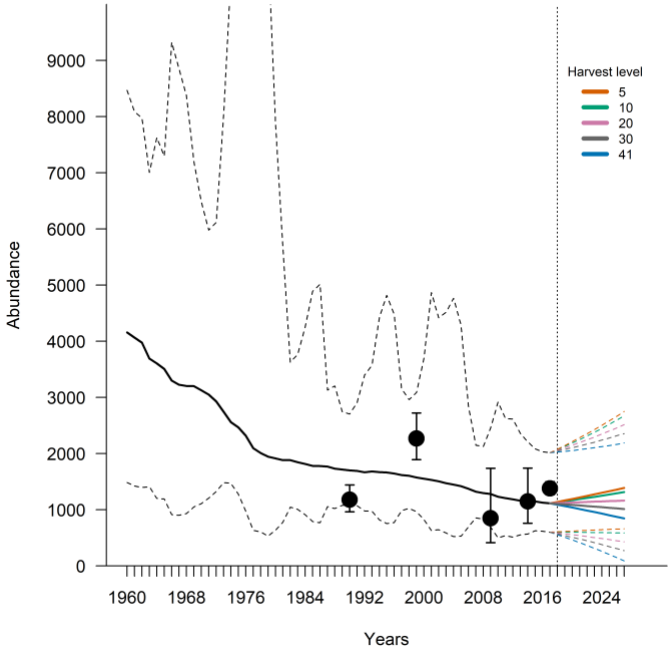
Abundance
9000
8000
7000
6000
5000
4000
3000
2000
1000
0
1960
1968
1976
1984
1992
2000
2008
2016
2024
Years
Harvest level
5
10
20
30
41

B

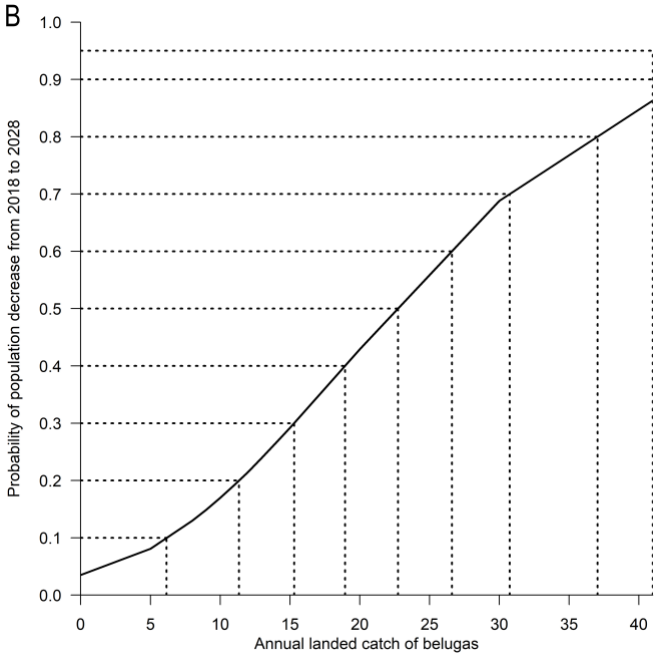
Probability of population decrease from 2018 to 2028
1.0
0.9
0.8
0.7
0.6
0.5
0.4
0.3
0.2
0.1
0.0
0
5
10
15
20
25
30
35
40
Annual landed catch of belugas

C

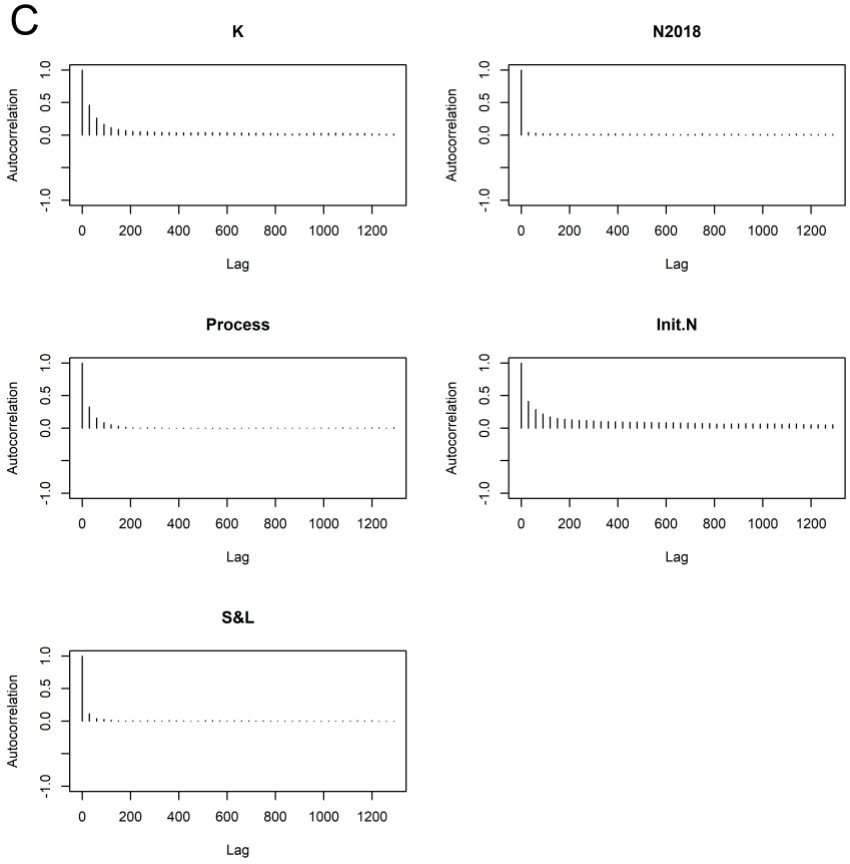
K
N2018
Process
Init.N
S&L
Autocorrelation
-1.0
0.0
0.5
1.0
0
200
400
600
800
1000
1200
Lag

D

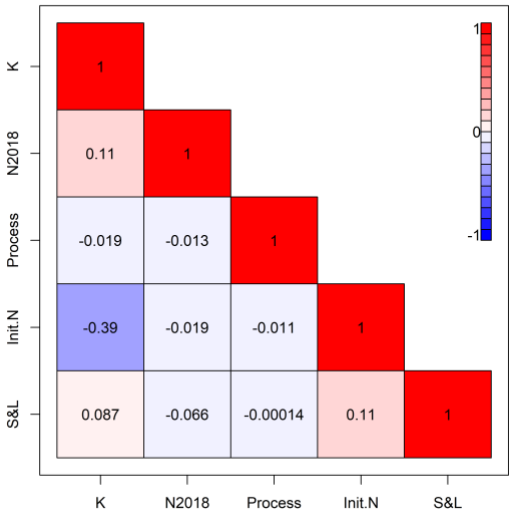
K
N2018
Process
Init.N
S&L
1
0.11
-0.019
-0.013
-0.39
-0.019
-0.011
0.087
-0.066
-0.00014
0.11
1
0
-1

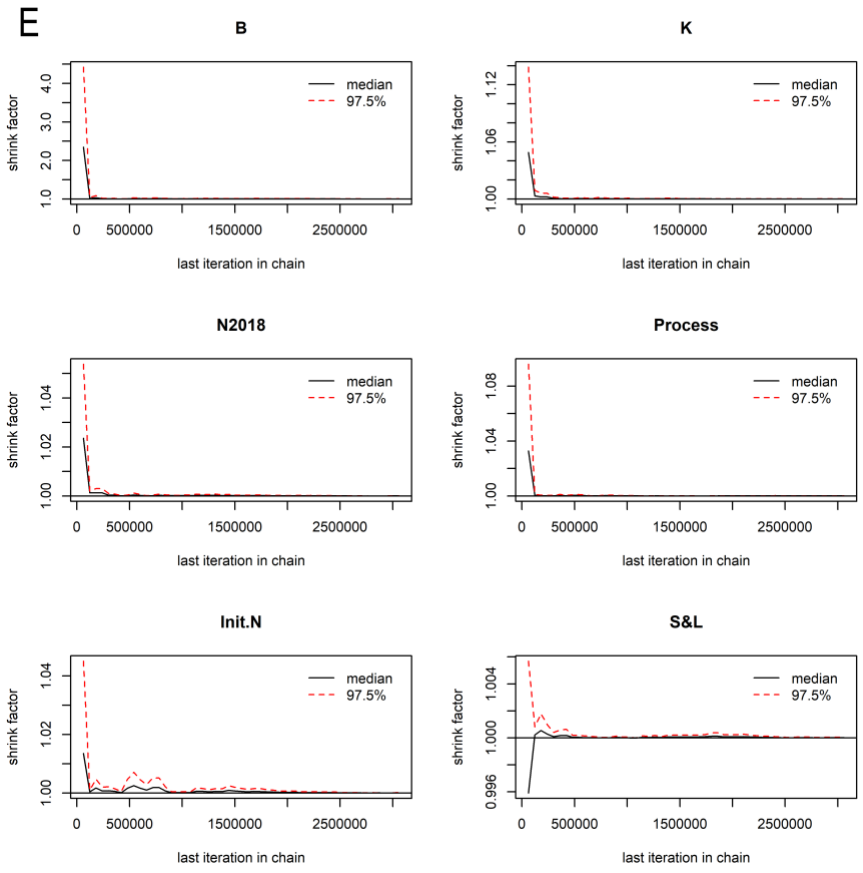
E
B
K
N2018
Process
Init.N
S&L
shrink factor
median
97.5%
last iteration in chain
0
500000
1500000
2500000

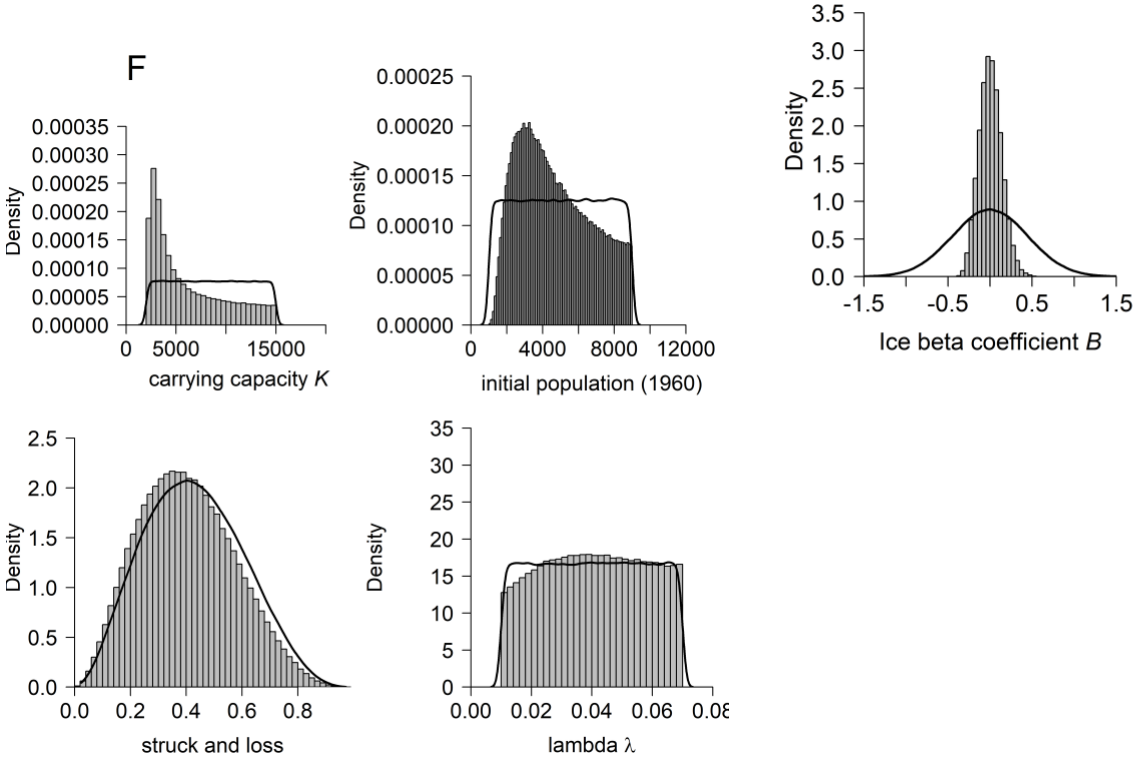
F
Density
carrying capacity K
initial population (1960)
Ice beta coefficient B
struck and loss
lambda λ

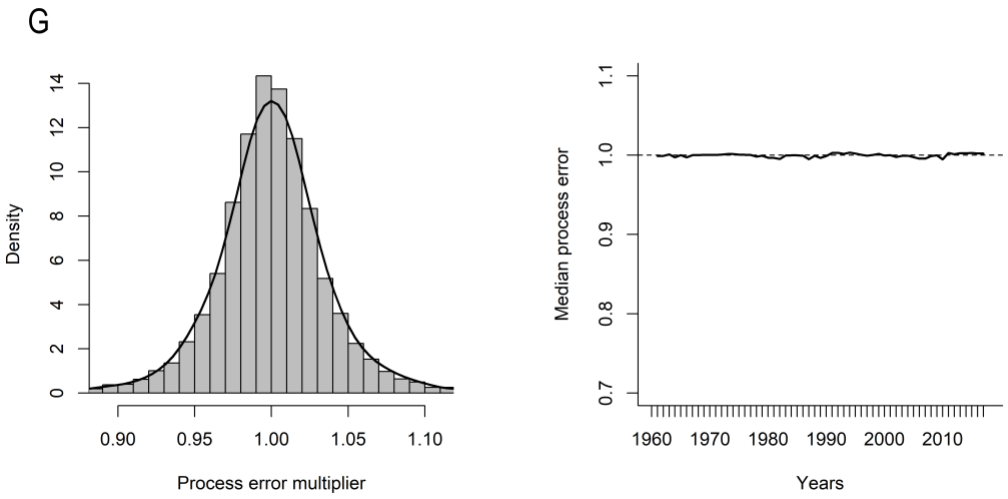

Appendix 2. Figure 2. Model fitted to harvest data (1960–2017), adjusted aerial survey data (1990-2017), and environmental covariate ICE. A) Population estimates show survey estimates (mean ± 95% confidence intervals), median (solid line) estimate, 2.5th, 97.5th quantiles (dashed lines), and future projections under various harvest scenarios (coloured lines). Plots are: B) probability of decline after 10 years, C) autocorrelation plots showing correlation in successive lags of the chain, D) cross correlation showing correlation between variables within the model, E) Gelman plots showing convergence by comparing between and within chain variance, F) priors (lines), posterior (histograms) for B, C, K, theta, initial population and S&L, and G) process error plots showing prior and posterior distributions and time series of median process errors.

Appendix 2. Table 2. Model outputs for the CS beluga stock model incorporating environmental covariate SST (see Table 2). The mean, standard deviation (SD), median (50th Q), 25th and 75th quantiles (25th Q, 75th Q), 95% credibility intervals (2.5%CI, 97.5%CI) are given for the following model parameters and their priors: beta coefficient for SST I, carrying capacity (K), process error (process), survey precision (surv), starting population (startpop), struck and loss (S&L), and population size in 2018 (N_{2018}). $\widehat{R}$ is the Brooks-Gelman-Rubin statistics; values near 1 indicate convergence of chains. N.eff is the number of effective chains after considering autocorrelation.

Parameter	Mean	SD	2.5%CI	25th Q	50th Q	75th Q	97.5%CI	$\widehat{R}$	n.eff
C	0.013	0.031	-0.05	-0.007	0.013	0.033	0.07	1.001	170000
C.prior	-0.001	0.447	-0.88	-0.302	-0.002	0.3	0.877	1.001	5.00x10^5
K	6396.698	3787.006	2168.384	3098.18	5119.492	9258.739	14382.99	1.001	190000
K.prior	8509.137	3752.556	2322.446	5261.523	8516.761	11761.27	14678.32	1.001	490000
R	1	0	1	1	1	1	1	1	1
deviance	77.067	2.479	73.564	75.359	76.604	78.289	83.178	1.001	5.00x10^5
Lambda$_{max}$	0.038	0.017	0.011	0.023	0.036	0.051	0.068	1.001	5.00x10^5
Lambda$_{max}$.prior	0.04	0.017	0.011	0.025	0.04	0.055	0.069	1.001	5.00x10^5
prec.process	1518.697	1222.805	124.354	626.27	1204.059	2070.887	4688.018	1.001	110000
prec.process.prior	1500.503	1226.751	107.473	606.216	1183.626	2056.156	4687.576	1.001	5.00x10^5
prec.surv	6.412	3.227	1.747	4.05	5.877	8.192	14.119	1.001	5.00x10^5
prec.surv.prior	6.249	3.951	1.038	3.339	5.44	8.289	16.035	1.001	5.00x10^5
startpop	4969.63	2086.528	1563.678	3234.958	4821.177	6665.549	8740.688	1.001	380000
startpop.prior	4997.314	2309.409	1199.233	2998.617	4997.69	6995.024	8798.933	1.001	310000
struck.and.lost	0.416	0.171	0.116	0.288	0.408	0.536	0.762	1.001	380000

struck.and.lost. prior	0.429	0.175	0.119	0.298	0.422	0.553	0.777	1.001	250000
N_{2018}	1315.234	502.839	601.211	987.486	1233.854	1542.798	2510.734	1.001	150000

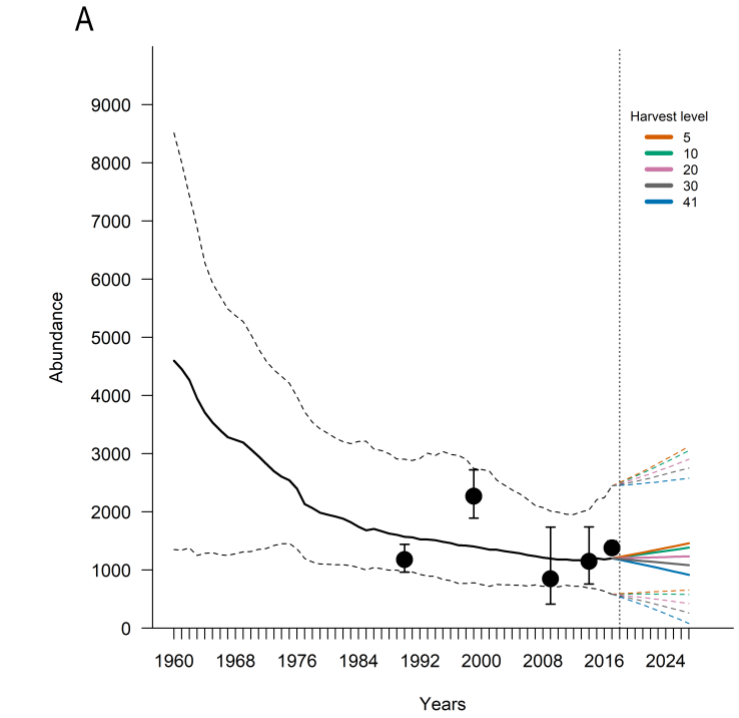
A
Abundance
Years
Harvest level
5
10
20
30
41
0
1000
2000
3000
4000
5000
6000
7000
8000
9000
1960
1968
1976
1984
1992
2000
2008
2016
2024

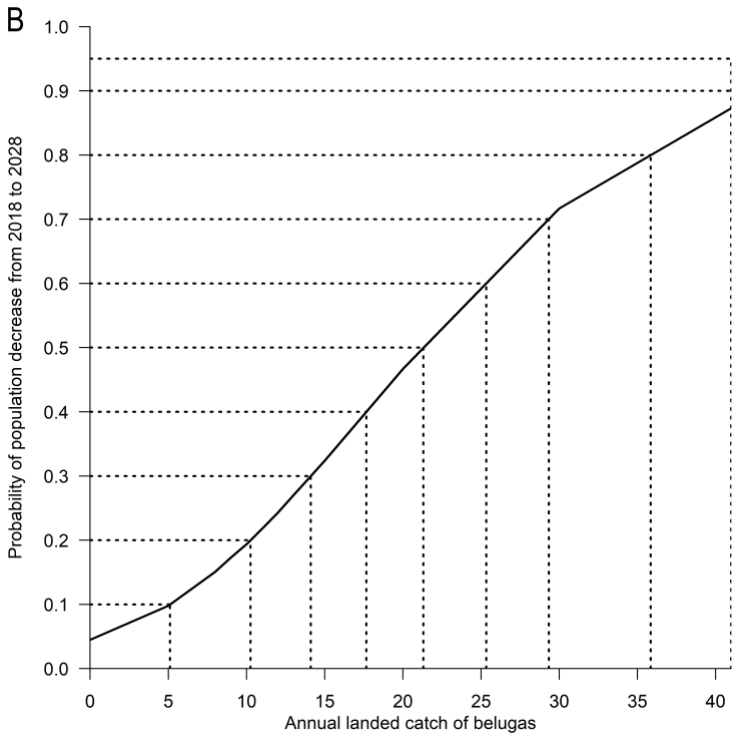
B
Probability of population decrease from 2018 to 2028
Annual landed catch of belugas
0.0
0.1
0.2
0.3
0.4
0.5
0.6
0.7
0.8
0.9
1.0
0
5
10
15
20
25
30
35
40

C

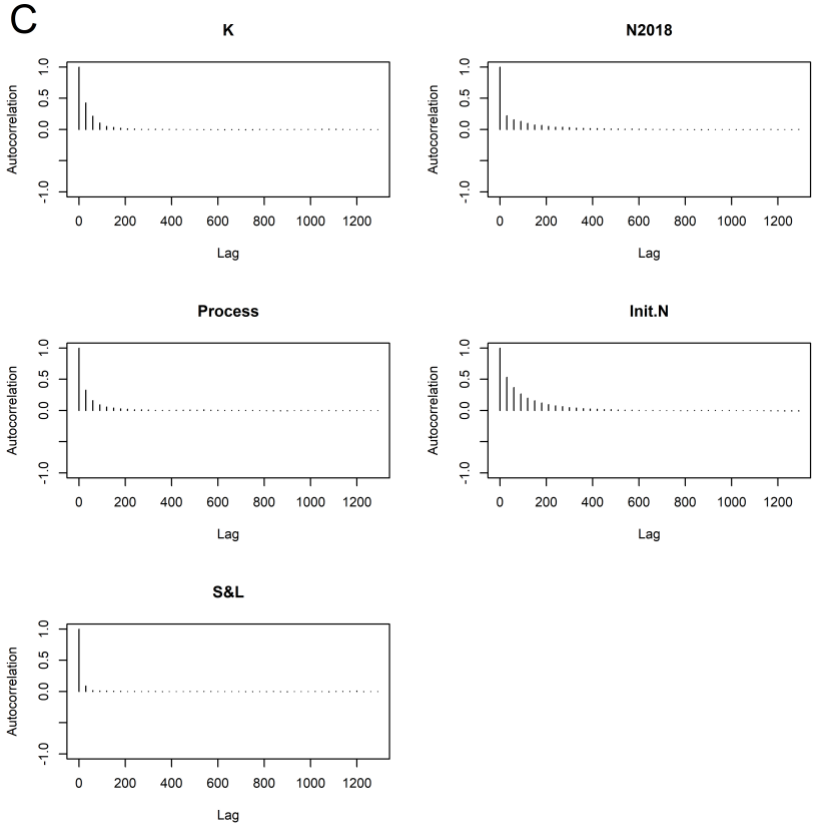
K
N2018
Process
Init.N
S&L
Autocorrelation
Lag
-1.0
0.0
0.5
1.0
0
200
400
600
800
1000
1200

D

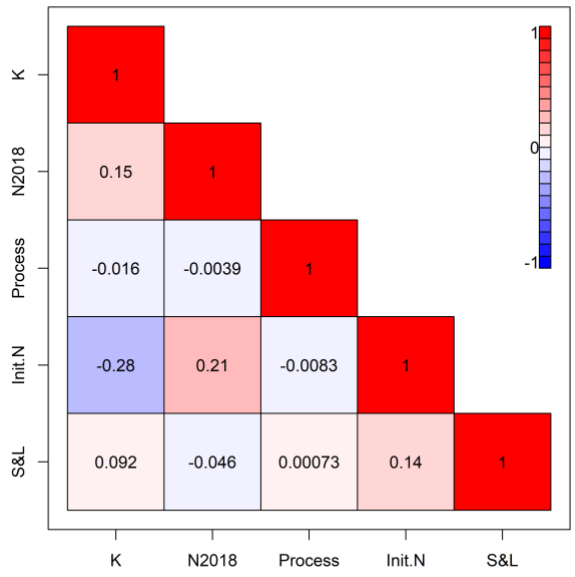
K
N2018
Process
Init.N
S&L
1
0.15
-0.016
-0.0039
-0.28
0.21
-0.0083
0.092
-0.046
0.00073
0.14
1
0
-1

E

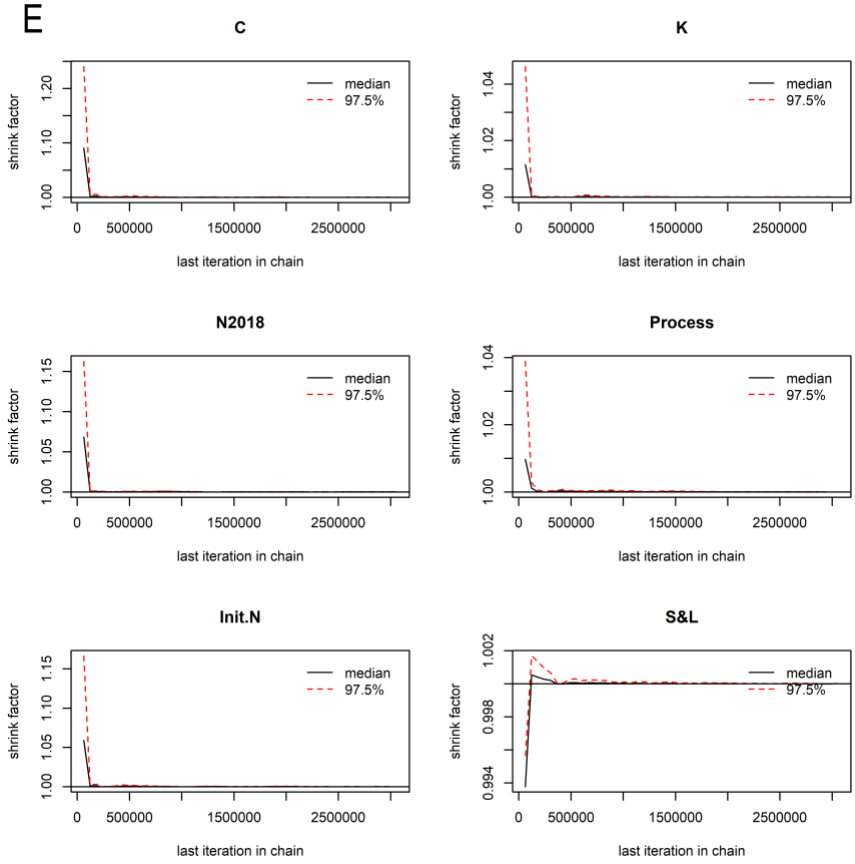
C
K
N2018
Process
Init.N
S&L
median
97.5%
shrink factor
last iteration in chain

F

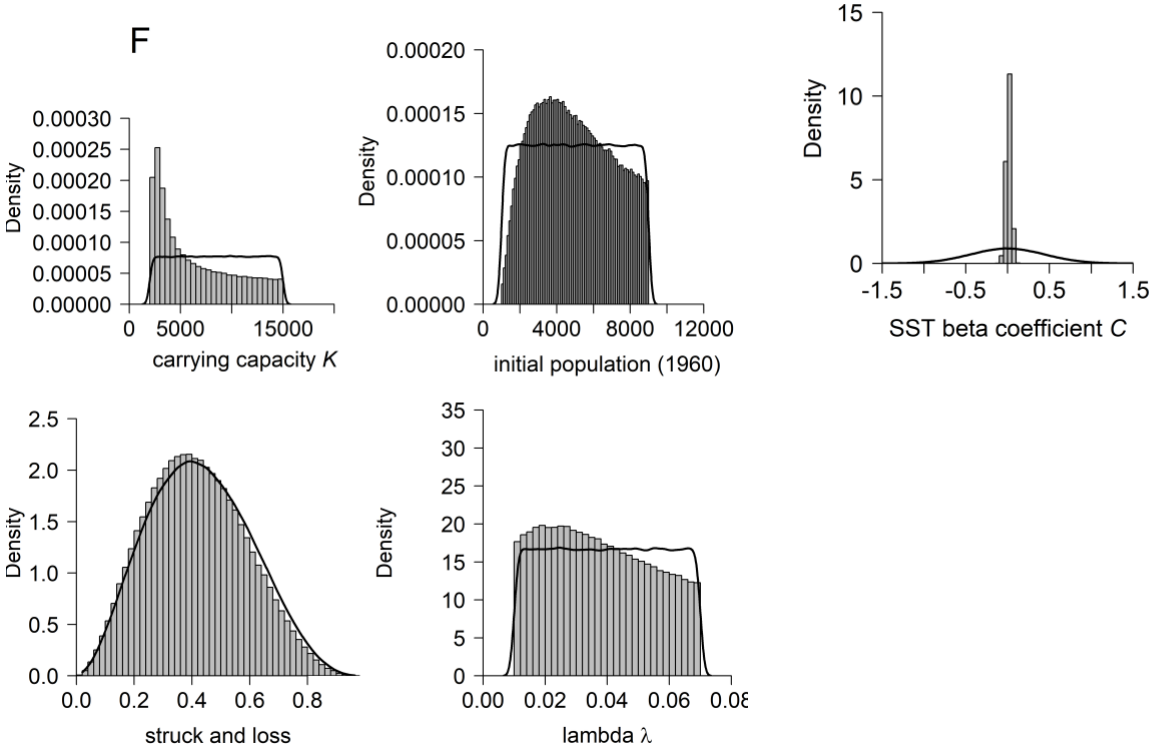
Density
carrying capacity K
initial population (1960)
SST beta coefficient C
struck and loss
lambda λ

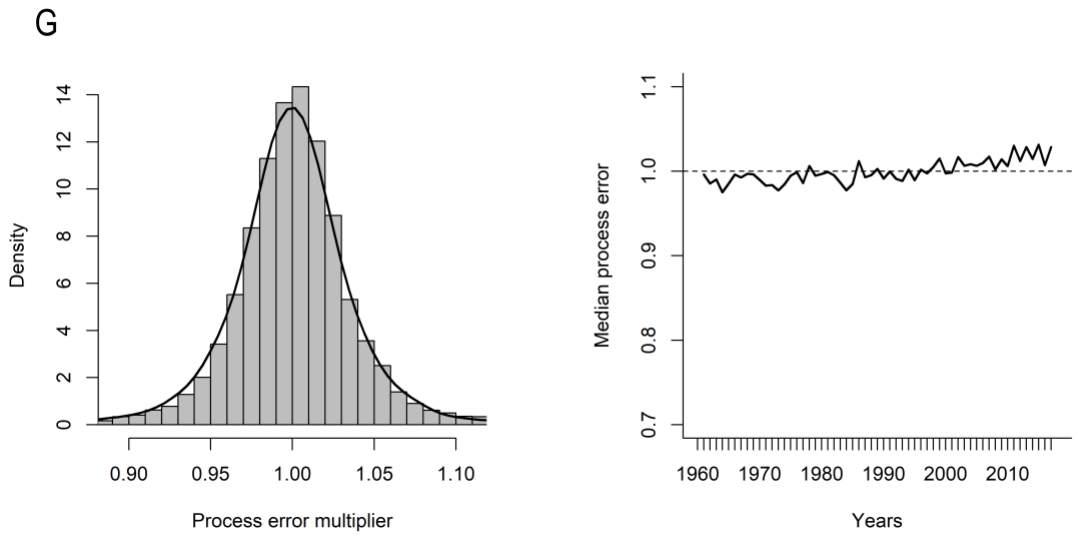

Appendix 2. Figure 3. Model fitted to harvest data (1960–2017), adjusted aerial survey data (1990-2017), and environmental covariate SST. A) Population estimates show survey estimates (mean ± 95% confidence intervals), median (solid line) estimate, 2.5th, 97.5th quantiles (dashed lines), and future projections under various harvest scenarios (coloured lines). Plots are: B) probability of decline after 10 years, C) autocorrelation plots showing correlation in successive lags of the chain, D) cross correlation showing correlation between variables within the model, E) Gelman plots showing convergence by comparing between and within chain variance, F) priors (lines), posterior (histograms) for B, C, K, theta, initial population and S&L, and G) process error plots showing prior and posterior distributions and time series of median process errors.

R code details for CS beluga population model

The CS beluga population estimates alongside their standard errors, harvest/catch data, and the environmental covariates (all as described in the main text) are loaded into the R session. Harvest levels for future projections are also defined.

```
#catch data
catch<-read.c“v("cumsdcatchtest_1960_mod.”sv", header=T)
CUMB=catch$CUMBERLAND
#year range
start.year=catch$YEAR[1]
last.year=catch$YEAR[nrow(catch)]
Nyears=last.year-start.year+1

#Cumberland Sounds survey data
#survey years
survey.year=c(1990,1999,2009,2014,2017)
#survey abundance estimates
survey=c(1180,2270,849,1151,1381)
#survey standard errors
survey.se=c(121,211,321,246,59)

#number of surveys
Nsurv=length(survey.year)
#survey year number (i.e., 1 = starting year)
surv.year=survey.year-start.year+1

#sea ice data
#for March
iceconc<-read.c“v("CSiceZscoreMARCH.”sv", header=T)
ICE=iceconc$ZscoreICE

#sea surface temperature
#for August
sstdata <-read.c“v("CSsstZscoreAUGUST.”sv", header=T)
SST=sstdata$ZscoreSST

#future projections
#number of years to project into future
N.fut.years=10
#future catch levels
Fut.lev=c(5,10,20,30,41)
#number of catch levels
N.lev=length(Fut.lev)

#compile data for model
```

```
dataDL<-list(Nyears=Nyears, Nsurv=Nsurv, N.fut.years=N.fut.years,
             N.lev=N.lev, Fut.lev=Fut.lev, surv.year=surv.year,
             survey=survey, CUMB=CUMB, ICE=ICE, SST=SST)
```

The model is built, and the priors, as described in the main text (Table 1), are defined using JAGS syntax.

```
modelJAGS <- function(){

struck.and.lost ~ dbeta(3,4)
struck.and.lost.prior ~ dbeta(3,4)

#precision parameter of log-normal survey error (=inverse of variance)
prec.surv ~ dgamma(2.5,0.4)
prec.surv.prior ~ dgamma(2.5,0.4)

#precision parameter of log-normal process error (=inverse of variance)
prec.process ~ dgamma(1.5,0.001)
prec.process.prior ~ dgamma(1.5,0.001)

lambda ~ dunif(0.01,0.07)
lambda.prior ~ dunif(0.01,0.07)

K~ dunif(2000,15000)
K.prior~dunif(2000,15000)

startpop ~ dunif(1000,9000)
startpop.prior ~ dunif(1000,9000)

R<-1

#coefficient for sea ice concentration
B ~ dnorm(0,5)
B.prior ~ dnorm(0,5)

#coefficient for sea surface temp
C ~ dnorm(0,5)
C.prior ~ dnorm(0,5)
```

State process is defined, where CUMB refers to catch history, and all other parameters are defined above or in the main text.

```
#for year 1
Nstart[1] <- startpop
Nfin[1] <- max(.01, Nstart[-] - (CUMB[1])*(1+struck.and.lost))
```

```
#for year 2 onward
for (year in 2:Nyears)
{ #inclusion of environmental covariates in process error
  ice[year] <- B*ICE[year-1]
  sst[year] <- C*SST[year-1]
  process[year] <- ice[year] + sst[year]
  proc.error[year] ~ dlnorm(process[year],prec.process)

  #density dependent growth
  Nstart[year] <-(Nfin[year-1]*(1+(lambda*(1-(Nfin[year-1]/K)^R)))*
                  proc.error[year])
  Nfin[year] <- max(.01,Nstart[yea-] - (CUMB[year])*(1+struck.and.lost) )
}
```

Observation process is defined using model estimates from survey years.

```
#observation process
for (surv.ser in 1:Nsurv)
{   survey.pred[surv.ser] <- (Nstart[surv.year[surv.ser]])
    survey.med[surv.ser] <- log(max(.001,survey.pred[surv.ser]))
    survey[surv.ser] ~ dlnorm(survey.med[surv.ser],prec.surv)
}
```

Finally, future predictions for the first future year are created using the final year of the model recreated trajectory, and from year 2 onward future years are predicted using the prediction from the previous year. This concludes the model structure, so the model is then closed and written as a JAGS model.

```
#future predictions
for (lev in 1:N.lev)
#for year 1
{   for (year in 1:1)
    { fut.error[lev,year] ~ dlnorm(0,prec.process)
    #prediction at the start of the year
    fut.Nstart[lev,year] <- max(1,(Nfin[Nyears]*(1+(lambda*
          (1-(Nfin[Nyears]/K)^R)))*fut.error[lev,year] ) )
    #prediction after harvest
    fut.Nfin[lev,year] <- max(1,(fut.Nstart[lev,yea-] - Fut.lev[lev]*
          (1+struck.and.lost)) )
    #probability of decline
    P.less[lev,year] <- step(Nfin[Nyears]-fut.Nfin[lev,year])
    }

#for year 2 onward
    for (year in 2:N.fut.years)
```

```
    { fut.error[lev,year] ~ dlnorm(0,prec.process)
    #prediction at the start of the year
   fut.Nstart[lev,year] <- max(1,(fut.Nfin[lev,year-1]*(1+(lambda*
          (1-(fut.Nfin[lev,year-1]/K)^R)))*fut.error[lev,year] ))
        #prediction after harvest
    fut.Nfin[lev,year] <- max(1,(fut.Nstart[lev,yea-] - Fut.lev[lev]*
          (1+struck.and.lost))  )
        #probability of decline
    P.less[lev,year] <- step(Nfin[Nyears]-fut.Nfin[lev,year])
    }
}
#end of model
}

write.model(modelJAGS, modelJAGS <- paste0(getwd"),"/modelJAGS."ug"))
```

The MCMC model features are defined and the model can be run.

```
#number of chains
Nchains = 5

Final_NIter = 100000
Thining = 30
Burnin = 60000
Effective_NIter = Burnin + Final_NIter * Thining

#initial values
Inits <- rep(list(list()),Nchains)

#RUN model
m <- jags.parallel(model.file=modelJAGS,
            n.chains = Nchains,
            n.thin = Thining,
            n.iter = Effective_NIter,
            n.burnin = Burnin,
            dat = dataDL,
            inits = Inits,
            parameters.to.save=     "c""K", "K.pr"or","R", "R.pr"or",
                  "  "prec.surv.pr"or", "prec.s"rv", "lambda.pr"or",
                  "  "lam"da", "startpop.pr"or", "start"op",
                  "  "struck.and.lost.pr"or", "struck.and.l"st",
                  "  "prec.process.pr"or", "prec.proc"ss", "N"in",
                  "  "fut.N"in", "proc.er"or","B", "B.pr"or","C",
                  "  "C.pr"or", pas"e("P.le"s[", 1:N.le","",",N.fut.yea"s""]
",
                       s""="")))
```

Appendix 3

R code details for ECWG bowhead whale MRC models

Capture history is loaded into R as a data frame with a column (ch) that has all capture periods as a caracter string, with 1 for years with captures and 0 for years without. Identification of captures as described in the main text. The data is then processed by functions in package 'marked' to get setup for use in the model.

```
library(marked)

# Select column with capture history from data set
bcap <- caphist %>% sele“t(”ch")

# Process the data for the model
# Use model“= ""JS" for Cormack Jolly-Seber model and
#   change to model“= ”JS" for Jolly-Seber model
bcap.proc=process.data(bcap, model“= ""JS")
bcap.ddl=make.design.data(bcap.proc)
```

The model stucture is set up with Phi (apparent survival) and p (probability of capture) varying annually (time) or constant (dot). The four models as described in the main text are then run.

```
#Set up model structure and run models
fit.models=function()
{
  Phi.time=list(formula=~time)
  Phi.dot=list(formula=~1)
  p.dot=list(formula=~1)
  p.time=list(formula=~time)
  cml=create.model.list“c(""h""""p"))
  results=crm.wrapper(cml,data=bcap.proc, ddl=bcap.ddl, hessian = TRUE, exter
nal=FALSE,accumulate=FALSE)
  return(results)
}
bcap.models=fit.models()

# Look at ranking of each model
bcap.models
```

Once the top model has been determined, parameters are isolated and the p parameter is used to estimate abundance.

```
#Look at parameters from top model (model 2)
model2<- bcap.models[[2]]
paramtable2 = model2$results$reals
paramtable2

# Isolate p estiamtes for abundance estimate for CJS model
ptable <- paramtable2$p
# Order p estimates in order of years
ptable <- ptable[order(ptable$time),]

# Estimate annual abundance estimates for CJS model
obs = gregex“r”"1", bcap$ch)
n_obs = summary(as.factor(unlist(obs)))
estim_abundance = n_obs[-1]/ptable$estimate[1:8]
ucl_abundance = n_obs[-1]/ptable$ucl[1:8]
lcl_abundance = n_obs[-1]/ptable$lcl[1:8]
estim_abundance
```

Outputs from non-preferred mark-recapture models for EC-WG bowhead whales, and metadata for all captures.

Appendix 3. Table 1. Estimated apparent survival rate (Φ), and probability of capture (*p*) from the top Cormack-Jolly-Seber mark recapture model for ECWG bowhead whales sampled from 2012-2021. No samples were taken in 2015.

Φ				
Year	**Estimated Survival Rate**	**SE**	**Lower Confidence Limit**	**Upper Confidence Limit**
All	0.9877	0.0924	0.000026	1
p				
Year	**Estimated probability of capture**	**SE**	**Lower Confidence Limit**	**Upper Confidence Limit**
2013	0.0455	0.0147	0.0240	0.0846
2014	0.0315	0.0097	0.0170	0.0573
2015	-	-	-	-
2016	0.0125	0.0050	0.0057	0.0271
2017	0.0241	0.0085	0.0120	0.0478
2018	0.0025	0.0020	0.0006	0.0116
2019	0.0247	0.0113	0.0100	0.0599
2020	0.0136	0.0074	0.0047	0.0389
2021	0.0107	0.0065	0.0032	0.0347

Appendix 3. Table 2. Comparison of AIC results for the four tested Cormack-Jolly-Seber mark recapture models for ECWG bowhead whales sampled from 2012-2021.

Model	Number of Parameters	AIC	ΔAIC
constant Φ annual p_t	9	921.60	0.00
annual Φ_t annual p_t	16	932.44	10.84
constant Φ constant p	2	939.27	17.66
annual Φ_t constant p	9	943.71	22.11

Appendix 3. Table 3. Comparison of AIC results for the four tested Jolly-Seber mark recapture models for ECWG bowhead whales sampled from 2012-2021 from all sampling locations.

Model	Number of Parameters	AIC	ΔAIC
constant Φ annual p_t	12	994.74	0.00
annual Φ_t annual p_t	19	1004.46	9.72
constant Φ constant p	4	1109.19	114.45
annual Φ_t constant p	11	2636.99	1642.25

Appendix 3. Table 4. Comparison of AIC results for the four tested Jolly-Seber mark recapture models for ECWG bowhead whales sampled from 2012-2021 from Pangnirtung.

Model	Number of Parameters	AIC	ΔAIC
constant Φ annual p_t	12	737.48	0.00
annual Φ_t annual p_t	19	750.34	12.87
annual Φ constant p	11	899.16	161.68
constant Φ_t constant p	4	951.17	213.70

Appendix 4

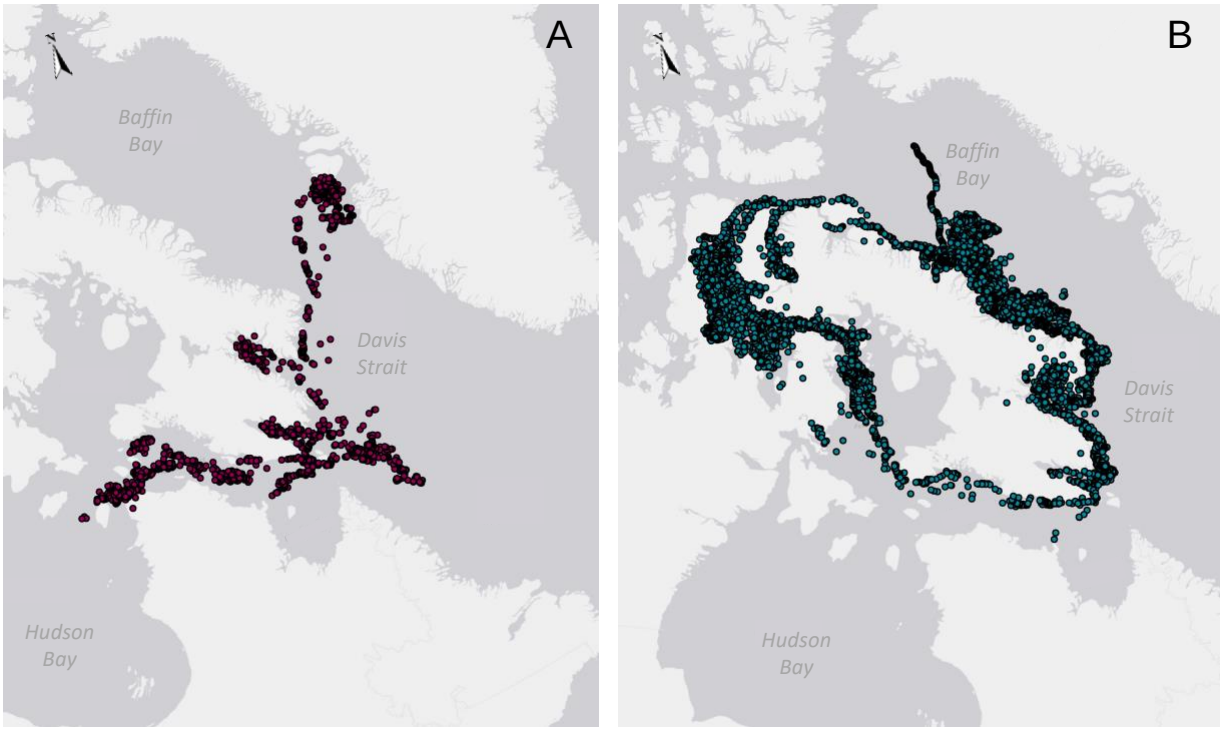

Appendix 4. Figure 1. Tracks from satellite tagged bowhead whales from the EC-WG population. A) Locations in March from 29 individuals tagged from 2007-2017. B) Locations in August from 105 individuals tagged from 2005-2019.

Evidence of model convergence for a stochastic stock production model for EC-WG bowhead whales.

1)

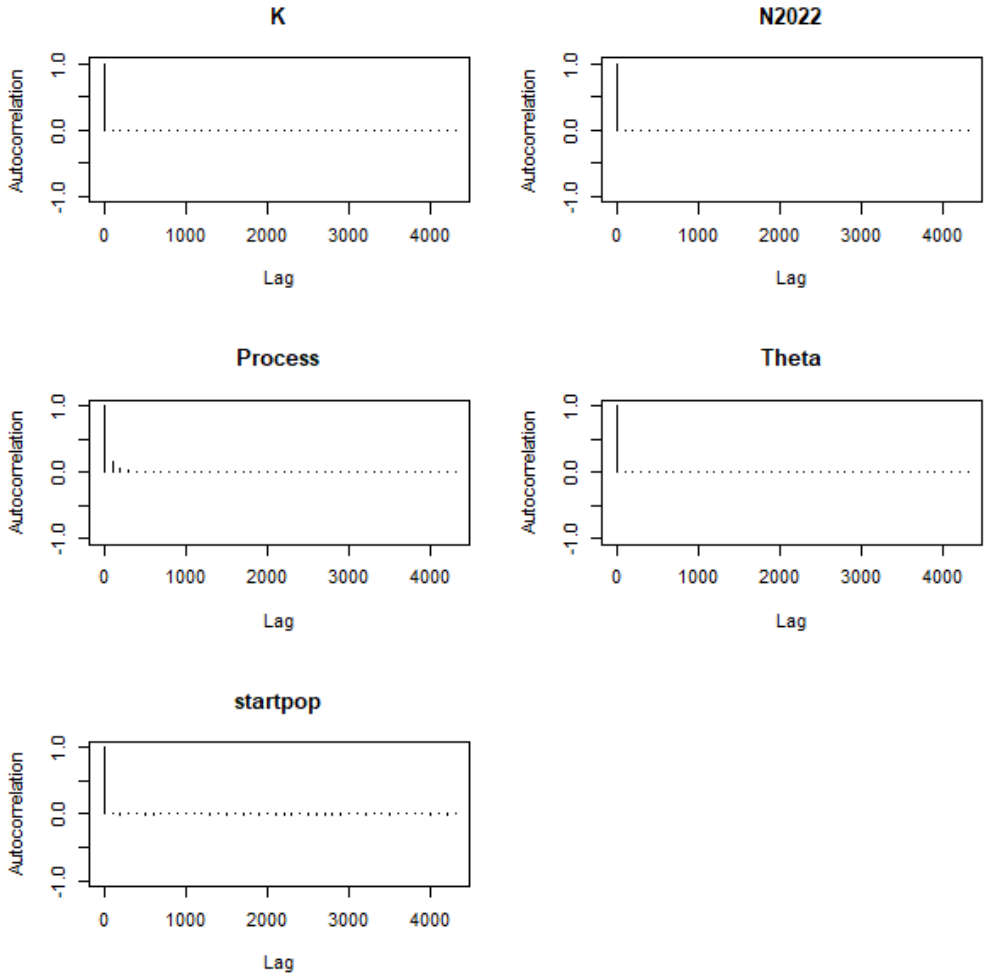

2)

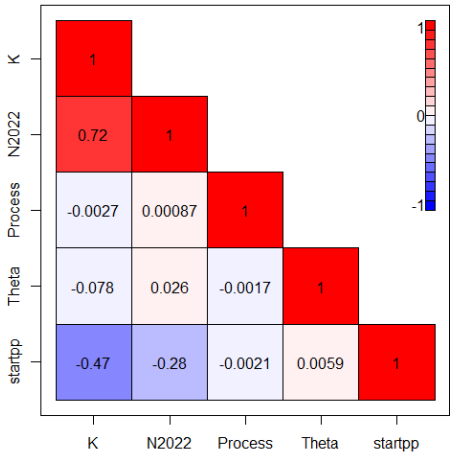
K
N2022
Process
Theta
startpp
1
0.72
1
-0.0027
0.00087
1
-0.078
0.026
-0.0017
1
-0.47
-0.28
-0.0021
0.0059
1
1
0
-1

3)

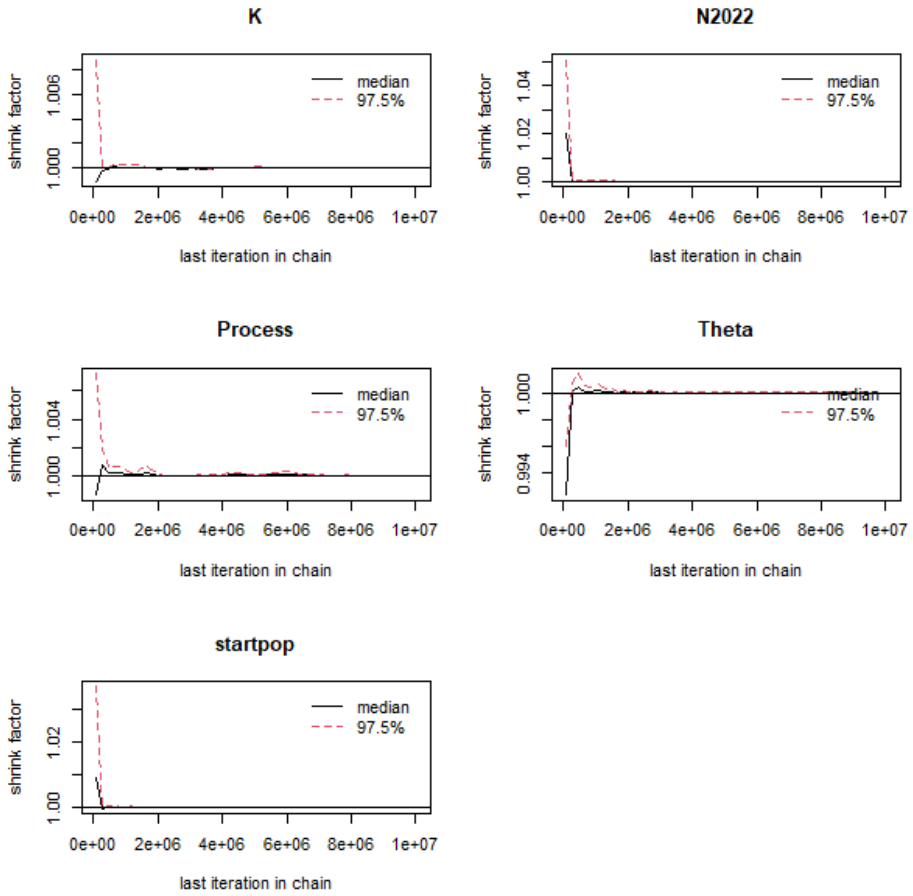
K
N2022
Process
Theta
startpop
shrink factor
median
97.5%
last iteration in chain
0e+00
2e+06
4e+06
6e+06
8e+06
1e+07

4)

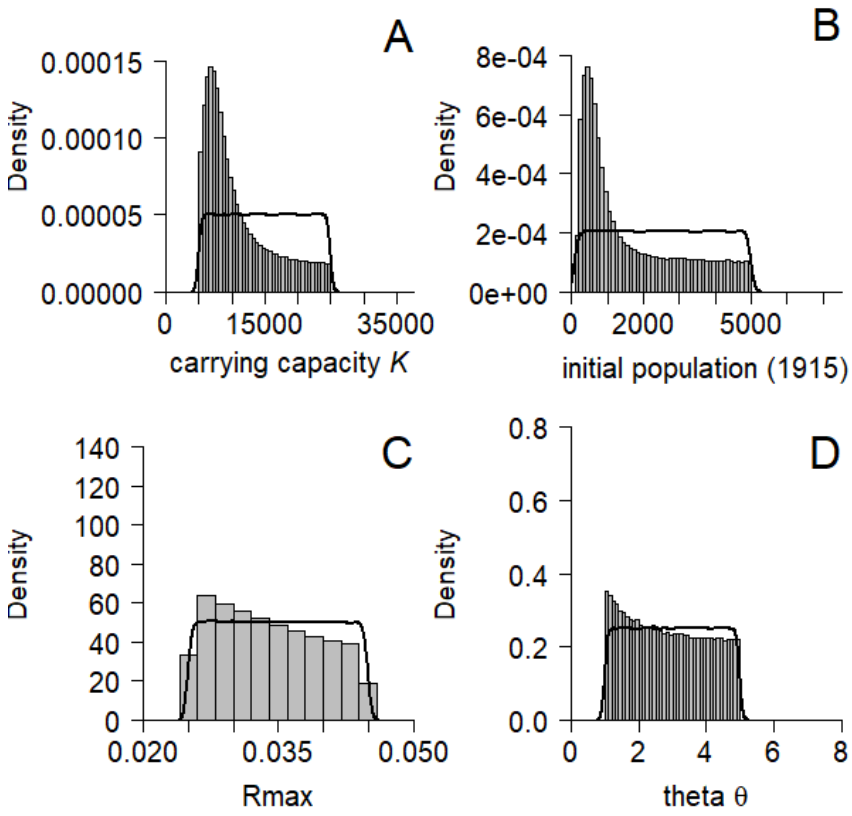

Appendix 4. Figure 2. Model fitted to harvest data (1915–2022), adjusted aerial survey data (1981, 2002, 2013), and mark-recapture estimates (2013, 2017). Parameters are defined as: K (carrying capacity), N2022 (population abundance in 2022), initN (starting population), R (theta or density dependence shaping parameter), and process (process error). Plots are: 1) autocorrelation plots showing correlation in successive lags of the chain, 2) cross correlation showing correlation between variables within the model, 3) Gelman plots showing convergence by comparing between and within chain variance, 4) priors (lines), posterior (histograms) for K (carrying capacity, A), initial population (B), maximum growth rate (C), and theta (D).

Appendix 4. Table 1. Model output for the EC-WG bowhead whale stock model where theta=1. The mean, standard deviation (SD), median (50^{th} Q), 25^{th} and 75^{th} quantiles (25^{th} Q, 75^{th} Q), 95% credibility intervals (2.5%CI, 97.5%CI) are given for the following model parameters: carrying capacity (K), process error (process), survey precision (surv), starting population (startpop), struck and loss (S&L), and population size in 2022 (N_{2022}). $\widehat{R}$ is the Brooks-Gelman-Rubin statistics; values < 1.05 indicate convergence of chains. N.eff is the number of effective chains after considering autocorrelation.

Parameters	Mean	SD	2.5% CI	25% Q	50% Q	75% Q	97.5% CI	$\widehat{R}$	n.eff
K	12362.322	5357.523	5481.353	7962.54	10910.161	16155.546	23921.444	1.001	30000
theta	1	0	1	1	1	1	1	1	1
deviance	94.348	2.092	91.028	92.884	94.17	95.436	99.264	1.001	24000
Rmax	0.034	0.006	0.025	0.029	0.034	0.039	0.044	1.001	17000
prec.process	15028.454	12138.196	1134.412	6112.812	11952.701	20596.911	46479.099	1.001	30000
prec.surv	3.884	1.862	1.153	2.534	3.582	4.899	8.362	1.001	25000
startpop	1724.271	1292.42	271.885	691.375	1262.415	2551.698	4698.179	1.001	30000
struck.and.lost	0.28	0	0.28	0.28	0.28	0.28	0.28	1	1
N_{2022}	8504.837	2231.176	5137.082	6902.543	8204.17	9758.047	13720.686	1.001	18000

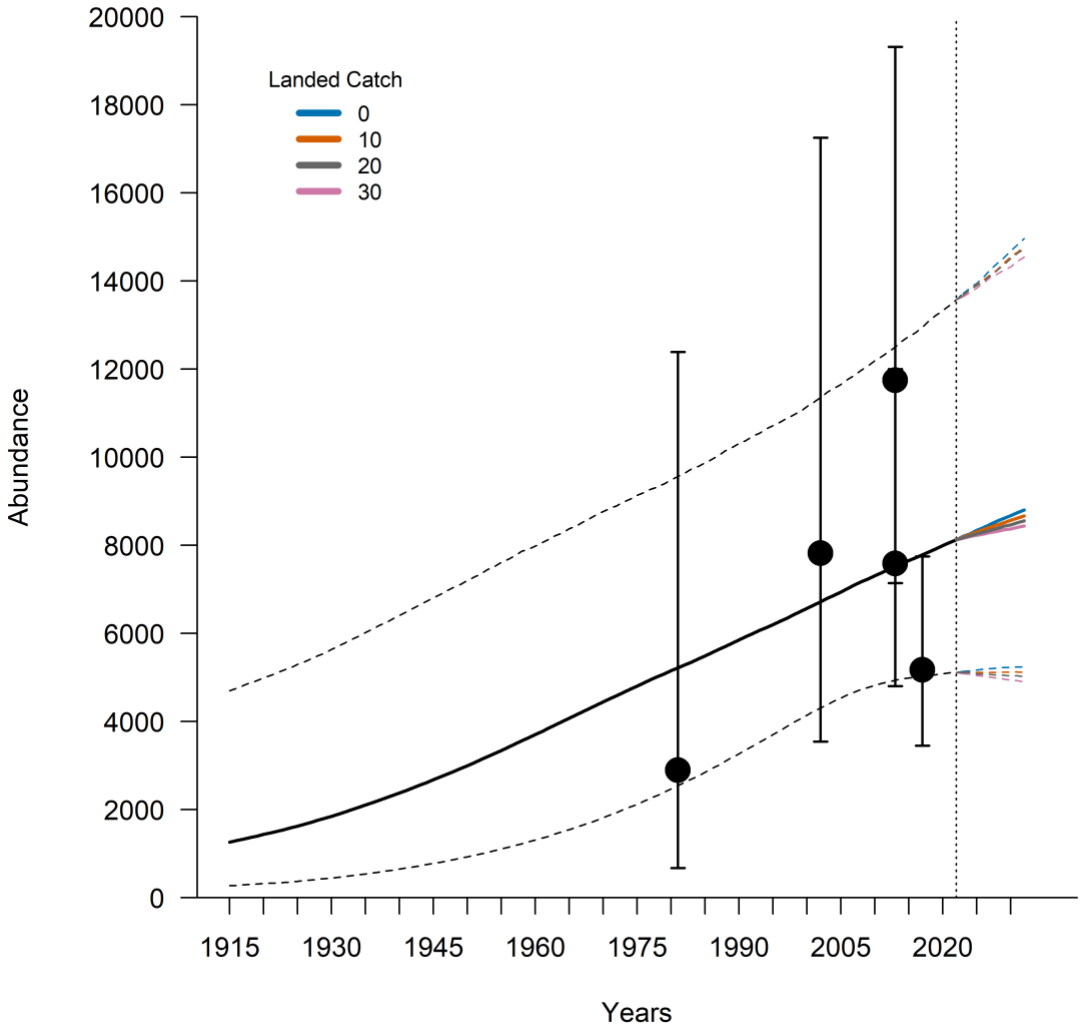

Appendix 4. Figure 3. Future population projections for EC-WG bowhead whales under four different harvest scenarios based on population estimates from a stochastic stock production model where theta=1 fitted to extrapolated aerial survey estimates flown in 1981, 2002, and 2013, and genetic mark recapture estimates from 2013 and 2017 (black dots ± 95% log-normal CI). The solid line indicates the posterior median estimates and dashed lines show 95% credible intervals.

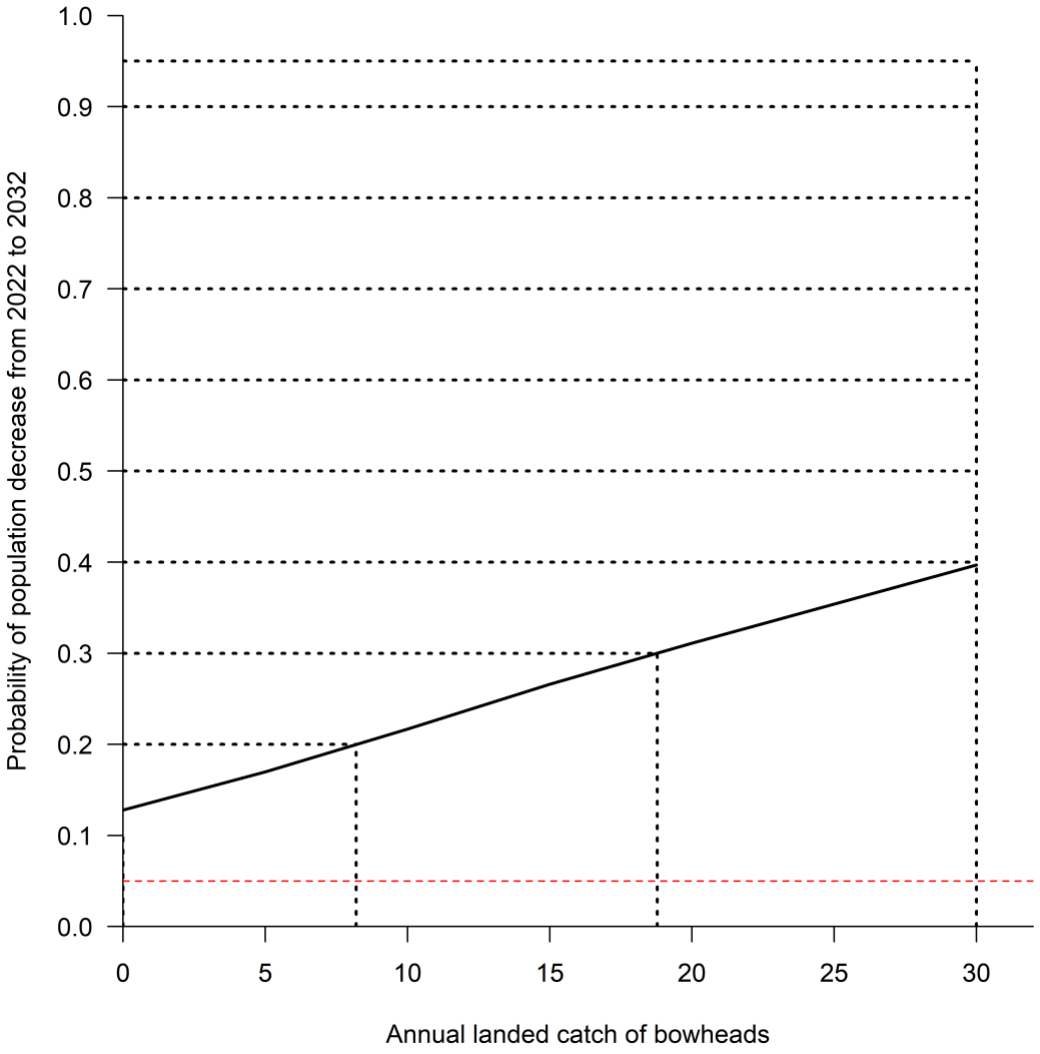

Appendix 4. Figure 4. Probability of EC-WG bowhead whale stock decreasing from the 2022 abundance estimate after 10 years of harvest, as a function of the number of reported bowhead whales removed from the stock every year. Estimates from population model where R=1. Dotted lines indicate levels of harvest (x-axis) corresponding to the probability of decline (y-axis). Red dotted line indicates low risk of decline.